

**Short-term and Long-term SPI Drought Forecasts Using Wavelet Neural Networks  
and Wavelet Support Vector Regression in the Awash River Basin of Ethiopia**

**By**

**Anteneh Belayneh**

A thesis submitted to McGill University  
in partial fulfillment of the requirements for the degree of  
**Master of Science**

Department of Bioresource Engineering  
MacDonald Campus of McGill University  
Ste. Anne de Bellevue, Quebec, Canada  
**June 2012**

Copyright © Anteneh Belayneh, 2012

## Abstract

Ethiopia's climate variability coupled with the country's heavy reliance on rain-fed agriculture make it vulnerable to the impacts of drought. This vulnerability is evident in the Awash River Basin, where a significant proportion of the population is dependent on international food assistance for survival. Given this vulnerability to drought, effective drought forecasts are an essential tool for effective water resource management as well as mitigation of some of the more adverse consequences of drought. This study forecast the Standard Precipitation Index (SPI) on both short-term and long-term lead times. For short-term forecasts this study computed SPI 1 and SPI 3, short-term drought indicators which represent agricultural drought. For long-term forecasts, SPI 12 and SPI 24 were computed. These two indices are long-term drought indicators which represent hydrological drought conditions.

The SPI forecasts were done using five data driven models. Forecasts were compared between two machine learning techniques: artificial neural networks (ANNs) and support vector regression (SVR). The results from these two techniques were compared to a traditional stochastic forecast model, namely an autoregressive integrated moving average (ARIMA) model. In addition, ANN and SVR models were coupled with wavelet analysis (WA) to produce wavelet-neural network (WA-ANN) and wavelet-support vector regression (WA-SVR) models. This study proposed and explored, for the first time, SVR and WA-SVR methods for short term and long term SPI drought forecasting at different lead times.

Traditionally, the number of wavelet decompositions of a time series (for forecasting applications) are determined either by trial and error or using the formula  $L = \text{int}[\log(N)]$ , with  $N$  being the number of samples. This study found that in almost all cases the approximation series after decomposition, and not the detail series, yielded the best forecast results. The decomposition level which had the approximation that yielded the best forecast results was determined to be the appropriate decomposition.

With regards to ANN model architecture, traditionally the optimal number of neurons in the hidden layer is either determined using a trial and error procedure, or is determined empirically to be  $\log(N)$  or  $2n+1$ , where  $n$  is the number of input layers. This

study combined all these approaches. The empirical methods helped establish upper and lower bounds for the optimal number of neurons within the hidden layer. After an interval was determined, a trial and error procedure was used to determine the optimal number of neurons in the hidden layer.

The forecasts in this study were evaluated using a measure of persistence,  $R^2$ , RMSE, and MAE. The forecast results indicate that WA-ANN and WA-SVR models were the most accurate methods for forecasting the SPI on both short and long-term time scales.

## Résumé

La variabilité du climat de l'Éthiopie combinée à la forte dépendance de ce pays sur l'agriculture dépendant de la pluie le rend vulnérable aux impacts des sécheresses. Cette vulnérabilité est évidente dans le bassin de la rivière Awash, où une grande proportion de la population dépend de l'aide alimentaire internationale pour survivre. Étant donné cette vulnérabilité aux sécheresses, des prévisions efficaces d'inondations sont un outil essentiel pour la gestion efficace de ressources hydriques ainsi que pour mitiger les conséquences les plus graves des sécheresses. Cette étude prévoit l'Indice de Précipitations Standard (IPS) sur des temps de défilement à court et à long terme. Pour les prévisions à court terme, cette étude s'est penchée sur IPS 1 et IPS 3, des indicateurs de sécheresse à court terme qui représentent la sécheresse agricole. Pour les prévisions à long terme, IPS 12 et IPS 24 ont été calculés. Ces deux indices sont des indicateurs de sécheresse à long terme qui représentent des conditions de sécheresse hydrologique.

Les prévisions d'IPS ont été effectuées en employant cinq modèles à base de données (data-driven models). Des prévisions ont été comparées entre deux techniques d'apprentissage automatique (machine learning) : les réseaux de neurones artificiels (RNA) et les supports de régression vectorielle (SRV). Les résultats de ces deux techniques ont été comparés à un modèle académique traditionnel de prévision, soit un modèle autorégressif intégré de moyenne mobile (ARIMM). De plus, les modèles RNA et SRV ont été combinés à une analyse d'ondelettes (AO) pour produire des modèles d'ondelettes-réseaux de neurones (AO-RNA) et des modèles d'ondelettes-supports de régression vectorielle (AO-SRV). Cette étude propose et examine, pour la première fois, des méthodes SRV et AO-SRV pour des prévisions de sécheresse IPS à court et long terme à des temps de défilement différents.

Traditionnellement, le nombre de décompositions d'ondelettes dans une série temporelle (pour les applications de prévision) sont déterminées soit par essai et erreur ou en utilisant la formule  $L = \text{int}[\log(N)]$ , N représentant le nombre d'échantillons. Cette recherche permis de constater que dans presque tous les cas, la série d'approximation après décomposition, et non la série détail, produisait les meilleurs résultats de prévision. Le niveau de décomposition dont l'approximation avait produit les meilleurs résultats

prévisionnels a déterminé la décomposition appropriée. Par rapport au modèle d'architecture RNA, traditionnellement, le nombre optimal de neurones dans une couche cachée est obtenu en utilisant une méthode d'essai et erreur, ou alors est fixé empiriquement à  $\log(N)$  ou  $2n+1$ , où  $n$  est le nombre de niveaux de input de données. Cette étude a combiné toutes ces approches. Les méthodes empiriques ont aidé à déterminer les limites supérieures et inférieures pour le nombre optimal de neurones au sein de la couche cachée. Après avoir procédé à la détermination d'un intervalle, l'essai et l'erreur ont été utilisés pour parvenir au nombre optimal de neurones dans un niveau caché.

Les prévisions dans cette recherche ont été évaluées selon les mesures de la persistance, du coefficient de détermination ( $R^2$ ), de la déviation de valeur efficace (RMSE), et de l'erreur moyenne absolue (MAE). Les résultats de prévision indiquent que les modèles AO-RNA et AO-SRV étaient les méthodes les plus justes pour prévoir les IPS à des échelles à court comme à long terme.

## **Acknowledgements**

First and foremost, I would like to thank my parents for all their support and encouragement. Without their constant encouragement it would not have been possible to finish this work.

My supervisor, Dr. Jan F. Adamowski, was fundamental to the completion of this thesis. His insights, encouragement and ability to keep me on track were instrumental throughout the duration of this work. He has always provided me with useful advice and comments on how to best improve my work. Thank you for your patience and encouragement.

Dr. Bahaa Khalil was also very important and helpful for the completion of this work. His help with the development of all the models was greatly needed. I am very thankful for the time you spent in helping me whenever I run into problems and always taking the time to help me improve my work.

I would also like to thank the Meteorological Services of Ethiopia. They provided all the data used for this study. I would like to thank this agency for being dedicated to the collection of climatic data.

The use of the OnlineSVR software for the development of the support vector regression models would not have been possible without Francesco Parrella, who developed the program and was very helpful on how to use it.

## Contributions of Authors

Chapters 3 and 4 of this thesis have been prepared for submissions as manuscripts to peer-reviewed journals. Chapter 3 is being prepared for submission to the Journal of Agricultural Management and Chapter 4 is being prepared for submission to the Journal of Hydrology. Part of Chapter 3 has been submitted to the Journal of Applied Computational Intelligence and Soft Computing and was accepted with revisions. Part of chapter 4 has been accepted to the Northeast Agricultural and Biological Engineering Conference - NABEC-CSBE/SCGAB Joint Meeting and Technical Conference on Ecological Engineering, which will be held in Orillia, Ontario from July 15 – 18, 2012.

The author of this thesis was responsible for gathering data, determining the step-by-step procedures involved in the methodology for data analysis, performing the data analysis, and preparing the two manuscripts for journal submissions. Dr. Jan Adamowski is the supervisor of this thesis; he provided the original idea for this thesis, and provided guidance and advice regarding many different aspects covered by this thesis. He also reviewed and edited this thesis and is a co-author of the two manuscripts of this thesis (chapters 3 and 4). Dr. Bahaa Khalil of the Department of Bioresource Engineering at McGill University is also a co-author of the two manuscripts (chapters 3 and 4). He provided statistical and technical guidance during the data analysis and helped review and edit the thesis. He also assisted in compiling the MATLAB codes used to analyze the data.

### **List of papers for journal submissions and conferences associated with this thesis:**

**Belayneh, A.,** Adamowski, J., Khalil, B., 2012. Short-term SPI drought forecasting in the Awash River Basin in Ethiopia using wavelet-neural networks and wavelet-support vector regression. To be submitted to the Journal of Agricultural Management.

**Belayneh, A., Adamowski, J., Khalil, B., 2012.** Long-term SPI drought forecasting in the Awash River Basin in Ethiopia using wavelet-neural network and wavelet-support vector regression models. To be submitted to the Journal of Hydrology .

**Belayneh, A., Adamowski, J., 2012.** Standard precipitation index drought forecasting using neural networks, wavelet neural networks and support vector regression. Accepted by the Journal of Applied Computational Intelligence and Soft Computing.

**Belayneh, A., Adamowski, J., Khalil, B., 2012.** Long-term SPI drought forecasting in the Awash River Basin in Ethiopia using wavelet-neural network and wavelet-support vector regression models. NABEC-CSBE/SCGAB Joint Meeting and Technical Conference on Ecological Engineering.

# Table of Contents

Abstract	2
Résumé	4
Acknowledgements	6
Contributions of Authors	7
Table of Contents	9
List of tables	11
List of figures	11
List of Acronyms	13
<b>1.1 Introduction</b>	15
<b>1.2 Objectives</b>	18
<b>1.3 Thesis Outline</b>	19
Chapter 2: Literature Review	20
<b>2 Overview of Drought</b>	20
<b>2.1 Drought Definitions and Forms</b>	20
<b>2.1.1 Types of Drought</b>	21
<b>2.2 Droughts as Natural Hazards</b>	22
<b>2.3 Drought Impacts</b>	23
<b>2.3.1 Impacts of Drought in Developed Regions</b>	24
<b>2.3.2 Impacts of Drought in Developing Regions</b>	25
<b>2.3.3 Major Causes of Drought in Ethiopia</b>	25
<b>2.4 Drought Monitoring</b>	27
<b>2.4.1 Drought Monitoring in Ethiopia</b>	28
<b>2.5 Overview of Drought Indices</b>	29
<b>2.5.1 Satellite Data Based Drought Indices</b>	30
<b>2.5.2 Vegetation Condition Index</b>	30
<b>2.5.3 Normalized Difference Vegetation Index (NDVI)</b>	30
<b>2.6 Data Driven Drought Indices</b>	31
<b>2.6.1 Percent of Normal</b>	32
<b>2.6.2 The Palmer Drought Severity Index (PDSI)</b>	32
<b>2.6.3 Crop Moisture Index</b>	33
<b>2.6.4 The Deciles Index</b>	33
<b>2.6.5 Standardized Precipitation Index (SPI)</b>	34
<b>2.7 Comparison of Drought Indices</b>	35
<b>2.7.1 Selection of Forecasting Index</b>	37
<b>2.8 Overview of the Types of Forecasting Models used in this Study</b>	38
<b>2.8.1 Short versus Long-term Drought Forecasting</b>	40
<b>2.8.2 Stochastic Models</b>	41
<b>2.8.3 Auto Regressive Moving Integrated Average Models (ARIMA)</b>	41
<b>2.8.4 Artificial Neural Networks</b>	43
<b>2.8.5 Feed Forward Neural Networks</b>	44
<b>2.8.6 Coupled Wavelet Transforms and ANNs</b>	48
<b>2.8.7 Coupled WA-ANNs for Drought Forecasting</b>	49
<b>2.8.8 Support Vector Regression (SVR) and Coupled Wavelet SVR Models</b>	50
Connecting Text to Chapter 3	52

Chapter 3	53
<b>3.1 Introduction</b>	53
<b>3.2 Theoretical Development</b>	58
<b>3.2.1 Development of SPI Series</b>	58
<b>3.2.2 Autoregressive Integrated Moving Average (ARIMA) Models</b>	62
<b>3.2.3 Artificial Neural Network Models</b>	63
<b>3.2.4 Support Vector Regression Models</b>	64
<b>3.2.5 Wavelet Transforms</b>	67
<b>3.3 Study Areas</b>	68
<b>3.3.1 Upper Awash Basin</b>	69
<b>3.3.2 Middle Awash Basin</b>	69
<b>3.3.3 Lower Awash Basin</b>	70
<b>3.3.4 Estimating Missing Rainfall</b>	70
<b>3.4. Methodology</b>	71
<b>3.4.1 SPI Calculation</b>	72
<b>3.4.2 ARIMA Model Development</b>	73
<b>3.4.3 Wavelet Transformation</b>	73
<b>3.4.4 ANN Models</b>	74
<b>3.4.5 WA-ANN Models</b>	75
<b>3.4.6 Support Vector Regression Models</b>	76
<b>3.4.7 WA-SVR Models</b>	76
<b>3.4.8 Performance Measures</b>	76
<b>3.5. Results and Discussion</b>	78
<b>3.5.1 SPI 1 forecasts</b>	79
<b>3.5.2 SPI 3 forecasts</b>	83
<b>3.5.3 Discussion</b>	86
<b>3.6 Conclusion</b>	89
<b>References</b>	90
Connecting Text to Chapter 4	97
<b>Chapter 4</b>	98
<b>4.1 Introduction</b>	98
<b>4.2 Theoretical Development</b>	101
<b>4.2.1 SPI</b>	101
<b>4.2.2 ARIMA Models</b>	102
<b>4.2.3 ANN Models</b>	103
<b>4.2.4 Support Vector Regression</b>	104
<b>4.2.5 Wavelet Transforms</b>	106
<b>4.3 Awash River Basin</b>	108
<b>4.3.1 Upper Awash Basin</b>	109
<b>4.3.2 Middle Awash Basin</b>	109
<b>4.3.3 Lower Awash Basin</b>	109
<b>4.3.4 Estimating Missing Rainfall</b>	110
<b>4.4 Methodology</b>	110
<b>4.4.1 SPI Calculation</b>	111
<b>4.4.2 Model Inputs</b>	112
<b>4.4.3 ARIMA Models</b>	112

4.4.4 ANN Models	113
4.4.5 SVR Models	114
4.4.6 Wavelet Decomposition	114
4.4.7 WA-ANN Models	115
4.4.8 WA-SVR Models	115
4.4.9 Performance Measures	116
4.5 Results and Discussion	117
4.5.1 SPI 12 Forecasts	118
4.5.2 SPI 24 Forecasts	119
4.5.3 Discussion	<b>Error! Bookmark not defined.</b>
4.6 Conclusion	127
References:	129
Chapter 5: Summary and Conclusions	134
5.1 Summary	134
5.2 Short-term Drought Forecasts	136
5.2.1 SPI 1 Forecasts	137
5.2.2 SPI 3 Forecasts	137
5.3 Long-term SPI Forecasts	137
5.3.1 SPI 12 and SPI 24 Forecasts	138
5.4 General Forecasting Observations	138
5.5 Contribution to Research	139
5.6 Future Research	140
5.7 Conclusions	141
References:	142

## List of tables

Table 1: Drought Classification based on SPI (McKee et al., 1993).	59
Table 2: Descriptive Statistics of the Awash River Basin	71
Table 3: Model Inputs for the best data driven models (L=monthly forecast lead time)	79
Table 4.1: The best ARIMA, ANN and SVR models for 1 and 3 month forecasts of SPI 1.	80
Table 5: The best WA-ANN and WA-SVR models for 1 and 3 month forecasts of SPI 1	81
Table 6: The best ARIMA, ANN and SVR models for 1 and 3 month forecasts of SPI 3	84
Table 7: The best WA-ANN and WA-SVR models for 1 and 3 month forecasts of SPI 3.	85
Table 8: Descriptive Statistics for Awash Basin.	110
Table 9: Model Inputs for the best data driven models (L = forecast lead time in months)	118
Table 10: The best ARIMA, ANN and SVR models for 6 and 12 month forecasts of SPI 12.	120
Table 11: The best WA-ANN and WA-SVR models for 6 and 12 month forecasts of SPI 12	121
Table 12: The best ARIMA, ANN and SVR models for 6 and 12 month forecasts of SPI 24.	122
Table 13: The best WA-ANN and WA-SVR models for 6 and 12 month forecasts of SPI 24.	123

## List of figures

Figure 1: Awash River Basin (Source: Edossa et al., 2010).	70
Figure 2: Autocorrelation plot for the selection of candidate SPI 1 models.	82
Figure 3: Autocorrelation plot for the selection of candidate SPI 3 models.	82
Figure 4: SPI 3 forecast results for the best WA-ANN model at the Bati station for 1 month lead time.	87
Figure 5: SPI 3 forecast results for the best WA-SVR model at the Bati Station for 1 month lead time.	88
Figure 6: Awash River Basin (Source: Edossa et al., 2010).	109

<b>Figure 7: SPI 24 forecast results for the best WA-ANN model at the Bati station for 6 months lead time.</b>	<b>125</b>
<b>Figure 8: SPI 12 forecast results for the best WA-ANN model at the Dubti Station for 6 months lead time.</b>	<b>126</b>
<b>Figure 9: SPI 24 forecast results for the best WA-ANN model at the Dubti Station for 6 months lead time.</b>	<b>126</b>

## List of Acronyms

ANFIS	Artificial neuro-fuzzy inference system
ANN	Artificial neural network
AR	Autoregressive
ARMA	Autoregressive moving average
ARIMA	Autoregressive integrated moving average
BPN	Back-propagation network
CMI	Crop Moisture Index
CWT	Continuous wavelet transform
DMSNN	Direct multi-step neural network
DWT	Discrete wavelet transform
EB	European Blocking
EDI	Effective Drought Index
EU	European Union
HSNNDA	Hybrid stochastic neural network direct approach
HSNNRA	Hybrid stochastic neural network recursive approach
LM	Levenberg Marquardt
MA	Moving average
MAE	Mean absolute error
MLP	Multi-layer perceptron
MLR	Multiple linear regression
NAO	North Atlantic Oscillation
NDVI	Normalized Vegetation Index
NIR	Near Infrared
NMSA	National Meteorological Services Agency
PDSI	Palmer drought severity index
PERS	Persistence index
PHDI	Palmer hydrological drought index
PN	Percent of Normal
RBF	Radial Basis Function
RED	Red bands
RMSE	Root mean square error
RMSNN	Recursive multi-step neural network
SPI	Standard Precipitation Index
SSE	Sum of squared errors
SVC	Support vector classification
SVM	Support vector machines
SVR	Support vector regression
VCI	Vegetation condition index
WA	Wavelet analysis
WA-ANN	Wavelet neural networks
WA-SVR	Wavelet support vector regression

## List of Mathematical Symbols

$g(x)$  = gamma distribution

$\alpha$  = the shape parameter

$\beta$  = scale parameter

$x$  = amount of precipitation in mm

$\Gamma(\alpha)$  = value taken by gamma function

$G(x)$  = cumulative probability that a certain amount of rain has been observed for a given month and for a specific time scale

$q$  = probability of no precipitation

$H(x)$  = the cumulative probability of precipitation observed

$z_t$  = the observed time series

$\phi(B)$  = polynomial of order  $p$

$\theta(B)$  = polynomial of order  $q$

$p$  = order of non-seasonal auto-regression

$q$  = order of non-seasonal moving average

$d$  = number of regular differencing

$N$  = the number of samples

$m$  = the number of hidden neurons

$n$  = number of input neurons

$t$  = time step

$l$  = loss function

$R_{emp}$  = empirical risk function

$R_{reg}$  = regular risk function

$\left\| \overset{\rightarrow}{W} \right\|$  = regression vector

$K(x, x_i)$  = Kernel function

$\Psi$  = wavelet function

$s$  = wavelet scale parameter

$\tau$  = the wavelet translation

$*$  = the complex conjugate

$J$  = integer controlling wavelet scale

$K$  = integer controlling wavelet translation

$s_o$  = fixed dilation step

$h$  = low pass filter

$c_i(k)$  = the approximation of the wavelet signal

$X_0$  = original SPI values

$X_n$  = normalized SPI values

# **Chapter 1: Introduction**

## **1.1 Introduction**

Throughout history, most human settlements, however small or prosperous, have had to contend with drought. The 20<sup>th</sup> century has seen its share of droughts (Glantz, 1994). The early 1970s were a turning point in global awareness about the need to better understand the drought phenomenon, its causes and consequences, and to develop mitigation strategies to cope with its consequences (Glantz, 1994). The occurrence of severe droughts throughout Africa and India, North America, China, the Soviet Union, Australia, and Western Europe in the 1980s once again underscored the vulnerability of developed and developing societies to drought (Glantz, 1994). Even today, with the advancement of technology and instant communication, agricultural and livestock production in developed as well as developing countries can be sharply reduced by drought related stresses. There is little surprise when drought related crop failures occur in developing countries, yet developed countries such as the United States and Canada have not been able to prevent their agricultural systems from also being affected by drought. Thus, no country can claim to be immune from the impacts of drought.

Droughts often become highly visible when they are associated, rightly or wrongly, with famine. Famine is an acute shortage of food. Prolonged drought is but one of many possible causes; others include overproduction, poverty, the ravages of war, and destruction of crops and grazing by fire, locusts, other pests and diseases (Whitmore, 2005). Yet, for the most part droughts can occur without precipitating a famine. Indeed famines have frequently taken place in the absence of drought conditions (Glantz, 1994). Often, drought, which has been described as a ‘creeping’ phenomenon, combines with other societal and environmental conditions to produce famine-like conditions. Drought has also been blamed for environmental degradation and desertification, prompting mass migration of people and internal unrest. While drought may play an important factor in each of the aforementioned processes, it often proves to have been one of many intervening factors (Whitmore, 2005).

The most popular perception of a drought is as a meteorological phenomenon, characterized by a lack of rainfall compared with an expected amount for a given time period. For some, a drought exists when rainfall is 75% of the long-term average for a given period, while others might consider it to occur at 60% or 50% of the long-term average (Glantz, 1994). Some researchers have suggested that drought should be defined in terms of societal factors. They have argued that, before a reduction in precipitation becomes a concern to society, it usually adversely affects the established economy of the region (Sanford, 1978). Definitions of what constitutes a drought will vary depending on expectations about moisture needs for specific human activities within a given area. Thus, there can be agricultural drought and hydrological drought, as well as meteorological drought, which may lead to disagreements regarding whether a drought has in fact occurred.

In general, natural disasters have disproportionate impacts on the Gross Domestic Product (GDP) of developing countries as compared with that of developed countries (UN, 2009). Due to the relative lack of infrastructure and ability to cope with natural disasters, sub-Saharan countries are especially vulnerable to the effects of drought. Drought is not the sole cause of famine, yet in sub-Saharan countries a prolonged period of drought coupled with other societal processes can lead to a famine (Sanford, 1978). Indeed, hundreds of millions of people in the world today do not enjoy food security. They do not have “access at all times to enough food for an active and healthy life” (Boken, 2005). Many of these individuals are among the quarter-billion people living in the climatically vulnerable dry-lands of sub-Saharan Africa (Boken, 2005).

An example of a sub-Saharan country that is highly vulnerable to the impacts of drought is Ethiopia, which will be the focus of this research study. Ethiopia is a landlocked country on the horn of Africa. Covering an area of approximately 1.14 million km<sup>2</sup>, Ethiopia (3°24` and 14°53` North; and 32°42` and 48°12` East) is bordered by Sudan to the west, Somalia and Djibouti to the east, Eritrea to the north and Kenya to the south. It is a country that is periodically affected by droughts and famine. In some years almost the entire country is subjected to drought (NMSA, 1996). Ethiopia’s weather and climate are extremely variable both temporally and spatially. The heavy dependence of the

population on rain-fed agriculture has made the people and the country's economy extremely vulnerable to the impacts of droughts. The drought of the early 1970s was responsible for 100,000 deaths in the Sahel and 200,000 deaths in Ethiopia (Boken, 2005) and was soon followed by another drought from 1983-85 that was responsible for between 400,000 and 1 million deaths (Boken, 2005).

Ethiopia's heavy reliance on agriculture, combined with its susceptibility to frequent climate extremes, has left it in a precarious position (Edossa et al., 2010). 85% of Ethiopia's population is engaged in agriculture (Edossa et al., 2010). Agriculture supplies a significant proportion of the raw materials for the agro-industries, and accounts for 52% of the gross product and 90% of the export earnings (Mersha and Boken, 2005). The dependency of most of the population on rain-fed agriculture makes the country's economy vulnerable to the effects of weather and climate.

Drought records in Ethiopia span more than 2000 years, but are mostly qualitative in nature. Reports from 1950 onwards are well documented and supported by scientific data (Mersha and Boken, 2005). Between 1950 and 1988 there were 38 droughts in Ethiopia. The 1957-58 drought and its related impacts led to famine in Tigray province and the 1972-73 famine caused by drought claimed 200,000 lives in Wollo province. Although the famine caused by the drought of 1984-85 remains well known to the world community, less serious, but nonetheless significant droughts occurred in the years 1987, 1988, 1991-92, 1993-94, 1999, and 2002 (Edossa et al., 2010).

Given the adverse consequences of droughts, and the vulnerability of Ethiopia, the need to predict drought is great because severe and prolonged droughts have multidimensional impacts on the progress and development of the country's economy as well as potentially adverse effects on the environment and society as a whole. This study will attempt to forecast drought in Ethiopia on both short and long-term time scales. Data driven models will be used to forecast future drought events. A suitable drought index for the Awash River Basin within Ethiopia will be computed. The Awash River Basin will further be separated into three sub-basins to ensure the methods for drought forecasting are effective in regions with differing physical characteristics. The data driven models to be used are

traditional stochastic models for time series forecasting (namely Box-Jenkins autoregressive integrated moving average models), and more recent models (namely artificial neural networks, artificial neural networks pre-processed with wavelet transforms, support vector regression, and support vector regression pre-processed with wavelet transforms).

The Awash River is a transboundary river whose riparians include Ethiopia, Djibouti and Somalia with 92.74% of the river basin area in Ethiopia (Edossa et al., 2010). The Awash River basin has been divided into three sub-basins: the Upper basin, Middle basin and Lower basin on the basis of various factors such as location, altitude, climate, topography and agricultural development. The Upper Awash Basin has a unimodal rainfall distribution and a temperate climate, while both the Middle and Lower Awash Basins have a bimodal rainfall distribution with semi-arid climates. Given the differences in climatology and rainfall distribution the Awash Basin was analysed as three separate sub-basins to determine whether the climate of a given sub-basin had an impact on drought forecasts or whether drought forecasts were more effective in a given climatology.

## **1.2 Objectives**

The primary objective of this research is to determine the most accurate data driven method to forecast the Standard Precipitation Index (SPI) on both short and long-term time scales to effectively forecast drought in the Awash River Basin of Ethiopia. This involves the proposal and testing of a new method of drought forecasting based on support vector regression and the coupling of wavelet transforms with support vector regression. The forecasting methods that will be compared include traditional times series forecasting methods such as ARIMA models as well as ANNs and ANNs that have their data pre-processed using wavelet transforms (WA-ANN). In addition, time series forecasting using support vector regression (SVR) and support vector regression using data pre-processed with wavelet transforms (WA-SVR) will be compared, as this has not been explored in the literature to date. Both short and long-term forecasts with the various methods will be compared to assess which method is the most effective

forecasting tool for a given time scale in the three selected sub-basins of the Awash River.

The specific objectives of this research are:

- To generate SPI values from the raw monthly precipitation data for the three sub-basins
- To evaluate all five data driven model types for short-term drought forecasting of SPI values
- To evaluate all five data driven model types for long-term drought forecasting of SPI values

### **1.3 Thesis Outline**

This thesis has been written as a series of chapters. Chapter 1 is an introduction of the research topic and objectives. Chapter 2 is a literature review containing an overview of drought concepts and definitions that will define drought in its various forms and place drought in the context of natural hazards. Some of the impacts of droughts will be detailed, with emphasis on why the impacts of drought are different from other natural hazards, and the need for an effective drought monitoring and forecasting system will be discussed. Chapter 2 will also discuss drought monitoring, its importance and current monitoring strategies within Ethiopia. An overview of drought indices will be given and the most suitable drought index will be selected for Ethiopia. An overview and description of the forecast models to be used for both short and long-term drought will be given and the reasoning behind the distinction between these two forecast lengths will also be explained. Chapter 3 describes the theoretical development and methodology used to forecast SPI 1 and SPI 3 for lead times of 1 and 3 months which are representative of short-term drought forecasts. Chapter 4 describes the theoretical development and methodology used to forecast SPI 12 and SPI 24 for lead times of 6 and 12 months, which are representative of long-term drought forecasts. Chapter 5 provides some overall conclusions and recommendations for future research.

## **Chapter 2: Literature Review**

### **2 Overview of Drought**

#### **2.1 Drought Definitions and Forms**

Drought is a normal and recurrent feature of climate. It occurs in all climatic zones and its characteristics vary significantly from region to region. Unfortunately, even though drought is a common and recurring phenomenon, it lacks a single, absolute definition. While drought affects virtually all sectors of an economy, it does so in such a variety of ways that each sector is apt to have its own concept of drought, and its own criteria for gauging the severity of drought (Whitmore, 2005). In fact, within any one sector there may be many conflicting criteria. In the agricultural sector, a hot dry spell may constitute a damaging drought for a grain farmer but be just what a fruit farmer requires to ripen his or her fruit (Whitmore, 2005). This example shows that the concept of drought is relative rather than absolute.

Defining drought is therefore difficult (Redmond, 2002). There are more than 150 definitions of drought in the literature (Boken, 2007). Often, the difference between an estimated water demand and an expected water supply in a region becomes the basis to define a drought for the region. According to the Glossary of Meteorology (1957), drought is “a period of abnormally dry weather sufficiently prolonged for the lack of water to cause serious hydrological imbalance in the affected area. Drought is a relative term; therefore any discussions in terms of a precipitation deficit must refer to the particular precipitation-related activity that is under discussion”. This definition implies that drought cannot be viewed solely as a physical phenomenon, rather it should be considered in relation to its impacts on society. The American Meteorological Society (AMS) (1997) separates drought into four categories: meteorological, agricultural, hydrological and socioeconomic. Each type of drought has specific characteristics and affects different aspects of society.

Meteorological drought is usually defined as a deficit in precipitation over a period of time, while agricultural drought occurs when there is not enough soil moisture to meet

the needs of a particular crop at a particular time. Agricultural drought occurs after a meteorological drought because agriculture is usually the first economic sector affected by drought. Hydrologic drought refers to deficiencies in surface and groundwater resources due to lack of precipitation over an extended period of time. Finally, socio-economic drought is associated with the failure of water resource systems to meet water demands, thus associating drought with the supply and demand of a specific economic good (AMS, 1997). Socio-economic drought occurs when the demand for an economic good exceeds the water supply (Mishra and Singh, 2010). Drought produces several impacts that affect many sectors of the economy. This is because water is integral in the production and distribution of almost all goods and services (Bordi and Sutera, 2007).

### **2.1.1 Types of Drought**

Some droughts are regular and predictable, as in regions where a pronounced rainy season each year is followed by a dry season. These seasonal droughts are a fairly regular, normal feature of the climate, to which local ecosystems and farming practices have adapted over time. At the other end of the spectrum are sporadic and sometimes prolonged and acute droughts (Whitmore, 2005). The following section will list and briefly describe the main forms of drought.

#### Seasonal Drought

Regular seasonal drought is a common, well-defined climatic feature especially for the mid-latitudes. Sometimes the bulk of the rain falls in the summer, followed by a virtually dry winter. In a Mediterranean type of climate the opposite occurs, where winter is the rainy season, with the summers tending to be warm and dry.

#### Irregular Drought

Irregular droughts are synonymous with intermittent, erratic, sporadic and unpredictable droughts. They result from the vagaries of rainfall, and are amongst the most damaging and difficult droughts to handle. Even though these droughts are irregular, they are still a normal, integral part of a region's climate and will continue to occur. Irregular droughts often occur in sub-humid regions (Whitmore, 2005).

## Partial Drought

Partial droughts are another damaging form of drought and are very difficult to detect. While the soil moisture deficit is not sufficiently severe to cause the symptoms of drought it is nevertheless sufficient to reduce the uptake of nutrients from the soil. Thus, crop growth and yield may be well below optimum levels.

## **2.2 Droughts as Natural Hazards**

A natural hazard is defined as a threat of a naturally occurring event that will have a negative effect on people or the environment (Mishra and Singh, 2010). Drought is a type of natural hazard that is further aggravated by the growing global water demand (Mishra and Singh, 2010). Occurrences of drought are dependent on atmospheric conditions as well as the hydrologic processes which feed moisture to the atmosphere. Once dry hydrologic conditions are established the positive feedback mechanism of droughts set in, where the moisture depletion from upper soil layers lowers evapotranspiration rates, which in turn, lowers the relative humidity of the atmosphere. A lower relative humidity corresponds to a lower chance of precipitation. Only disturbances which carry enough moisture from outside the dry region will be able to produce sufficient rainfall to end drought conditions (Mishra and Singh, 2010).

Droughts rank first among all natural hazards when measured in terms of the number of people affected (Byun and Willhite, 1999). Droughts differ from other natural hazards in several ways. First, the onset and the end of a drought are difficult to determine. The impacts of a drought increase slowly and often accumulate over a considerable period and may linger years after the end of the drought. Second, defining a drought is difficult which may lead to confusion due to the lack of a universal definition of drought. Third, unlike other natural hazards the impacts of drought are non-structural and spread over large geographical areas, which results in difficulty in the quantification of impact and for the provision of relief (Mishra and Singh, 2010). Human activities can directly trigger a drought unlike other natural hazards, with exacerbating factors such as over-farming, excessive irrigation, deforestation and overuse of available water resources.

Droughts produce a complex web of impacts that span many sectors of a society, including the economic sector and may reach well beyond the area experiencing drought. Half the earth's terrestrial surfaces are susceptible to droughts, which makes them a widespread phenomenon (Kogan, 1997). Almost all major agricultural lands are located in areas susceptible to drought (Mishra and Singh, 2010).

### **2.3 Drought Impacts**

In recent years, large scale intensive droughts have been observed on all continents, affecting large areas in Europe, Africa, Asia, Australia, South America, Central America, and North America. The increased attention on droughts is a direct consequence of the high economic and social costs incurred as a result of droughts. The main impacts of drought can be distinguished in three categories: i) economic; damage to agricultural production, economic damage to forest production, economic damage to industries connected to agricultural production, unemployment caused by production decrease and economic damage to reduced navigability of streams; ii) environmental; lack of feed and drinking water, increase of salt concentration (in streams and irrigated areas), loss in natural and artificial lakes, damages to river life, damage to air quality and damage to landscape quality; iii) social; inconveniences due to water system rationing, risks for health connected with increase of pollution concentration and discontinuous water system, inequity in drought impacts and mitigation measures distribution, risks on public security due to more frequent fires and abandonment of activities and in extreme cases of emigration (Rossi et al., 2007).

The impacts of drought differ significantly geographically. The following section will describe and differentiate between the impacts of drought in developed and developing regions. Impacts of drought in North America and Europe will be compared and contrasted to the impacts of drought in Africa.

### **2.3.1 Impacts of Drought in Developed Regions**

During the last two decades, the impacts of droughts in the United States have increased significantly with an increased number of droughts as well as an increase in their severity (Mishra and Singh, 2010). For example, a 1988 drought had a significant impact on the US economy (approximately \$40 billion). Nearly 10% of the total land area of the United States experienced either severe or extreme droughts at any given time during the 20<sup>th</sup> century. From 1980 to 2003 in the United States, drought accounted for 10 of the 58 weather-related disasters (Ross and Lott, 2003). Droughts accounted for \$144 billion of the estimated \$349 billion total cost of all weather-related disasters in the US (Ross and Lott, 2003). Hence, in economic terms alone droughts are the costliest natural disasters in the United States.

In Canada, most regions have experienced droughts, however, the Canadian Prairies are more susceptible mainly due to the high variability of precipitation in both time and space in the region (Environment Canada, 2004). Six of the ten costliest disasters in Canadian history have been droughts (Environment Canada, 2004). During the past two centuries, at least 40 long-duration droughts occurred in Western Canada. In the southern regions of Alberta, Saskatchewan, and Manitoba, multi-year droughts were observed in the 1890s, 1930s, and 1980s. Droughts in Eastern Canada are usually shorter, smaller in area, less frequent, and less intense; nonetheless, some major droughts occurred during the 20th century. Over much of the Prairies, several consecutive seasons of below average precipitation have led to one of the most severe prairie droughts on record, devastating many water dependent activities in 2001 and 2002 (Environment Canada, 2004). As well, in 2001 the aggregate level of the Great Lakes plunged to their lowest points in more than 30 years, with Lake Superior and Lake Huron displaying near record.

In Europe, major drought events have been observed over the last 30 years. Most notably a drought in 1976 affected the areas of Northern and Western Europe, while a drought in 1989 and 1991 affected most of Europe. More recently, in 2003 a prolonged drought affected most of Europe. The most serious drought in the Iberian Peninsula in 60 years occurred in 2005, reducing overall EU cereal yields by an estimated 10% (United Nations

Environment Programme, 2006). Since 1991, the yearly average economic impact of droughts in Europe has been €5.3 billion, with the economic damage of the 2003 drought in Europe amounting to at least €8.7 billion (Mishra and Singh, 2010).

### **2.3.2 Impacts of Drought in Developing Regions**

Since the late 1960s, the Sahel, a semiarid region in West Africa between the Sahara desert and the Guinea coast rainforest, has experienced a drought of unprecedented severity (Mishra and Singh, 2010). The drought has had a devastating impact on this ecologically vulnerable region and was a major impetus for the establishment of the United Nations Convention on Combating Desertification and Drought (Zeng, 2003). While the frequency of droughts in the region is thought to have increased from the end of the 19<sup>th</sup> century, three long droughts have had dramatic environmental and societal effects upon the Sahel nations. Famine followed severe droughts in the 1910s, the 1940s, the 1960s, the 1970s and 1980s although a partial recovery occurred from 1975 to 1980. While at least one particularly severe drought has been confirmed in each century since the 1600s, the frequency and severity of the recent Sahelian drought stands out. Famine and dislocation on a massive scale - from 1968 to 1974 and again in the early and mid 1980s - was blamed on two spikes in the severity of the 1960–1980s drought periods (Mishra and Singh, 2010).

### **2.3.3 Major Causes of Drought in Ethiopia**

The purpose of this study, as mentioned earlier, is to forecast short term and long term drought in Ethiopia. Ethiopia's vulnerability to drought and the past consequences of several droughts has been briefly outlined in the previous chapter. The following section will briefly describe the major causes of drought in Ethiopia. The major causes of drought in the context of Ethiopia are atmospheric circulation, method of cultivation, selection of cropping pattern, inappropriate land use and deforestation. The following paragraphs will give a brief description of how each of these factors contributes to drought in Ethiopia.

## Atmospheric Circulation

Droughts in Ethiopia occur mainly due to rainfall variability (Mersha and Boken, 2005). Seasonal and annual rainfall variations in Ethiopia are associated with the macro-scale pressure systems and monsoon flows related to the changes in the pressure systems. If any one of the rain-producing pressure systems weakens, in any given season, there will be abnormal rainfall behaviour during the season. A study by Engida (1999) indicates that the area with stable rainfall activity has decreased, while the area with highly variable rainfall has substantially increased. As a result the frequency of droughts has increased.

## Soil Erosion

Most Ethiopian farmers are still continuing to use unsustainable and inefficient methods of cultivation resulting in the erosion of topsoil by the wind and rains. Ethiopian farmers have failed to adapt, over the past century, to innovation in design, materials, or application of technology (irrigation, mechanization, agronomic techniques). The basic ox-drawn, single-tine plough has remained the basis of production throughout the Ethiopian highlands. Due to soil erosion, water does not infiltrate into the soil. Instead it is wasted as runoff (Mersha and Boken, 2005). This results in a depletion of soil moisture and soil nutrients. The annual soil loss due to erosion is estimated at 1.9-3.5 billion tons (Mersha and Boken, 2005). Furthermore, the amount of soil loss on cultivated land is between 4 and 10 times greater than the amount of soil loss on grazing land (Mersha and Boken, 2005).

## Deforestation

Deforestation is another important contributor to drought in Ethiopia. Historical sources indicate that dense forests might have once covered 35-40% of Ethiopia's total area. Currently forests cover approximately 2.7% of the country's area (Mersha and Boken, 2005). The main driving forces behind deforestation are the expansion of agricultural land, unrestrained exploitation of forest resources, overgrazing and the establishment of new settlements into forested land coupled with increasing population pressure (Mersha and Boken, 2005).

## Overgrazing

Ethiopia's livestock population is the largest in Africa, with 30,000,000 cattle, 24,000,000 sheep, 18,000,000 goats, 7,000,000 horses, 1,000,000 camels and 53,000,000 poultry (FAOSTAT, 2006). About 70 percent of the cattle and sheep and 30 percent of the goats are in the highlands above 1,500 metres. Ethiopian rangelands account for almost 90% of the desertified lands (Mabbutt, 1984). Overgrazing of these rangelands by livestock has caused degradation of vegetation and the compaction and erosion of the soil by both wind and water.

## Land Ownership

Another important factor contributing to drought recurrence is the problem of land ownership. Communal ownership is believed to lead to mismanagement, particularly, overgrazing and inefficient removal of wood for fuel (Mersha and Boken, 2005). The ability to transfer land sales and leasing also allows lands to be used by farmers who earn the highest return from it through mobility of draft animals, farm implements and labour. The system of land tenure in Ethiopia has had varying and significant impacts on land management. From a historical perspective, it is believed that Ethiopia's small holders are uncertain about the security of rights to the land. This has resulted in cultivation for short term needs rather than long term yield.

## **2.4 Drought Monitoring**

To minimize the impacts of drought an effective and timely monitoring system is required. Effective monitoring of droughts helps develop an early warning system. An objective evaluation of drought condition in a particular area is the first step for planning water resources in order to prevent and mitigate the impacts of future occurrences of drought. In order to objectively evaluate droughts, several indices have been developed to evaluate the water supply deficit in relation to the time duration of precipitation shortage (Bordi and Sutera, 2007). Usually these drought indices are based on the amount of precipitation and they measure the deviation of actual precipitation from a historically established norm. Some of these drought indices take into account other additional

climatological indices such as temperature, evapotranspiration or soil moisture. Drought indices developed over short-term time scales are useful in monitoring meteorological drought and agricultural drought. Likewise, indices developed over long-term time scales are useful for monitoring hydrologic and socioeconomic drought (Cacciamani et al., 2007). An overview and comparison of drought indices is given in section 2.5.

An important aspect of drought monitoring and the development of an early warning system is the ability to effectively forecast future drought events. Forecasting future dry events in a region is very important for finding sustainable solutions to water management and risk assessment of drought occurrences (Bordi and Sutera, 2007). Drought forecasting techniques vary from the use of stochastic methods to the use of satellite data imagery. Recently neural networks have become increasingly popular tools for drought forecasting. The section on models will describe different forecasting tools and the tools used in this study.

#### **2.4.1 Drought Monitoring in Ethiopia**

As drought is a recurrent phenomenon in Ethiopia several monitoring and mitigation strategies exist. The National Meteorological Services Agency (NMSA) of Ethiopia regularly produces a 10 day bulletin that gives an analysis of rainfall based on the long term average or normal. This bulletin is then circulated to a wide range of users, ranging from local development agents to decision makers at a national level. Rainfall analysis is both qualitative and quantitative and includes reports concerning the onset of the rainy season, which is reported as early, normal or late. Rainfall distribution is expressed as: deficient or excess, erratic or even. Rainfall is compared with the normal by computing the percentage deviation. In addition to rainfall analysis, the normalized vegetation index (NDVI) is provided, which is a satellite data driven index widely used to monitor vegetation and drought conditions. The NMSA produces a regular 10-day bulletin regarding NDVI variation that compares the current vegetation condition with normal or conditions of the previous year. The NMSA also uses the NDVI to produce monthly and seasonal precipitation forecasts.

As mentioned earlier, an important part of integrating droughts into water resource management is the development of an early warning system. Due to a slow evolution in time, drought is often a phenomenon whose consequences take a significant amount of time with respect to its inception to be perceived by the socio-economic sector (Cancelliere et al., 2007). In light of this feature, an effective mitigation of the most adverse impacts of drought is possible, more than in the case of other extreme hydrological events, provided a drought monitoring system is able to promptly warn of the onset of a drought (Rossi, 2004). An accurate selection of indices for drought identification, providing a synthetic and objective description of drought conditions, represents a key point for the implementation of an efficient drought warning system (Cancelliere et al., 2007). Most drought indices were developed with the intent to monitor current drought conditions although some of them can be used to forecast the possible evolution of an ongoing drought. The following section will provide an overview of some of the drought indices commonly used and compare their strengths and weaknesses as they relate to forecasting drought in Ethiopia.

## **2.5 Overview of Drought Indices**

A drought index is a prime variable for assessing the effect of a drought and defining different drought parameters, which include intensity, duration, severity and spatial extent (Mishra and Singh, 2010). It should be noted that a drought variable should be able to quantify the drought for different time scales for which a long time series is essential. The most commonly used time scale for drought analysis is a year, followed by a month (Mishra and Singh, 2010). The yearly time scale can be used to abstract information on the regional behaviour of droughts, while the monthly time scale is more appropriate for monitoring the effects of drought in situations related to agriculture, water supply and groundwater abstractions. A time series of drought indices provides a framework for evaluating drought parameters of interest (Mishra and Singh, 2010).

Several drought indices have been developed to quantify a drought, each having its own strength and weakness. The most common drought indices include the Palmer drought severity index (PDSI), the commonly used percent of normal (PN), rainfall anomaly

index (RAI), deciles, crop moisture index (CMI), Bhalme and Mooly drought index (BMDI), surface water supply index (SWSI), national rainfall index (NRI), standardized precipitation index (SPI), and reclamation drought index (RDI). Drought indices can be classified into two groups, satellite data driven drought indices and data driven drought indices.

### **2.5.1 Satellite Data Based Drought Indices**

Since the 1970s, several studies have used satellite land observation data to monitor a variety of dynamic land surface processes. Satellite remote sensing provides a synoptic view of the land and a spatial context for measuring drought impacts which have proved to be a valuable source of timely, spatially continuous data with improved information on monitoring vegetation dynamics over large areas. The following section will briefly describe some of the satellite data driven drought indices used for the purposes of drought monitoring.

### **2.5.2 Vegetation Condition Index**

The Vegetation Condition Index (VCI) is computed from satellite advanced very high resolution radiometer (AVHRR) radiance data adjusted for land, climate, ecology and weather conditions. The VCI shows promise when used for drought detection and tracking (Kogan, 1997). The VCI allows detection of drought and measurement of the time of its onset and its intensity, duration and impact on vegetation (Mishra and Singh, 2010). However, since the VCI is based on vegetation, it is primarily useful for the summer growing season only.

### **2.5.3 Normalized Difference Vegetation Index (NDVI)**

The Normalized Difference Vegetation Index (NDVI) is a satellite data driven index widely used to monitor vegetation and drought conditions (Mersha and Boken, 2005). The NDVI isolates green vegetation from its background using Landsat MSS digital data. It is expressed as the difference between the near-infrared (NIR) and red bands normalized by their sum ( $NDVI = (NIR - RED) / (NIR + RED)$ ). The NDVI is the most commonly used vegetation index because it has a desirable measurement scale ranging

from -1 to 1 with zero being the approximate value for no vegetation. Negative values represent non-vegetative surfaces, while values closer to 1 are representative of dense vegetation (Anyamba et al., 2005). The NDVI also has the ability to reduce external noise factors such as topographical effects and sun-angle variations.

The NDVI is one of the drought monitoring systems used by the NMSA of Ethiopia. The NMSA produces a regular 10-day bulletin regarding NDVI variation that compares the current vegetation condition with normal or last-year conditions (Mersha and Boken, 2005). The NMSA also provides monthly and seasonal forecasts using the NDVI. The bulletin is distributed to higher officials and NGOs engaged in early warning activities (Mersha and Boken, 2005). The models and forecasts developed in this study of SPI 1, SPI 3, SPI 12 and SPI 24 for both short and long-term lead times can be used by the NMSA to augment what is already being done with their NDVI forecasts. SPI 1 and SPI 3 are representative of short-term drought conditions and can represent agricultural drought. Effective forecasts of these two indices with warning times of 1 and 3 months will be a useful tool for agricultural systems and enable farmers in Ethiopia to modify their practices in preparation for an oncoming drought. SPI 12 and SPI 24 are representative of long-term drought conditions and represent hydrological drought conditions. Effective forecasts of SPI 12 and SPI 24, with warning times of 6 and 12 months, will augment the monthly and seasonal forecasts of the NMSA and give water resource managers in Ethiopia advanced warning regarding the onset of a drought, thereby helping them effectively plan ahead.

## **2.6 Data Driven Drought Indices**

Data driven drought indices use precipitation, either as the sole input or in combination with other meteorological elements. A combination of meteorological variables could be precipitation and temperature or precipitation and soil moisture. The following section discusses commonly used data driven drought indices, their strengths, and their limitations and offers a comparison between the different indices.

### **2.6.1 Percent of Normal**

The Percent of Normal (PN) is a drought index that requires precipitation as its only input, usually over a minimum 30 year historical period. It is calculated by dividing actual precipitation by normal precipitation, typically considered to be a 30-year mean, and multiplying this by 100% (Bordi and Sutera, 2007). The Percent of Normal can be computed for a variety of time scales. Usually these time scales range from a single month to a group of months representing a particular season, to an annual or wet year (Bordi and Sutera, 2007). Normal precipitation is considered to be 100% for a specific location.

The Percent of Normal is limited as a tool for a comparison of climatic conditions of different areas. The reason for this limitation is precipitation on monthly or seasonal scales does not have a normal distribution. As a result the mean precipitation is not the same as the median precipitation. The median precipitation is the value exceeded by 50% of the precipitation in a long-term climate record. This limitation of the Percent of Normal, with respect to comparing different climatic regions, has been overcome by other standardized drought indices such as the PDSI and SPI.

### **2.6.2 The Palmer Drought Severity Index (PDSI)**

The Palmer Drought Severity Index (PDSI) was developed by Palmer (1965) and was the first comprehensive effort to assess the total moisture status of a region (Mishra and Singh, 2010). The index is based on the water balance, using a concept of supply and demand over a two-layer soil model. The basis of the PDSI is the difference between the amount of precipitation required to retain a normal water balance level and the actual precipitation (Bordi and Sutera, 2007). Several coefficients are calculated which define local hydrological norms related to temperature and precipitation. The calculation of the coefficients above depends heavily on the soil water capacity of the underlying layer (Bordi and Sutera, 2007). Since the inception of the PDSI, modified versions such as the Palmer Hydrologic Drought Index (PHDI) have evolved. The PHDI is commonly used for water supply monitoring.

There are several limitations of the PDSI, which include an inherent time scale making PDSI more suitable for agricultural impacts and less so for hydrologic droughts. The PDSI assumes that all precipitation is rain, making values obtained during winter months and high elevations often questionable. The PDSI also assumes that runoff only occurs after all soil layers have been saturated, leading to an underestimation of runoff (Mishra and Singh, 2010). In addition, the PDSI can be slow respond to developing and diminishing droughts (Mishra and Singh, 2010).

### **2.6.3 Crop Moisture Index**

The crop moisture index (CMI) was developed by Palmer (1968) to evaluate short term moisture conditions across major crop producing regions. Computation of CMI involves the use of weekly values of temperature and precipitation to compute a simple moisture budget. The CMI responds rapidly to changing conditions and this rapid response to changing short-term conditions may provide misleading information about long-term conditions.

Another limitation of the CMI is its sensitivity to potential evapotranspiration. An increase in CMI may occur with an increase in potential evapotranspiration. An increase in the CMI value indicates wetter moisture conditions; however there is no natural case where an increase in potential evapotranspiration would produce wetter moisture conditions. The second limitation of the CMI is that it is not a long term drought monitoring tool, due to its rapid response to changing short-term conditions. CMI is best suited for measuring agricultural drought during warm seasons (Heim, 2002).

### **2.6.4 The Deciles Index**

The deciles index was developed by Gibbs and Maher (1967) and has widespread use in Australia (Morid et al., 2006). In the computation of the deciles index, monthly precipitation totals from a long-term record are first ranked from highest to lowest to construct a cumulative frequency distribution. The distribution is then split into 10 parts (tenths of distribution or deciles). The first decile is the precipitation value not exceeded

by the lowest 10% of all precipitation values in a record. The second decile is between the lowest 10 and 20% and so forth. By comparing the amount of precipitation in a month (or during a period of several months) with the long-term cumulative distribution of precipitation amounts in that period, the severity of drought can be assessed (Morid et al., 2007). The deciles are grouped into five classes, two deciles per class. If precipitation falls into the lowest 20% (deciles 1 and 2), it is classified as “much below normal”. Deciles 3 to 4 (20 to 40%) indicate “below normal” precipitation, deciles 5 to 6 (40 to 60%) indicate “near normal” precipitation, 7 and 8 (60 to 80%) indicate “above normal” precipitation and 9 and 10 (80 to 100%) indicate “much above normal” precipitation. In the aforementioned method, monthly rainfall time series are normalized using the Box–Cox transformation (Morid et al., 2006). A disadvantage of the deciles index is that a long climatological record is needed to calculate the deciles accurately.

### **2.6.5 Standardized Precipitation Index (SPI)**

The standardized Precipitation Index (SPI) was developed by McKee et al. (1993). A number of advantages arise from the use of the SPI index. The index is based on precipitation alone making its evaluation relatively simple (Cacciamani et al., 2007). Secondly, the index makes it possible to describe the drought on time scales that typically describe the four types of drought described earlier. In the context of this study, the SPI will enable the forecast of drought on both short and long-term time scales. As mentioned earlier, indices developed over short term time scales are useful in monitoring meteorological drought and agricultural drought. Likewise, indices developed over long term time scales are useful for monitoring hydrologic and socio-economic drought (Cacciamani et al., 2007). A third advantage of the SPI is its standardization which makes it particularly suited to compare drought conditions among different time periods and regions with different climates (Cacciamani et al., 2007).

The SPI index is based on an equi-probability transformation of aggregated monthly precipitation into a standard normal variable (Cancelliere et al., 2007). The computation of the index requires fitting a probability distribution to aggregated monthly precipitation series (3, 6, 12, 24, 48 months). The probability density function is then transformed into

a normal standardized index whose values classify the category of drought characterizing each place and time scale (Cacciamani et al., 2007). The SPI can only be computed when sufficiently long (at least 30 years) and possibly continuous time-series of monthly precipitation data are available (Cacciamani et al., 2007).

The SPI may be used for monitoring both dry and wet conditions (Morid et al., 2006). Positive SPI values indicate greater than median precipitation and negative values indicate less than median precipitation. The 'drought' parts of the SPI range are arbitrarily split into categories of near normal, moderately dry, severely dry and extremely dry (Morid et al., 2006). Each of these categories is defined by a range of SPI values. For example, the near normal category is defined by a range of SPI values from 0.5 to -0.5, while the severely dry category is defined by a range of SPI values from -1.5 to -2. A more negative SPI value is indicative of a more severe drought condition.

A disadvantage of the SPI index is that it is not always easy to find a probability distribution that models the raw precipitation data. Another disadvantage is that it is not always possible to access reliable time-series data to produce a robust estimate of the distribution parameters. The application of the index in arid regions on time scales of less than three months can result in misleading SPI values (Cacciamani et al., 2007). To overcome the possible lack of a probability distribution that models the raw precipitation data, several probability distributions can be used. The use of different probability distributions affect the SPI values as the SPI is based on the fitting of a distribution to precipitation time series. The gamma distribution (McKee et al., 1993; Edwards and McKee, 1997; Mishra and Singh, 2009), Pearson Type III distribution (Guttman, 1999) and lognormal, extreme value, and exponential distributions have been widely applied to simulations of precipitation distributions.

## **2.7 Comparison of Drought Indices**

It was determined that for this study a data driven drought index would be used to forecast drought, as opposed to a satellite based drought index. As mentioned above, satellite based drought indices are sensitive to changes in vegetative land cover over a given spatial and temporal scale. However, in areas where vegetative cover is minimal as

in the Somali Region of Ethiopia, some satellite based drought indices such as the VCI, are not very effective. In addition, satellite based drought indices are not as effective in detecting the onset of droughts, due to the time it takes for the effects of a drought to be apparent on vegetative surfaces. Given the fact that the NMSA of Ethiopia already conducts drought forecasts using the NDVI using a data driven index will both augment those forecasts and bring the advantages of data driven indices to their drought forecasts and monitoring systems.

Of the aforementioned data driven drought indices the PDSI (Kim and Valdes, 2003; Morid et al., 2006; Cutore et al., 2008; Karamouz et al., 2009; Hwang & Carbone, 2009) and the SPI (Tsakiris & Vangelis, 2004; Mishra, 2005; Mishra & Desai, 2006; Mishra et al., 2007; Cancelliere et al., 2007a; Cancelliere et al., 2007b; Cacciamani et al., 2007; Bordi & Sutera, 2007; Bacanli et al., 2008) have found widespread application in the field of drought forecasting. The main strength of these two drought indices is the fact that they are standardized. For the purposes of comparing drought conditions of different areas, which often have different hydrological balances, the most important characteristic of a drought index is its standardization (Bordi & Sutera, 2007). Standardization of a drought index ensures independence from geographical position as the index in question is calculated with respect to the average precipitation in the same place (Cacciamani et al., 2007).

There has been a lot of comparison between SPI and PDSI for forecasting droughts. One of the differences between the two indices is the special characteristics of the PDSI vary from site to site while those of the SPI do not. Another difference is the PDSI has a complex structure with an exceptionally long memory, while the SPI is an easily interpreted, simple moving average process. This characteristic makes the SPI useful as the primary drought index because it is simple, spatially invariant in its interpretation and probabilistic, allowing it to be used in risk and decision making analysis. The SPI is also more representative of short-term precipitation than the PDSI and is thus a better indicator for soil moisture variation and soil wetness (Mishra and Singh, 2010). The SPI also provides a better spatial standardization than does the PDSI with respect to extreme

drought events (Lloyd-Hughes and Saunders, 2002). The SPI has also been found to be better than the PDSI in detecting the onset of a drought event (Hayes et al., 1999).

Given the very complex empirical derivations of the PDSI, the fact that the PDSI assumes parameters such as soil characteristics are uniform over a climatic zone, and that the underlying computations are based on the climates of the mid-western United States, it was decided that the PDSI is not the most suitable drought index for Ethiopia. The SPI, however, is independent from a geographic position, relatively simple to compute and allows for the quantification of both short and long-term drought. Given these advantages, it was decided that the SPI is the most suitable drought index for drought forecasting in Ethiopia.

### **2.7.1 Selection of Forecasting Index**

The SPI is the most feasible drought index for Ethiopia because only precipitation data is required for its development. It is also a standardized index allowing it to be used over different climatic regions and temporal scales. Finally, the SPI has been developed and applied in developing countries. Mishra (2005), Mishra and Desai (2006) and Mishra et al. (2007) developed the SPI for the purpose of drought forecasting in the Kansabati River basin of India. The SPI has also been used as a tool to link meteorological and hydrological drought in the Awash River Basin of Ethiopia (Edossa et al., 2010). Given the advantages of using the SPI over the PDSI, in addition to the fact that the SPI has been used in an Ethiopian context (Edossa et al., 2010), selecting the SPI as the forecasting index was deemed appropriate.

The SPI has the ability to quantify the precipitation deficit for multiple time scales (Tsakiris and Vangelis, 2004). These time scales reflect the impact of drought on the availability of water resources. Streamflow, groundwater and reservoir storage reflect the longer-term precipitation anomalies, while soil moisture conditions respond to precipitation anomalies on a relatively short scale. For these reasons, the SPI was originally calculated for 3, 6, 12, 24 and 48 month time scales (Tsakiris and Vangelis, 2004). A 3-month SPI reflects short and medium-term moisture conditions and provides a seasonal estimation of precipitation. It compares the precipitation over a specific 3-month

period with the precipitation totals from the same 3-month period for all the years included in the historical record. A relatively normal 3-month period could in the middle of a longer-term drought that would only be visible at longer time scales. The 3-month SPI can be misleading in regions where it is normally dry during that 3-month period. A 6-month SPI can be very effective showing the precipitation over distinct seasons, indicating medium-term trends in precipitation. Information from a 6-month SPI may be associated with anomalous stream flows and reservoir levels (Tsakiris and Vangelis, 2004). The SPI is considered to be more sensitive to conditions at this time than the Palmer Index. A 12-month SPI reflects long-term precipitation patterns. The longer SPI tend towards zero unless a specific trend is occurring. At these time scales, SPI values are likely tied to streamflows, reservoir levels, and even groundwater levels (Tsakiris and Vangelis, 2004).

## **2.8 Overview of the Types of Forecasting Models used in this Study**

Up to this point drought has been defined and a need for a monitoring and forecasting system has been established. The SPI was selected as the drought index to be forecasted in Ethiopia, based on its advantages over other indices and its prior use in the context of developing countries, as well as its prior use in Ethiopia. Yet to be addressed is how the SPI will be forecasted and why. The following section will outline which forecast models will be used for the forecasting of SPI and the reasoning behind the selection of the models will also be given.

This study is aimed at forecasting SPI values for drought on both a short and long term basis. Five different types of forecast methods are explored and compared. The first type of method explored in this study is traditional stochastic models. Stochastic models include multiple linear regression (MLR), Markov Chain models, transition probabilities, autoregressive moving average (ARMA) models and autoregressive integrated moving average models (ARIMA). The most widely used stochastic models for the purpose of drought forecasting are ARMA/ARIMA models (Mishra and Desai, 2005; Mishra and Desai, 2006; Mishra et al., 2007; Han et al., 2010), and this is the type of stochastic model explored in this study. The second type of method for forecasting the SPI that is

explored in this study are artificial neural networks (ANNs). ANNs have become an increasingly popular tool for modelling time-series data and have been used in several studies as a tool for forecasting both the SPI and the PDSI (Mishra and Desai, 2006; Bacanli et al., 2008; Barros and Bowden, 2008; Cutore et al., 2009; Karamouz et al., 2009; Marj and Meijerink, 2011). The third type of method explored in this study is the coupling of an ANN with a discrete wavelet transform. Coupling discrete wavelet transforms with ANNs (WA-ANN) has very recently been explored for several hydrologic applications such as river flow forecasting (Adamowski, 2007; Adamowski and Sun, 2010; Ozger et al., 2012), precipitation forecasting (Partal and Kisi, 2007), forecasting peak urban water demand (Adamowski, 2010; Chen et al., 2012), forecasting evapotranspiration (Partal, 2009), and one application in drought forecasting (Kim and Valdes, 2003). Given that only one study has been published that explores the application of the WA-ANN method in drought forecasting, there is a need for additional studies.

The fourth forecasting method explored in this study is the use of support vector regression (SVR). SVRs are a soft computational technique that has been increasingly used in the field of hydrology over the last decade. SVRs have been used to forecast future water levels in Lake Erie (Khan and Coulibaly, 2006) and to forecast monthly discharge time series (Wang et al., 2009). The fifth forecasting method explored in this study is the coupling of discrete wavelet transforms with support vector regression (WA-SVR). Recently, WA-SVR has been explored as a tool to forecast monthly streamflow in Turkey (Kisi and Cimen, 2011). To the best knowledge of the author, there are no studies that explore the ability of SVR and WA-SVR to forecast a given drought index. Given the absence of such studies, this study is an important step in assessing whether these two methods are effective methods of forecasting drought on both short and long-term time scales. The following sections will first detail the distinction between short-term and long-term drought forecasting, and then discuss the properties of each of the five types of forecasting methods mentioned above.

### **2.8.1 Short versus Long-term Drought Forecasting**

The literature that exists on drought forecasting considers forecasts of 1-3 months lead times to be short-term drought forecasts, and forecasts of 4-12 months lead times to be medium to long-term drought forecasts (Kim and Valdes, 2003; Mishra and Desai, 2005; Mishra et al., 2006; Morid et al., 2007; Bordi and Sutera 2007; Cacciamani et al., 2007; Cancelliere et al., 2007). Forecasting short-term drought is useful for monitoring the effects of droughts on agricultural systems and is essential in managing water resources. Forecasting long-term drought helps understand the regional behaviour of a drought.

For short-term drought forecasts this study will explore forecasting SPI 1 and SPI 3 into the future for lead times of 1 and 3 months. Stochastic forecasts of the SPI for brief time steps (< 3 months) are sometimes considered misleading, especially in regions that receive low precipitation (Cacciamani et al., 2007). However this study is aiming to forecast the SPI, not only with the use of stochastic methods, but also using neural networks, support vector regression and both neural networks and support vector regression that have wavelet decomposed data as their inputs. Neural networks have been shown to provide reliable results for SPI forecasts (Mishra and Desai, 2006; Mishra et al., 2007; Baccanli et al., 2008). The SPI has not, to the knowledge of the author, been forecast using support vector regression or both wavelet pre-processed neural networks and wavelet pre-processed support vector regression. By forecasting the SPI 1 and SPI 3, with lead times of 1 and 3 months, it will help determine which data driven model is best suited for short-term or seasonal drought forecasting.

In regards to medium to long-term forecasts, this study will also explore forecasting the SPI 12 and SPI 24 into the future with lead times of 6 and 12 months, similar to most long-term drought forecasts. Again, the same data driven methods will be used for forecasting and eventually compared to determine which forecast method is best suited for long-term drought forecasts.

## **2.8.2 Stochastic Models**

The forecast models used in this study are data driven models. Data driven forecasting methods have been extensively used in hydrologic forecasting. Their popularity stems from their rapid development times and their minimum information requirements in terms of input data compared to physically based models (Adamowski, 2008). In data driven forecasting, stochastic models have traditionally been used. The aforementioned ARMA and ARIMA models are the most commonly used stochastic models for both short term and long term drought forecasting (Mishra and Desai, 2005; Mishra and Desai, 2006; Mishra et al., 2007; Cancelliere et al., 2007; Han et al., 2010). Stochastic models, which are often referred to as time-series models, have been used in scientific, economic and engineering applications for the analysis of time series data (Mishra and Desai, 2005). Times series modeling techniques have been shown to provide a systematic empirical method for simulating and forecasting the behaviour of uncertain hydrological systems and for the purpose of quantifying the expected accuracy of the forecasts (Mishra and Desai, 2005). The following sections will describe the different classes of stochastic models and describe the models considered for both short-term and long-term drought forecasting in this study.

## **2.8.3 Auto Regressive Moving Integrated Average Models (ARIMA)**

One of the most widely used time series models is the ARIMA model. The popularity of the ARIMA model is due to its statistical properties as well as the Box-Jenkins methodology in the building process (Zhang, 2003). In addition, various exponential smoothing models can be implemented by ARIMA models (McKenzie, 1984). ARIMA models are quite flexible in that they can represent several different types of time series, such as, pure autoregressive (AR), pure moving average (MA) and combined AR and MA (ARMA) series (Zhang, 2003).

Autoregressive moving average models (ARMA) are a result of the coupling of autoregressive and moving average models. In ARMA models the current value of the time series is expressed as a linear aggregate of  $p$  previous values and a weighted sum of  $q$  previous deviations (original value minus fitted value of previous data) plus a random

parameter. ARMA models can only be used when the data is stationary. When an ARMA model is extended to non-stationary series by allowing differencing of data series it forms an ARIMA model. Box and Jenkins (1976) popularized ARIMA models. The general non-seasonal ARIMA model is AR to order  $p$  and MA to order  $q$  and operates on  $d^{th}$  difference of the time series  $z_i$ ; thus a model of the ARIMA family is classified by three parameters  $(p, d, q)$  that can have zero or positive integral values.

Time series often contain cyclical features (Mishra, 2005). These cyclic features with respect to hydrologic time series are of an annual cycle primarily due to the earth's rotation about the sun. Such time series are cyclically non-stationary. Once the deterministic cyclic effects have been removed from a time series, the ARIMA approach can be applied to obtain a linear model for the stochastic part of the series. Box et al. (1994) generalized the ARIMA model to deal with seasonality, and defined a general multiplicative seasonal ARIMA model, which is commonly known as a SARIMA model.

The study by Mishra and Desai (2005) used ARIMA and SARIMA models to forecast droughts using the SPI in the Kansabati River basin in India. The study forecasted the SPI with lead times of 1-6 months. The predicted results show reasonably good agreement with the observed data for lead times of 1-2 months and when the forecast lead time increased the relationship between the predicted and observed data decreased. ARIMA and SARIMA models were also used to forecast the SPI and compared to SPI forecasts done by ANNs and hybrid ARIMA-ANN models in the Kansabati River basin (Mishra and Desai, 2006; Mishra et al., 2007). Both studies showed that the results for the ARIMA models were inferior to the other forecast models for lead times of 4-6 months and their performances decreased with longer lead times. For lead times of 1-2 months there was no significant difference in the performance of all three types of models.

This study will forecast the SPI using ARIMA models. The stochastic models to be used in this study are ARIMA models due to their flexibility and because they have been extensively used to forecast droughts; as such, they serve as a good traditional method to compare with the other newer methods that are explored in this study.

#### **2.8.4 Artificial Neural Networks**

Traditionally used stochastic models such as MLR and ARIMA are effective in modeling and forecasting time series data that is linear. These stochastic models are basically linear models that assume the data in question is stationary. They have limited ability to capture non-stationarities and non-linearities in the data. Thus, it is necessary to consider alternative models when non-linearity plays a significant role in the forecasting (Mishra and Desai, 2006). Non-linearity plays a significant role in the forecasting of most hydrologic data, including drought data. As an alternative, ANNs have been used to forecast hydrologic time series, including drought. In recent decades, ANNs have shown great ability in modelling and forecasting nonlinear time series in hydrology and water resources engineering due to their innate nonlinear property and flexibility for modelling.

ANNs are non-linear data driven models which can provide powerful solutions to many complex modelling problems. They have many features which make them attractive for use in forecasting. One such feature is their rapid development. ANNs are easy to develop as they do not require very detailed knowledge about the physical characteristics of the study area. Another feature is their rapid execution time. Once ANNs are calibrated they are rapid to run, and require very little execution time. In addition they have parsimonious data requirements compared to other traditional models. This parsimony in terms of data requirements is ideal for developing countries where hydrologic data may be sparse or incomplete.

Some of the characteristics of ANNs that make them attractive for hydrologic modelling are that they are able to recognize the relation between the input and output variables without explicit considerations. ANNs work well even when the training sets contain noise and measurement errors (Mishra and Desai, 2006), and they are able to adapt to solutions over time to compensate for changing circumstances. Apart from hydrology, ANNs have been widely used to model time series in various fields of applications such as dynamic systems, non linear signal processing, pattern recognition, identification and classification (BuHamra et al., 2003). ANNs have been used as an alternative for both linear and non-linear time series forecasting (Egrioglu et al., 2008). ANNs are able to

mimic a large class of nonlinear functions, and therefore they are ideal candidates to develop empirical (regression type) models. An ANN model is based on a connectionist approach to computation involving several transformation elements (neurons), interconnected and distributed over different layers (Cutore et al., 2009). In general, ANNs consist of an input layer, through which information reaches the network, one or more hidden layers, into which information is routed, and a layer of output, through which the results are provided (ASCE 2000a,b).

There are several classes of ANN models of which the feed-forward back propagation model and the adaptive neural network based fuzzy inference system (ANFIS) have found applications in drought forecasting. The back propagation model is the most commonly used class of neural networks for drought forecasting (Mishra and Desai, 2006; Mishra et al., 2007; Morid et al., 2007; Cutore et al., 2009; Karamouz et al., 2009; Marj and Meijerink, 2011; Adamowski and Karapataki, 2011), although ANFIS models have found some applications in drought forecasting (Bacanli et al., 2008). The following paragraphs describe the structures of these two neural networks and detail instances in which they have been applied to drought forecasting.

### **2.8.5 Feed Forward Neural Networks**

The most popular type of neural network for time series forecasting is the feed-forward model (Mishra and Desai, 2006). A typical feed-forward model consists of three layers; the input layer, the output layer and the hidden layer. The input nodes are the previous lagged observations, while the output provides the forecast for the future values (Mishra and Desai, 2006). Hidden nodes with appropriate nonlinear transfer functions are used to process the information received by the input nodes. To build a model for forecasting, the neural network is processed through three stages: the training stage where the network is trained to predict future data, based on past and present data; the testing stage where the network is tested to stop training or to keep training; and the validation stage where the network ceases training and is used to forecast future data and to calculate different measures of error. The back propagation network (BPN), developed by Rumelhart et al. (1986) is the most prevalent of the supervised learning models of ANN. BPN uses the

steepest gradient descent method to correct the weight of the interconnectivity neuron. BPN solves the interaction of the processing of processing elements by adding hidden layers.

In the learning process of BPN, the interconnection weights are adjusted using the error convergence technique to obtain a desired output for a given input. In general, the error at the output layer in the BPN model propagates backward to the input layer through the hidden layer in the network to obtain the final desired output. The gradient descent method is utilized to calculate the weight of the network and adjusts the weight of interconnections to minimize the output error. Another element of ANNs is the activation function. It determines the relationship between inputs and outputs of a node and a network and introduces a degree of the nonlinearity that is valuable for most ANN applications. The well-known activation functions are logistic, hyperbolic tangent, sine (or cosine) and the linear functions. Among them, the logistic transfer function is the most popular one (Mishra and Desai, 2006).

There are two different approaches with respect to neural networks for forecasting several time steps ahead: the recursive multi-step neural network approach (RMSNN) and the direct multi-step neural network approach (DMSNN). The RMSNN is similar to ARIMA models in forecasting as it has a single output node. A recursive multi-step approach is based on one output node, forecasting a single step ahead, and the network is applied recursively, using the previous predictions as inputs for the subsequent forecasts. The DMSNN is a forecast approach based on multiple outputs, when several nodes are included in the output layer, and each output node represents one time step to be forecasted.

Several authors have used ANNs for the purpose of forecasting droughts. Morid et al. (2007) used ANNs to predict quantitative values of drought indices in the province of Tehran in Iran. The drought indices they predicted are the SPI and the effective drought index (EDI). They used a feed forward neural network with standard BPN. The study forecast SPI values of 1-12 months for a forecast lead time of 1 month. The study presented forecast results for SPI 3-12 because they deemed these forecasts as

particularly important for drought forecasting. The best ANN models developed in the study were for a lead time of 6 months for both the SPI and the EDI.

A study Mishra and Desai (2006) compared ARIMA/SARIMA models with RMSNN and DMSNN for drought forecasting. The models were applied to forecast drought using SPI as the drought index in the Kansabati River basin of India. The study forecasted SPI for 1-6 months lead time. Their results show that as lead times increase, the simulated error between observed and predicted SPI values increase for all three model types. The simulated values for 1-month lead time were not significantly different from observed values for all three models. The RMSNN approach seems to provide very good results for 1-month lead time in comparison to DMSNN and ARIMA models. When a longer lead time of 4 months is considered the DMSNN approach outperforms RMSNN and ARIMA models. The performance of the ARIMA models provides good results up to a 2-month lead time but is inferior in comparison to the DMSNN approach.

In another study, Cutore et al. (2009) developed models to forecast the PHDI in Sicily, based on ANNs and tried to extend these models to include inputs from large scale climatic indexes, the NAO and the European Blocking (EB). The ANN forecasting model had an input vector consisting of monthly PHDI and climatic index data, and an output vector consisting of monthly Palmer index predictions. The study used single layer feed forward networks. The study performed forecasts of Palmer Index values for 1-4 months lead time. The study adopted two different forecasting techniques to forecast at different time horizons. The first one is what they termed the direct approach, in which different ANNs were developed for each forecasting horizon. The second approach used what they termed the iterative approach, in which ANNs able to predict 1 month ahead were considered and forecasted values were used as inputs. These two schemes are analogous to the RMSNN and the DMSNN. Results of the study indicate that the NAO and the EB series are significantly correlated with Palmer index series for winter and autumn months, with special references to the last decades. The forecasting models based on the two different neural networks approaches indicated some improvements in terms of  $R^2$  when NAO and especially EB are considered. The comparison between the two forecasting schemes indicated some improvements in terms of predictive capability when the

iterative approach for the winter and autumn months was applied. No significant differences in forecasting quality for the other months were obtained for the varying forecasting approaches.

A study by Barua et al. (2011) developed an ANN based drought forecasting approach using a time series of NADI values. In forecasting future drought conditions, the NADI produces the overall dryness within the system as compared to the traditional forecasting of rainfall deficiency, which considers only the meteorological droughts (Barua et al., 2011). As in other studies (Mishra and Desai, 2006 and Cutore et al., 2009) this study had two different ANN approaches: the RMSNN and the DMSNN. Overall, both models were capable of forecasting drought conditions reasonably well for forecasts of 6 months lead time. Moreover, it was found that both models show the same performance for 1 month lead time forecasts. Nevertheless, the RMSNN model provides slightly better forecasts than the DMSNN model for lead times of 2-3 months and the DMSNN model provided slightly better forecasts than the RMSNN model for forecast lead times of 4-6 months. Beyond the forecast lead time of 6 months, poor forecasts were observed for both modeling approaches.

In addition to comparing the performance of stochastic models and ANNs with respect to forecasting SPI values, Mishra et al. (2007) developed hybrid models that combine the advantages of both stochastic and ANN models. Using the SPI time series, the hybrid models as well as the individual stochastic and ANN models were applied to forecast droughts in the Kansabati River basin in India, and their performances were compared. The hybrid models were found to forecast droughts with greater accuracy. The study compared the forecast capabilities of 5 different models; an ARIMA model, a RMSNN, DMSNN, a hybrid stochastic neural network with a direct approach (HSNNDA), and a hybrid stochastic neural network with a recursive approach (HSNNRA). The performance of these models was evaluated over lead times of 1-6 months. The results of the study indicated that the hybrid models performed better in forecasting the SPI in the Kansabati basin. For a lead time of 1 month the HSNNRA performed better than any other model. However, when the lead times increase, the performance of all the

recursive-based models in the study deteriorated and the HSNNDAs were found to perform better.

### **2.8.6 Coupled Wavelet Transforms and ANNs**

A number of studies in the fields of hydrology and water resources have coupled neural networks with wavelet transforms, based on data pre-processing using wavelet transforms. As a pre-processing tool wavelet transforms provide useful decompositions of original time series, so that data that has been pre-processed improves the ability of a forecasting model by capturing information on various resolution levels (Adamowski, 2008). In addition, it has also been found that pre-processing data with wavelet transforms can lead to models that better represent the true features of the underlying system by eliminating ‘noise’ (Adamowski, 2008).

The wavelet transform is a mathematical tool that provides a time-frequency representation of a signal in the time domain (Dabueches, 1990; Partal and Kisi, 2007). Wavelet transforms are useful functions for the analysis of time-series that contain non-stationarities. Wavelet analysis allows the use of long-term intervals for low frequency information and shorter intervals for high frequency information, and is capable of revealing aspects of data like trends, breakdown points, and discontinuities that other signal analysis techniques might miss (Kim and Valdes, 2003). In addition, wavelet analysis can often compress or de-noise a signal (Kim and Valdes, 2003). The basic objective of wavelet transforms is to achieve a complete time-scale representation of localized and transient phenomena occurring at a different time scale (Labat et al., 2000).

The recent application of wavelet transforms in the fields of hydrology and water resources is partially linked with the ability of wavelets to deal with non-stationary data. ANNs and other linear or non-linear models are not usually effective in dealing with non-stationary data. In the field of hydrology, wavelet transforms have been used to: examine the rainfall–runoff relationship in a Karstic watershed (Labat et al., 1999), characterize daily streamflow (Smith et al., 1998; Saco and Kumar, 2000) and monthly reservoir inflow (Coulibaly et al., 2000), evaluate rainfall–runoff models (Lane, 2007), forecast

river flow (Adamowski, 2008; Adamowski and Sun, 2010; Ozger et al., 2012), forecast urban water demand (Chan et al., 2011) and forecast droughts (Kim and Valdes, 2003).

### **2.8.7 Coupled WA-ANNs for Drought Forecasting**

As mentioned above, models that couple neural networks with wavelet transforms have been recently used in hydrology. However, to the best knowledge of the author, the only application of neural networks with wavelet pre-processing for the purpose of drought forecasting was a study completed by Kim and Valdes (2003). Kim and Valdes (2003) developed a hybrid WA-ANN model to forecast regional drought in the Conchos River basin in Mexico. They used the PDSI to represent regional drought. The study by Kim and Valdes (2003) used the “a trous” wavelet transform with Mallat’s quadratic spline as a low pass filter to decompose the observed PDSI values.

Kim and Valdes (2003) evaluated their coupled model for four forecast lead times (1, 3, 6 and 12) months and five wavelet decomposition levels (1-5). The performance of their model was measured using various forecast skill criteria and then compared with a conventional ANN as well as persistence forecasts and climatological forecasts. Persistence forecasts are values of the predictand in the previous time step and climatological forecasts consist of climatologically averaged values. The ANN they used in their study was a three-layered feed-forward neural network. The study found that using a coupled model for drought forecasting was superior to using a conventional ANN forecast model. The forecasting skill of the coupled model was improved up to six-month lead time when compared to a conventional ANN (Kim and Valdes, 2003).

Given the results Kim and Valdes (2003) obtained by using wavelet transforms coupled with ANNs, it is expected that wavelet transforms will improve the ability of forecast models to predict future drought. However, additional research is needed since the study by Kim and Valdes (2003) is the only study that couples wavelet transforms and ANNs for drought forecasting. Studies coupling wavelet transforms and ANNs in hydrologic forecasting have concentrated more on river flow forecasting or forecasting urban water demand. This study will contribute to the literature on drought forecasts. Additional research is also needed on the use of other drought indices, such as the SPI, since the

study by Kim and Valdes used the PDSI to forecast drought. This study explores forecasting the SPI on both short and long-term time scales, using five different methods (traditional stochastic methods, ANNs, SVR, WA-ANN and WSVR) and compares each method to determine the most suitable method for forecasting SPI values on both short and long-term timescales. The results of this study will determine which forecasting model is appropriate to forecast drought conditions, using the SPI, with different lead times in the Awash River basin.

### **2.8.8 Support Vector Regression (SVR) and Coupled Wavelet SVR Models**

Support vector regression (SVR) was developed by Vapnik (1995) and is based on the structural risk minimization principle. The structural risk minimization principle theoretically minimizes the expected error of a learning machine and therein reduces the problem of overfitting. The structural risk minimization principle has been shown to be superior to the empirical risk minimization principle which is used by many conventional neural networks (Gunn et al., 1997). SVRs were developed to solve the classification problem in which it is shown that the generalization error is bounded by the sum of the training set error and a term depending on the VC (Vapnik-Chervonenkis) dimension of the model (Kisi and Cimen, 2008). SVRs have recently been extended to the domain of regression problems (Vapnik, 1999; Dibike et al., 2001; Liong and Sivapragasam, 2002).

Wavelet-support vector regression models (WA-SVR) are obtained by combining two methods, wavelet transforms and support vector regression (SVR). The WA-SVR model is a SVR model which uses wavelet decomposed sub-series as its inputs. WA-SVR has very recently begun to be investigated in hydrologic forecasting (Kisi and Cimen 2008; Kisi and Cimen 2011). The study by Kisi and Cimen (2008) used a coupled WA-SVR model to forecast monthly streamflow in Turkey. In their study, the original streamflow time series are decomposed into a certain number of sub-series components by the Mallat discrete wavelet algorithm. The WA-SVR is constructed so that the sub-series components of the original input time series are the inputs of the SVR and the original output time series are the output of the SVR. The study by Kisi and Cimen (2008) compared the ability of a WA-SVR model to forecast monthly streamflow to a single

SVR model. The comparison showed that the wavelet decomposed data could significantly increase the accuracy of the SVR model in forecasting monthly streamflows. The WA-SVR model increased the prediction correlation coefficient with respect to the single SVR model by 19–30%, and reduced the root mean square errors and mean absolute errors by 11–46% and 19–44%, respectively.

The present study develops, for the first time, the WA-SVR method for drought forecasting, and compares the ability of WA-SVR models to forecast drought with SVR models, ARIMA models, traditional ANN models and ANN models with wavelet decomposed data. While the three latter models have been used to forecast a given drought index to different degrees, SVR and WA-SVR have not. The results of this study will help determine whether these two methods are effective in forecasting SPI on both short and long-term time scales in Ethiopia.

## **Connecting Text to Chapter 3**

The chapter is a manuscript co-authored by the supervisor of this research Dr. Jan F. Adamowski, as well as Dr. Bahaa Khalil. The results of this chapter are being prepared to be submitted as a manuscript to the Journal of Agricultural Management. All literature cited in this chapter is listed in the reference section at the end of this chapter, as well as at the end of this thesis.

Chapter 3 covers the development of the SPI and the development of the five data driven forecasting models. SPI 1 and SPI 3 are computed as they are representative of short-term drought conditions and agricultural drought. The methodology for the development of neural network architectures as well as the parameters for support vector regression models is described. The process of wavelet decomposition is also discussed in Chapter 3. Once SPI 1 and SPI 3 are computed they are forecast by the five data driven models for lead times of 1 and 3 months, respectively. These forecasts are compared to determine which data driven model is the most effective drought forecasting tool.

## Chapter 3

### Short-term SPI drought forecasting in the Awash River Basin in Ethiopia using wavelet-neural networks and wavelet-support vector regression

Belayneh, A., Adamowski, J. and Khalil, B.

Department of Bioresource Engineering, Faculty of Agricultural and Environmental Sciences, McGill University, Quebec, Canada, H9X 3V9 Email:

anteneh.meshesha@mail.mcgill.ca

jan.adamowski@mcgill.ca

bahaa.khalil@mail.mcgill.ca

#### Abstract:

Droughts can cause significant damage to agricultural and other systems. An important aspect of mitigating the impacts of drought is an effective method of forecasting future drought events. In this study, five methods of forecasting drought for short lead times are explored in the Awash River Basin of Ethiopia. The Standard Precipitation Index (SPI) was the drought index chosen to represent drought in the basin. Machine learning techniques including artificial neural networks (ANNs) and support vector regression (SVR) were compared with coupled models (WA-ANN and WA-SVR) which pre-process input data using wavelet analysis (WA). This study proposed and tested, for the first time, the SVR and WA-SVR methods for short term drought forecasting. This study also used, for the first time, only the approximation series (derived via wavelet analysis) as inputs to the ANN and SVR models, and found that using just the approximation series as inputs for models gave good forecast results. The forecast results of all five data driven models were compared using several performance measures (RMSE, MAE,  $R^2$  and a measure of persistence). The forecast results of this study indicate that the coupled wavelet neural network (WA-ANN) models were the best models for forecasting SPI 1 and SPI 3 values over lead times of 1 and 3 months in the Awash River Basin.

**Keywords:** Standard precipitation index; Drought forecasting; Artificial Neural Networks; Support vector regression; Wavelet analysis; Autoregressive models; Africa

#### 3.1 Introduction

Drought is a natural phenomenon that occurs when precipitation is significantly lower than normal. Low precipitation levels can lead to severe hydrologic deficits. These deficits may cause low crop yields for agriculture, reduced flows for ecological systems, loss of biodiversity and other problems for the environment, in addition to adversely impacting the hydroelectric industry, as well as causing deficits in the drinking water supply which can negatively affect local populations. The less predictable characteristics

of droughts such as their initiation, termination, frequency and severity can make drought both a hazard and a disaster. Drought is characterized as a hazard because it is a natural accident of unpredictable occurrence but of recognizable recurrence (Mishra and Singh, 2010). Drought is also characterized as a disaster because it corresponds to the failure of the precipitation regime, causing the disruption of the water supply to natural and agricultural ecosystems as well as to other human activities (Mishra and Singh, 2010).

In recent years, large scale intensive droughts have been observed on all continents, affecting large areas in Europe, Africa, Asia, Australia, South America, Central America, and North America (Mishra and Singh, 2010). The increased attention regarding droughts is a direct consequence of the high economic and social costs incurred. The main impacts of drought can be distinguished in three categories: economic, environmental and social (Rossi et al., 2007). Between 1980 and 2003, drought accounted for \$144 billion of the \$349 billion total cost of all weather-related disasters in the US (Ross and Lott, 2003). Over the last 30 years, several major droughts have also been observed in Europe. One such drought occurred in 2005 on the Iberian Peninsula and resulted in an overall decline of approximately ten percent of total EU cereal yields. In addition, the yearly average economic impact of droughts in Europe has been estimated to be €5.3 billion since 1991 (Mishra and Singh, 2010). Droughts have also had a great impact in Africa, with the Sahel having experienced droughts of unprecedented severity in recorded history (Mishra and Singh, 2010). The impacts of drought on the Sahel were a major impetus for the establishment of the United Nations Convention on Combating Desertification and Drought (Zeng, 2003).

Droughts have had significant impacts in Ethiopia, where approximately 85% of the population (Edossa et al., 2010) is engaged in agriculture (primarily rain fed agriculture), and where agriculture comprises 52% of the country's GDP and 90% of its exports (Edossa et al., 2010). This heavy dependence on agriculture, coupled with a highly variable climate, has resulted in Ethiopia experiencing some of the more adverse consequences of drought, such as crop failures and in some cases a resulting famine. Droughts regularly lead to famine, as was the case during the 1957-58 drought in Tigray province and the 1972-73 drought which claimed over 200,000 lives in Wollo province.

Although the famine caused by the drought of 1984–85 remains well known to the world community, less serious, but nonetheless significant droughts occurred in the years 1987, 1988, 1991–92, 1993–94, 1999, and 2002 in Ethiopia (Edossa et al., 2010).

Due to their slow evolution in time, droughts are a phenomenon whose consequences take a significant amount of time with respect to their inception in order to be perceived by both ecological and socio-economic systems. Due to this feature, effective mitigation of the most adverse drought impacts is possible, more than in the case of the other extreme hydrological events such as floods, earthquakes or hurricanes, provided a drought monitoring system which is able to promptly warn of the onset of a drought and to follow its evolution in space and time is in operation (Rossi, 2007). An accurate selection of indices for drought identification, providing a synthetic and objective description of drought conditions and future drought conditions, represents a key point for the implementation of an efficient drought warning system (Cacciamani et al, 2007).

Most drought indices were developed with the intent to monitor current drought conditions. However, some indices can be used to forecast the possible evolution of an ongoing drought, in order to adopt appropriate mitigation measures and drought policies for water resources management (Cancelliere et al., 2007). This is because a drought index is expressed by a numeric number which is believed to be far more functional than raw data during decision making (Hayes, 1996). Several drought indices have been developed around the world in the past based on rainfall as the single variable, including the widely used Deciles (Gibbs and Maher, 1967), Standardized Precipitation Index (SPI) (McKee et al., 1993) and Effective Drought Index (EDI) (Byun and Wilhite, 1999). Another well-known index is the Palmer Drought Severity Index (PDSI) (Palmer, 1965), which considers temperature along with rainfall.

In this study the drought index chosen to forecast drought is the standard precipitation index (SPI), which was developed to quantify a precipitation deficit for different time scales (Guttman, 1999). The SPI was chosen as a drought index in this study because it is simple, spatially invariant in its interpretation, probabilistic and can be tailored to different time periods (Guttman, 1999). The SPI has been developed and applied as a

primary drought index in some developing countries. Mishra and Desai (2005), Mishra and Desai (2006) and Mishra et al. (2007) developed models to forecast the SPI for the purpose of drought forecasting in the Kansabati River basin of India. The SPI has also been used as a tool to link meteorological and hydrological drought in the Awash River Basin of Ethiopia (Edossa et al., 2010). The Awash River Basin is the study basin explored in this research and the SPI index will be used to forecast drought mainly because the SPI drought index requires precipitation as its only input. Furthermore, it has been determined that precipitation alone can explain most of the variability of East African droughts and that the SPI is an appropriate index for monitoring droughts in East Africa (Ntale and Gan, 2003).

In hydrologic drought forecasting, stochastic methods have been traditionally used to forecast drought indices. Markov Chain models (Paulo et al., 2005; Paulo and Pereira, 2008) and autoregressive integrated moving average models (ARIMA) (Mishra, 2005; Mishra and Desai, 2006; Mishra et al., 2007; Han et al., 2010) have been the most widely used stochastic models for hydrologic drought forecasting. The major limitation of these models is that they are linear models and they are not very effective in forecasting non-linearities, a common characteristic of hydrologic data.

In response to non-linear data, researchers in the last two decades have increasingly begun to forecast hydrological data using artificial neural networks (ANNs). ANNs have been used to forecast droughts in several studies (Mishra and Desai, 2006; Morid et al., 2007; Bacanlı et al., 2008; Barros and Bawden, 2008; Cutore et al., 2009; Karamouz et al., 2009; Marj and Meijerink, 2011). However, ANNs are limited in their ability to deal with non-stationarities in the data, a weakness also shared by ARIMA and other stochastic models.

Support Vector Machines (SVMs) are a relatively new form of machine learning that was developed by Vapnik (1995), and which have been recently used in the field of hydrological forecasting. The term SVM is used to refer to both classification and regression methods as well as the terms Support Vector Classification (SVC) and Support Vector Regression (SVR) to refer to the problems of classification and regression,

respectively (Gao et al., 2002). There are several studies where SVRs were used in hydrological forecasting. Khan and Coulibaly (2006) found that an SVR model was more effective at predicting 3-12 month lake water levels than ANN models. Kisi and Cimen (2009) used SVRs to estimate daily evaporation. Finally, SVRs have been successfully used to predict hourly streamflow (Asefa et al., 2006), and were shown to perform better than ANN and ARIMA models for monthly streamflow prediction (Wang et al., 2009 and Maity et al., 2010), respectively. However, to date SVRs have not been applied in drought forecasting.

Wavelet analysis, an effective tool to deal with non-stationary data, is an emerging tool for hydrologic forecasting and has recently been applied to: examine the rainfall–runoff relationship in a Karstic watershed (Labat et al., 1999), to characterize daily streamflow (Saco and Kumar, 2000) and monthly reservoir inflow (Coulibaly et al., 2000), to evaluate rainfall–runoff models (Lane, 2007), to forecast river flow (Adamowski, 2008, Adamowski and Sun, 2010, Ozger et al., 2012), to forecast groundwater levels (Adamowski and Chan, 2011), to forecast future precipitation values (Partal and Kisi, 2007), to forecast urban water demand (Chan et al., 2011) and for the purposes of drought forecasting (Kim and Valdes, 2003). The study conducted by Kim and Valdes (2003) is the only study to date that has explored the ability of a wavelet-neural network conjunction model (WA-ANN) to forecast a given drought index. However, the study by Kim and Valdes (2003) used their conjunction model to forecast the Palmer Index and not the SPI. Furthermore the ability to forecast drought using wavelet-support vector regression (WA-SVR) has not been explored to date.

The main objective of the present study was to compare traditional drought forecasting methods such as ARIMA models with machine learning techniques such as ANNs and SVR, along with ANNs with data pre-processed using wavelet transforms (WA-ANN), support vector regression (SVR), and a newly proposed drought forecasting method based on the coupling of wavelet transforms and support vector regression (WA-SVR) for short-term drought forecasting. The standardized precipitation index (SPI), namely SPI 1 and SPI 3, was forecast using the above mentioned methods for lead times of 1 and 3 months in the Awash River Basin of Ethiopia. As mentioned earlier, this is the first

study to forecast drought using the SVR and WA-SVR methods, and also the first study to forecast SPI using the WA-ANN method. Current drought forecasts in Ethiopia are done by the Meteorological Services Agency (NMSA), where they provide 10 day and monthly forecasts of the normalized vegetation index (NDVI). Forecasts of the SPI will augment the existing NMSA forecasts, especially considering that the NDVI and other satellite based drought indices are sensitive to changes in vegetative land cover, and have limited effectiveness in areas with minimal vegetative cover. Both SPI 1 and SPI 3 are short-term drought indicators, and forecast lead times of 1 and 3 months represent the shortest possible monthly lead time and a short seasonal lead time, respectively. As short-term drought indicators, SPI 1 and SPI 3 represent agricultural drought conditions. Given the fact that approximately 85% of Ethiopia's population is engaged in agriculture (Edossa et al., 2010), effective forecasts of these two drought indices are very important. The models developed in this research should prove to be very useful as they can complement the 10 day and monthly NDVI forecasts that the NMSA currently provides.

Section 2 of this paper explains the theoretical development behind the SPI and the different types of models used. Section 3 provides a brief description of the physical characteristics of the Awash River Basin. In section 4, the methodology used to forecast the SPI is described for each type of model. In section 5, the results are outlined and discussed, and conclusions are presented in section 6.

## **3.2 Theoretical Development**

This section first introduces the SPI and highlights some of the advantages of using it as a drought index. The theory behind the development of the SPI is described in some detail as well as the process of computation. This section then describes, in detail, the models proposed in this study to forecast the SPI, which are the ARIMA, ANN, WA-ANN, SVR and WA-SVR models.

### **3.2.1 Development of SPI Series**

The standardized Precipitation Index (SPI) was developed by McKee et al. (1993). A number of advantages arise from the use of the SPI index. First, the index is based on

precipitation alone making its evaluation relatively easy (Cacciamani et al., 2007). Secondly, the index makes it possible to describe drought on multiple time scales (Tsakiris and Vangelis, 2004; Mishra and Desai, 2006; Cacciamani et al., 2007). A third advantage of the SPI is its standardization which makes it particularly well suited to compare drought conditions among different time periods and regions with different climates (Cacciamani et al., 2007). A drought event occurs at the time when the value of the SPI is continuously negative; the event ends when the SPI becomes positive. Table 1 provides a drought classification based on SPI.

The computation of the SPI requires fitting a probability distribution to aggregated monthly precipitation series (1, 3, 6, 12, 24, 48 months). The probability density function is then transformed into a normal standardized index whose values classify the category of drought characterizing each place and time scale (Cacciamani et al., 2007). The SPI can only be computed when sufficiently long (at least 30 years), and possibly continuous, time-series of monthly precipitation data are available (Cacciamani et al., 2007).

**Table 1: Drought Classification based on SPI (McKee et al., 1993).**

<b>SPI Values</b>	<b>Class</b>
> 2	Extremely wet
1.5-1.99	Very wet
1.0-1.49	Moderately wet
-0.99 to 0.99	Near normal
-1 to -1.49	Moderately dry
-1.5 to -1.99	Very dry
<-2	Extremely dry

In most cases the probability distribution that best models observational precipitation data is the Gamma distribution (Cacciamani et al., 2007). The density probability function for the Gamma distribution is given by the expression (Cacciamani et al., 2007):

$$g(x) = \frac{1}{\beta^\alpha \Gamma(\alpha)} x^{\alpha-1} e^{-x/\beta}, \quad \text{for } x > 0 \quad (1)$$

where  $\alpha > 0$  is the shape parameter,  $\beta > 0$  is the scale parameter and  $x > 0$  is the amount of precipitation.  $\Gamma(\alpha)$  is the value taken by the standard mathematical function known as the Gamma function, which is defined by the integral (Cacciamani et al., 2007):

$$\Gamma(\alpha) = \int_0^{\infty} x^{\alpha-1} e^{-x} dx \quad (2)$$

In general, the Gamma function is evaluated either numerically or using the values tabulated depending on the value taken by parameter  $\alpha$ .

In order to model the data observed with a gamma distributed density function, it is necessary to estimate parameters  $\alpha$  and  $\beta$  appropriately. Different methods have been suggested in the literature for the estimate of these two parameters. For example, the Thom (1958) approximation is used for maximum probability in Edwards and McKee (1997):

$$\hat{\alpha} = \frac{1}{4A} \left( 1 + \sqrt{1 + \frac{4A}{3}} \right) \quad (3)$$

$$\hat{\beta} = \frac{\bar{x}}{\hat{\alpha}} \quad (4)$$

where for n observations

$$A = \sum_{i=1}^n \ln(x_i) \quad (5)$$

The estimate of the parameters can be further improved by using the interactive approach suggested in Wilks (1995).

After estimating coefficients  $\alpha$  and  $\beta$  the density of probability function  $g(x)$  is integrated with respect to  $x$  and we obtain an expression for cumulative probability  $G(x)$  that a certain amount of rain has been observed for a given month and for a specific time scale (Cacciamani et al., 2007):

$$G(x) = \int_0^x g(x) dx = \frac{1}{\hat{\beta} \hat{\Gamma}(\hat{\alpha})} = \int_0^x x^{\hat{\alpha}-1} e^{-x/\hat{\beta}} dx \quad (6)$$

The Gamma function is not defined by  $x = 0$  and since there may be no precipitation, the cumulative probability becomes (Cacciamani et al., 2007):

$$H(x) = q + (1 - q)G(x) \quad (7)$$

where  $q$  is the probability of no precipitation and  $H(x)$  is the cumulative probability of precipitation observed. The cumulative probability is then transformed into a normal standardized distribution with null average and unit variance from which we obtain the SPI index.

The above approach, however, is neither practical nor numerically simple to use if there are many grid points of many stations on which to calculate the SPI index. In this case, an alternative method is described in Edwards and McKee (1997) using the technique of approximate conversion developed in Abramowitz and Stegun (1965) that converts the cumulative probability into a standard variable  $Z$ . The SPI index is then defined as (Cacciamani et al., 2007):

$$Z = SPI = -\left(t - \frac{c_0 + c_1 t + c_2 t^2}{1 + d_1 t + d_2 t^2 + d_3 t^3}\right), \text{ for } 0 < H(x) \leq 0.5 \quad (8)$$

$$Z = SPI = +\left(t - \frac{c_0 + c_1 t + c_2 t^2}{1 + d_1 t + d_2 t^2 + d_3 t^3}\right), \text{ for } 0.5 < H(x) < 1 \quad (9)$$

where

$$t = \sqrt{\ln\left[\frac{1}{(H(x))^2}\right]}, \quad \text{for } 0 < H(x) \leq 0.5 \quad (10)$$

and

$$t = \sqrt{\ln\left[\frac{1}{1 - H(x)}\right]}, \quad \text{for } 0.5 < H(x) < 1 \quad (11)$$

where  $x$  is precipitation,  $H(x)$  is the cumulative probability of precipitation observed and  $c_0, c_1, c_2, d_0, d_1, d_2$  are constants with the following values:

$$\begin{array}{lll} c_0 = 2.515517 & c_1 = 0.802853 & c_2 = 0.010328 \\ d_0 = 1.432788 & d_1 = 0.189269 & d_2 = 0.001308 \end{array}$$

### 3.2.2 Autoregressive Integrated Moving Average (ARIMA) Models

The ARIMA model has several advantages over other stochastic models, such as exponential smoothing, its greater forecasting capability and its ability to provide greater information with respect to time-related changes (Mishra and Desai, 2005; Mishra et al., 2007). ARIMA models are amongst the most commonly used stochastic models for drought forecasting (Mishra and Desai, 2005; Mishra and Desai, 2006; Mishra et al., 2007; Cancelliere et al., 2007; Han et al., 2010). Autoregressive moving average models (ARMA) are a result of coupling autoregressive and moving average models and can be used when the data is stationary. A stationary time series can be defined when the data have a constant mean, variance and autocorrelation over time. Hydrologic time series generally present ascending or descending trends and are usually non-stationary, especially for short lead times. Non-stationary time series can be modeled by differencing the data series into a stationary time series. In ARMA models the current value of the time series is expressed as a linear aggregate of  $p$  previous values and a weighted sum of  $q$  previous deviations (original value minus fitted value of previous data) plus a random parameter. ARMA models can only be used when the data is stationary. When an ARMA model is extended to non-stationary series by allowing differencing of data series it forms an ARIMA model. Box and Jenkins (1976) developed ARIMA models. The general non-seasonal ARIMA model is autoregressive (AR) to order  $p$  and moving average (MA) to order  $q$  and operates on  $d^{th}$  difference of the time series  $z_t$ ; thus a model of the ARIMA family is classified by three parameters ( $p, d, q$ ) that can have zero or positive integral values.

The general non-seasonal ARIMA model may be written as (Box and Jenkins, 1976):

$$z_t = \frac{\theta(B)a_t}{\phi(B)\nabla^d} \quad (12)$$

$$\phi(B) = (1 - \phi_1 B - \phi_2 B^2 - \dots - \phi_p B^p) \quad (13)$$

and

$$\theta(B) = (1 - \theta_1 B - \theta_2 B^2 - \dots - \theta_q B^q) \quad (14)$$

where  $z_t$  is the observed time series.  $\phi(B)$  and  $\theta(B)$  are polynomials of order  $p$  and  $q$ , respectively. The orders  $p$  and  $q$  are the order of non-seasonal auto-regression and the

order of non-seasonal moving average, respectively. Random errors,  $a_t$  are assumed to be independently and identically distributed with a mean of zero and a constant variance.  $\nabla^d$  describes the differencing operation to data series to make the data series stationary and  $d$  is the number of regular differencing.

The time series model development consists of three stages: identification, estimation and diagnostic check (Box et al., 1994). In the identification stage, data transformation is often needed to make the time series stationary. Stationarity is a necessary condition in building an ARIMA model that is useful for forecasting (Zhang, 2001). The estimation stage of model development consists of the estimation of model parameters. The last stage of model building is the diagnostic checking of model adequacy. This stage checks if the model assumptions about the errors are satisfied. Several diagnostic statistics and plots of the residuals can be used to examine the goodness of fit of the tentative model to the observed data. If the model is inadequate, a new tentative model should be identified, which is subsequently followed, again, by the stages of estimation and diagnostic checking.

### **3.2.3 Artificial Neural Network Models**

ANNs are flexible computing frameworks for modeling a broad range of nonlinear problems. Over the past decade, ANNs have been extensively used in the field of hydrologic forecasting. They have many features which are attractive for forecasting such as their rapid development, rapid execution time and their ability to handle large amounts of data without very detailed knowledge of the underlying physical characteristics (ASCE, 2000a, b).

The ANN models used in this study have a feed forward Multi-layer perceptron (MLP) architecture which was trained with the Levenberg Marquardt (LM) back propagation algorithm. MLPs have often been used in hydrologic forecasting due to their simplicity. MLPs consist of an input layer, one or more hidden layers, and an output layer. The hidden layer contains the neuron-like processing elements that connect the input and output layers given by (Kim and Valdes, 2003):

$$\hat{y}_k(t) = f_0 \left[ \sum_{j=1}^m w_{kj} \cdot f_n \left( \sum_{i=1}^N w_{ji} x_i(t) + (w_{j0}) + w_{k0} \right) \right] \quad (15)$$

where  $N$  is the number of samples,  $m$  is the number of hidden neurons,  $x_i(t)$  = the  $i^{th}$  input variable at time step  $t$ ;  $w_{ji}$  = weight that connects the  $i^{th}$  neuron in the input layer and the  $j^{th}$  neuron in the hidden layer;  $w_{j0}$  = bias for the  $j^{th}$  hidden neuron;  $f_n$  = activation function of the hidden neuron;  $w_{kj}$  = weight that connects the  $j^{th}$  neuron in the hidden layer and  $k^{th}$  neuron in the output layer;  $w_{k0}$  = bias for the  $k^{th}$  output neuron;  $f_0$  = activation function for the output neuron; and  $\hat{y}_k(t)$  is the forecasted  $k^{th}$  output at time step  $t$  (Kim and Valdes, 2003).

MLPs were trained with the LM back propagation algorithm. This algorithm is based on the steepest gradient descent method and Gauss-Newton iteration. To apply the LM algorithm a scalar parameter  $u$  is required. The LM algorithm varies between the gradient descent algorithm (when  $u$  is large) and the Gauss-Newton algorithm (when the  $u$  is small). In the learning process, the interconnection weights are adjusted using the error convergence technique to obtain a desired output for a given input. In general, the error at the output layer in the model propagates backwards to the input layer through the hidden layer in the network to obtain the final desired output. The gradient descent method is utilized to calculate the weight of the network and adjusts the weight of interconnections to minimize the output error.

### 3.2.4 Support Vector Regression Models

Support vector machines (SVM) were introduced by Vapnik (1995) in an effort to characterize the properties of learning machines so that they can generalize well to unseen data (Kisi and Cimen, 2011). SVMs embody the structural risk minimization principle, unlike conventional neural networks which adhere to the empirical risk minimization principle. As a result, SVMs seek to minimize the generalization error, while ANNs seek to minimize training error. SVMs can be separated into two types: support vector classification (SVC) and support vector regression (SVR). Since this study is primarily concerned with forecasting the SPI, SVR was used.

Support vector regression (SVR) is used to describe regression with SVMs (Vapnik, 1995). In regression estimation with SVR the purpose is to estimate a functional dependency  $f(\vec{x})$  between a set of sampled points  $X = \{\vec{x}_1, \vec{x}_2, \dots, \vec{x}_l\}$  taken from  $R^n$  and target values  $Y = \{y_1, y_2, \dots, y_l\}$  with  $y_i \in R$  (the input and target vectors ( $x_i$ 's and  $y_i$ 's) refer to the monthly records of the SPI index). Assuming that these samples have been generated independently from an unknown probability distribution function  $P(\vec{x}, y)$  and a class of functions (Vapnik, 1995):

$$F = \left\{ f \mid f(\vec{x}) = (\vec{W}, \vec{x}) + B_s : \vec{W} \in R^n, R^n \rightarrow R \right\} \quad (16)$$

where  $\vec{W}$  and  $B_s$  are coefficients that have to be estimated from the input data. The main objective is to find a function  $f(\vec{x}) \in F$  that minimizes a risk functional (Cimen, 2008):

$$R \left[ f(\vec{x}) \right] = \int l(y - f(\vec{x}), \vec{x}) dP(\vec{x}, y) \quad (17)$$

where  $l$  is a loss function used to measure the deviation between the target,  $y$ , and estimate  $f(\vec{x})$ , values. As the probability distribution function  $P(\vec{x}, y)$  is unknown one cannot minimize the risk functional directly, but only compute the empirical risk function as (Cimen, 2008):

$$R_{emp} \left[ f(\vec{x}) \right] = \frac{1}{N} \sum_{i=1}^N l(y_i - f(\vec{x}_i)) \quad (18)$$

where  $N$  is the number of samples. This traditional empirical risk minimization is not advisable without any means of structural control or regularization. Therefore, a regularized risk function with the smallest steepness among the functions that minimize the empirical risk function could be used as (Cimen, 2008):

$$R_{reg} \left[ f(\vec{x}) \right] = R_{emp} \left[ f(\vec{x}) \right] + \gamma \left\| \vec{W} \right\|^2 \quad (19)$$

where  $\gamma$  is a constant ( $\gamma \geq 0$ ). This additional term reduces the model space and thereby controls the complexity of the solution leading to the following form of this expression (Smola, 1996; Cimen, 2008):

$$R_{reg} \left[ f(\vec{x}) \right] = C_c \sum_{x_i \in X} l_\epsilon(y_i - f(\vec{x}_i)) + \frac{1}{2} \left\| \vec{W} \right\|^2 \quad (20)$$

where  $C_c$  is a positive constant that has to be chosen beforehand. The constant  $C_c$  that influences a trade-off between an approximation error and the regression (weight) vector  $\left\| \vec{W} \right\|^2$  is a design parameter. The loss function in this expression, which is called an  $\epsilon$ -insensitive loss function ( $l_\epsilon$ ), and has the advantage that it will not need all the input data for describing the regression vector  $\left\| \vec{W} \right\|^2$ , can be written as (Cimen, 2008):

$$l_\epsilon(y_i - f(\vec{x}_i)) = \begin{cases} 0 & \text{for } |y_i - f(\vec{x}_i)| < \epsilon \\ |y_i - f(\vec{x}_i)| - \epsilon & \text{otherwise} \end{cases} \quad (21)$$

This function behaves as a biased estimator when it is combined with the regularization term ( $\gamma \left\| \vec{W} \right\|^2$ ). The loss is equal to 0 if the difference between the predicted and observed value is less than  $\epsilon$ . The nonlinear regression function is given by the following expression (Vapnik, 1995; Cimen, 2008):

$$f(x) = \sum_{i=1}^N (\alpha_i^* - \alpha_i) K(x, x_i) + B_s \quad (22)$$

where  $\alpha_i, \alpha_i^* \geq 0$  are the Lagrange multipliers,  $B_s$  is a bias term, and  $K(x, x_i)$  is the Kernel function which is based upon Reproducing Kernel Hilbert Spaces (Kisi and Cimen, 2011). The kernel function enables operations to be performed in the input space as opposed to the potentially high dimensional feature space. Hence an inner product in the feature space has an equivalent kernel in input space. Several types of functions are treated by SVR such as polynomial functions, Gaussian radial basis functions, multi-layer

perception functions, functions with splines, etc. (Kisi and Cimen, 2011). In this study, the radial basis function (RBF) was the kernel used.

### 3.2.5 Wavelet Transforms

The first step in wavelet analysis is to choose a mother wavelet ( $\psi$ ). The continuous wavelet transform (CWT) is defined as the sum over all time of the signal multiplied by scaled and shifted versions of the wavelet function  $\psi$  (Nason and Von Sachs, 1999):

$$W(\tau, s) = \frac{1}{\sqrt{|s|}} \int_{-\infty}^{\infty} x(t) \psi^* \left( \frac{t - \tau}{s} \right) dt \quad (23)$$

where  $s$  is the scale parameter;  $\tau$  is the translation and  $*$  corresponds to the complex conjugate (Kim and Valdes, 2003). The CWT produces a continuum of all scales as the output. Each scale corresponds to the width of the wavelet; hence, a larger scale means that more of a time series is used in the calculation of the coefficient than in smaller scales. The CWT is useful for processing different images and signals; however, it is not often used for forecasting due to its complexity and time requirements to compute. Instead, the successive wavelet is often discrete in forecasting applications to simplify the numerical calculations. The discrete wavelet transform (DWT) requires less computation time and is simpler to implement. DWT scales and positions are usually based on powers of two (dyadic scales and positions). This is achieved by modifying the wavelet representation to (Cannas et al., 2006):

$$\psi_{j,k}(t) = \frac{1}{\sqrt{|s_0^j|}} \psi \left( \frac{t - k\tau_0 s_0^j}{s_0^j} \right) \quad (24)$$

where  $j$  and  $k$  are integers that control the scale and translation respectively, while  $s_0 > 1$  is a fixed dilation step (Cannas et al., 2006) and  $\tau_0$  is a translation factor that depends on the aforementioned dilation step. The effect of discretizing the wavelet is that the time-space scale is now sampled at discrete levels. The DWT operates two sets of functions: high-pass and low-pass filters. The original time series is passed through high-pass and low-pass filters, and detailed coefficients and approximation series are obtained.

One of the inherent challenges of using the DWT for forecasting applications is that it is not shift invariant (i.e. if we change values at the beginning of our time series, all of the wavelet coefficients will change). To overcome this problem, a redundant algorithm, known as the  $\grave{a}$  trous algorithm can be used, given by (Mallat, 1998):

$$C_{i+1}(k) = \sum_{l=-\infty}^{+\infty} h(l)c_i(k + 2^i l) \quad (25)$$

where  $h$  is the low pass filter and the finest scale is the original time series. To extract the details,  $w_i(k)$ , that were eliminated in Eq. (25), the smoothed version of the signal is subtracted from the coarser signal that preceded it, given by (Murtagh et al., 2003):

$$w_i(k) = c_{i-1}(k) - c_i(k) \quad (26)$$

where  $c_i(k)$  is the approximation of the signal and  $c_{i-1}(k)$  is the coarser signal. Each application of Eq. (24) and (25) creates a smoother approximation and extracts a higher level of detail. Finally, the non-symmetric Haar wavelet can be used as the low pass filter to prevent any future information from being used during the decomposition (Renaud et al., 2002).

### 3.3 Study Areas

The Awash River Basin in Ethiopia was the area chosen for this study. Droughts are a common occurrence in Ethiopia. As agriculture, and especially rain-fed agriculture, is a major component of the country's economy, the potential for major detrimental impacts is very high. Furthermore, drought is one of the recurring natural hazards in the Awash River Basin (Edossa et al., 2010). Frequent and persistent droughts have led to food insecurity within the region, and a significant number of the basin inhabitants are reliant on international food assistance for survival (Edossa et al., 2010). Given these circumstances, effective agricultural drought forecasts are an important measure to provide a warning system for farmers, which can allow them to prepare for the advent of drought (for example by allowing them to switch to more drought resistant crops, etc...). The Awash River Basin (Figure 1) was separated into three smaller basins for the purpose

of this study on the basis of various factors such as location, altitude, climate, topography and agricultural development. The mean annual rainfall of the basin varies from about 1,600 mm in the highlands north east of Addis Ababa, to 160 mm in the northern point of the basin. The total amount of rainfall also varies greatly from year to year, resulting in severe droughts in some years and flooding in others. The total annual surface runoff in the Awash Basin amounts to some  $4,900 \times 10^6 \text{ m}^3$ . The sub-basins are called the Upper, Middle and Lower Awash Basins, respectively (Edossa et al., 2003). The reasoning behind the use of three sub-basins was to ensure the methods used in this study were effective in forecasting short-term drought in different conditions. The characteristics of each sub-basin are briefly described in the following sections. The rainfall record from 1970-2005 was used to generate the SPI time series for SPI 1 and SPI 3.

### **3.3.1 Upper Awash Basin**

The Upper Awash Basin has a temperate climate with annual mean temperatures ranging between 15-22°C and an annual precipitation of between 500-2000 mm (Edossa et al., 2010). Rainfall distribution in the Upper Awash Basin is unimodal. Seven rainfall gauges located in the Upper Awash River Basin were chosen for this study (Table 2). These stations were chosen because their precipitation records from 1970-2005 were either complete or relatively complete. Any station which had over 10% of their records missing was not selected.

### **3.3.2 Middle Awash Basin**

The Middle Awash Basin is in the semi-arid climatic zone with a long hot summer and a short mild winter. Annual rainfall varies between 200-1500 mm (Edossa et al., 2010). The rainfall distribution is bimodal in this sub-basin. Minor rains normally occur in March and April and major rains from July to August. Six rainfall gauges located in the Middle Awash Basin were selected using the same criteria as in the Upper Awash Basin and are shown in Table 2.

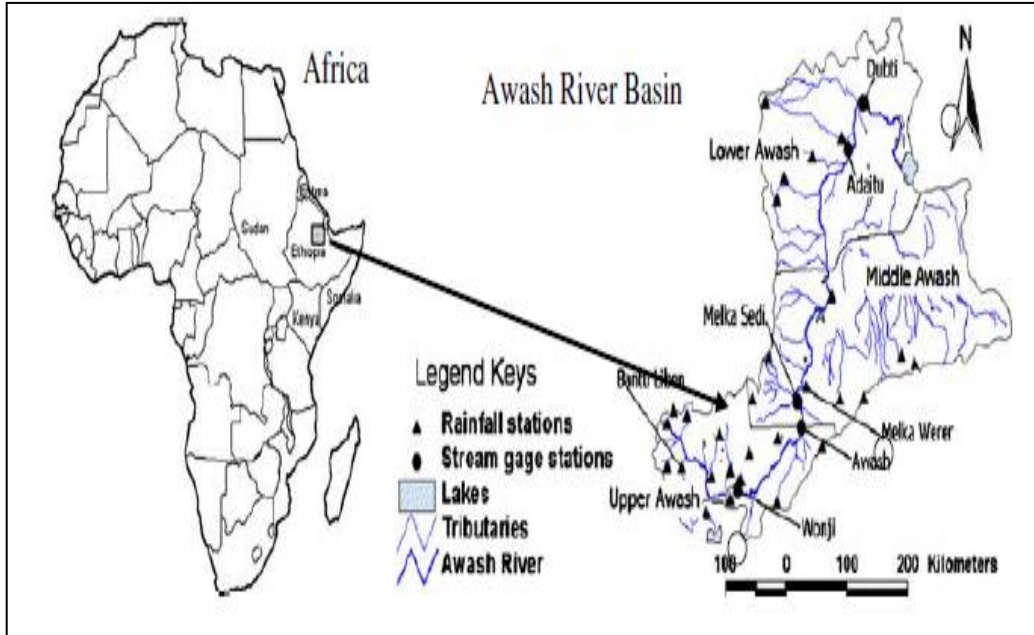


**Figure 1: Awash River Basin (Source: Edossa et al., 2010).**

### 3.3.3 Lower Awash Basin

The Lower Awash River Basin has a hot, semi-arid climate. The annual mean temperature of the region ranges between 22 and 32°C with average annual precipitation between 500 and 700 mm (Edossa et al., 2010). 5 rainfall gauges were selected from the Lower Awash Basin using the same criteria used in the two other sub-basins and are shown in Table 2.

### 3.3.4 Estimating Missing Rainfall

The normal ratio method, recommended by Linsley et al. (1988), was used to estimate the missing rainfall records at some stations. Using this method, rain depths for missing data are estimated from observations at three stations as close to and as evenly spaced around the station with the incomplete records as possible. The distance matrix was established for all rain gauge stations in the basin based on their geographic locations in order to assess proximity of stations with each other. Finally, all data sets were normalized using the equation:

$$X_n = \frac{X_0 - X_{\min}}{X_{\max} - X_{\min}} \quad (27)$$

where  $X_0$  and  $X_n$  represent the original and normalized data respectively, while  $X_{\min}$  and  $X_{\max}$  represent the minimum and maximum value among the original data.

**Table 2: Descriptive Statistics of the Awash River Basin**

Basin	Station	Mean annual Precipitation (mm)	Max annual Precipitation (mm)	Standard Deviation (mm)
Upper Awash Basin	Bantu Liben	91	647	111
	Tullo Bullo	94	575	114
	Ginchi	97	376	90
	Sebeta	111	1566	172
	Ejersalele	67	355	75
	Ziquala	100	583	110
	Debre Zeit	73	382	81
Middle Awash Basin	Koka	97	376	90
	Modjo	76	542	92
	Nazereth	73	470	85
	Wolenchiti	76	836	95
	Gelemsso	77	448	75
	Dire Dawa	51	267	54
Lower Awash Basin	Dubti	15	192	23
	Eliwuha	44	374	57
	Mersa	87	449	89
	Mille	26	268	40
	Bati	73	357	80

### 3.4. Methodology

The methodology section of this paper will detail, amongst other things, how the SPI was calculated, as well as how the SPI was forecasted over short term time scales using the different model types. Five different types of models were developed in this study: ARIMA, ANNs, WA-ANNs, SVRs and WA-SVRs. Two sets of inputs were developed from the SPI data. The monthly SPI was delayed ((t-1), (t-2), (t-3), etc) by an appropriate monthly time scale. The same delayed SPI data was decomposed using wavelet transforms.

All the data driven models developed in this study were recursive multi-step approach models which have one output node. In recursive models, a model is forecast one time-step ahead and the network is applied recursively, using the previous forecasts as inputs for the subsequent forecasts. For example, a forecast of 3 months lead time will have the outputs from forecasts of lead times of 1 and 2 months used as intermediate variables. These outputs are used as inputs for forecasts of 3 months lead time. Table 3 shows the inputs and intermediate variables used for the best data driven models. As shown in Table 3, forecasts of 3 months lead time have an input of  $SPI(t)$ , and intermediate variables  $SPI(t+2)$ ,  $SPI(t+1)$ ,  $SPI(t-1)$ , which include the forecast results of 1 and 2 months lead time ( $(SPI(t+1)$  and  $(SPI(t+2))$ ), respectively.

### **3.4.1 SPI Calculation**

The first step in the calculation of the SPI is to determine a probability density function that describes the long-term series of precipitation data (Cacciamani et al., 2007). Once this distribution is determined, the cumulative probability of an observed precipitation amount is computed. The gamma distribution function was selected to fit the rainfall data in this study. The SPI is a normalized index in time and space. This feature allows values in different geographic locations to be compared (Cacciamani et al., 2007). SPI values can be categorized according to classes. In this study, the near normal class is established from the aggregation of two classes:  $-1 < SPI < 0$  (mild drought) and  $0 \leq SPI \leq 1$  (slightly wet). SPI values are positive or negative for greater or less than mean precipitation, respectively. The time series of the SPI can be used for drought monitoring by setting application-specific thresholds of the SPI for defining drought beginning and ending times. Accumulated values of the SPI can be used to analyze drought severity. In this study, an SPI program, SPI\_SL\_6, developed by the National Drought Mitigation Centre at the University of Nebraska-Lincoln, was used to compute time series of drought indices (SPI) for each station in each sub-basin and for each month of the year at different time scales.

Using the rainfall records received from each rainfall gauge and the aforementioned SPI program, SPI values of 1 and 3 months were calculated. SPI 1 is very similar to the

percent of normal precipitation for a month. SPI 1 reflects relatively short-term conditions; its application can be related closely with short-term soil moisture and crop stress, especially during the growing season. Alternatively, a 3-month SPI compares the precipitation for that period with the same 3-month period over the historical record. For example, a 3-month SPI at the end of September compares the precipitation total for the July–September period with all the past totals for that same period. A 3-month SPI indicates short and medium term trends in precipitation and is still considered to be more sensitive to conditions at this scale than the Palmer Index. A 3-month SPI can be very effective in showing seasonal trends in precipitation. In contrast, longer SPI such as SPI 12 and 24 reflect long-term precipitation patterns. SPI 12 is a comparison of the precipitation for 12 consecutive months with the same 12 consecutive months during all the previous years of available data. Because these time scales are the cumulative result of shorter periods that may be above or below normal, the longer SPIs tend toward zero unless a specific trend is taking place.

In each sub-basin, for each station, SPI 1 and SPI 3 were computed. These SPI values were subsequently forecast over lead times of 1 and 3 months.

### **3.4.2 ARIMA Model Development**

Based on the Box and Jenkins approach, ARIMA models for the SPI time series were developed based on three steps: model identification, parameter estimation and diagnostic checking. The details on the development of ARIMA models for SPI time series can be found in the works of Mishra and Desai (2005) and Mishra et al., (2007).

In an ARIMA model, the value of a given times series is a linear aggregation of  $p$  previous values and a weighted sum of  $q$  previous deviations (Mishra and Desai, 2006). These ARIMA models are autoregressive to order  $p$  and moving average to order  $q$  and operate on  $d^{th}$  difference of the given times series. Hence, an ARIMA models is distinguished with three parameters  $(p,d,q)$  that can each have a positive integer value or a value of zero.

### **3.4.3 Wavelet Transformation**

When conducting wavelet analysis, the number of decomposition levels that is appropriate for the data must be chosen. Often the number of decomposition levels is chosen according to the signal length (Tiwari and Chatterjee, 2010) given by  $L = \text{int}[\log(N)]$  where  $L$  is the level of decomposition and  $N$  is the number of samples. According to this methodology the optimal number of decompositions for the SPI time series in this study would have been 3. In this study, each SPI time series was decomposed between 1 and 9 levels. The best results were compared at all decomposition levels to determine the appropriate level. The optimal decomposition level varied between models. Once a time series was decomposed into an appropriate level, the subsequent approximation series was either chosen on its own, in combination with relevant detail series or the relevant detail series were added together without the approximation series. With most SPI time series, choosing just the approximation series resulted in the best forecast results. In some cases, the summation of the approximation series with a decomposed detail series yielded the best forecast results. The appropriate approximation was used as an input to the ANN and SVR models. As discussed in Section 2.5, the ‘a trous’ wavelet algorithm with a low pass Haar filter was used.

#### **3.4.4 ANN Models**

The ANN models used to forecast the SPI were recursive models. The input layer for the models was comprised of the SPI values computed from each rainfall gauge in each sub-basin. The input data was standardized from 0 to 1.

All ANN models, without wavelet decomposed inputs, were created with the MATLAB (R.2010a) ANN toolbox. The hyperbolic tangent sigmoid transfer function was the activation function for the hidden layer, while the activation function for the output layer was a linear function. All the ANN models in this study were trained using the LM back propagation algorithm. The LM back propagation algorithm was chosen because of its efficiency and reduced computational time in training models (Adamowski and Chan, 2011).

There are between 3-5 inputs for each ANN model. The optimal number of input neurons was determined by trial and error, with the number of neurons that exhibited the lowest root mean square error (RMSE) value in the training set being selected. The inputs and outputs were normalized between 0 and 1. Traditionally the number of hidden neurons for ANN models is selected via a trial and error method. However a study by Wanas et al. (1998) empirically determined that the best performance of a neural network occurs when the number of hidden nodes is equal to  $\log(N)$ , where  $N$  is the number of training samples. Another study conducted by Mishra and Desai (2006) determined that the optimal number of hidden neurons is  $2n+1$ , where  $n$  is the number of input neurons. In this study, the optimal number of hidden neurons was determined to be between  $\log(N)$  and  $(2n+1)$ . For example, if using the method proposed by Wanas et al. (1998) gave a result of 4 hidden neurons and using the method proposed by Mishra and Desai (2006) gave 7 hidden neurons, the optimal number of hidden neurons is between 4 and 7; thereafter the optimal number was chosen via trial and error. These two methods helped establish an upper and lower bound for the number of hidden neurons.

For all the ANN models, 80% of the data was used to train the models, while the remaining 20% of the data was divided into a testing and validation set with each set comprising 10% of the data.

### **3.4.5 WA-ANN Models**

The WA-ANN models were trained in the same way as the ANN models, with the exception that the inputs were made up from either, the approximation series, or a combination of the approximation and detail series after the appropriate wavelet decomposition was selected. The model architecture for WA-ANN models consists of 3-5 neurons in the input layer, 4-7 neurons in the hidden layer and one neuron in the output layer. The selection of the optimal number of neurons in both the input and hidden layers was done in the same way as for the ANN models. The data was partitioned into training, testing and validation sets in the same manner as ANN models.

### **3.4.6 Support Vector Regression Models**

All SVR models were created using the OnlineSVR software created by Parrella (2007), which can be used to build support vector machines for regression. The data was partitioned into two sets: a calibration set and a validation set. 90% of the data was partitioned into the calibration set while the final 10% of the data was used as the validation set. Unlike neural networks the data can only be partitioned into two sets with the calibration set being equivalent to the training and testing sets found in neural networks. All inputs and outputs were normalized between 0 and 1.

All SVR models used the nonlinear radial basis function (RBF) kernel. As a result, each SVR model consisted of three parameters that were selected: gamma ( $\gamma$ ), cost (C), and epsilon ( $\epsilon$ ). The  $\gamma$  parameter is a constant that reduces the model space and controls the complexity of the solution, while C is a positive constant that is a capacity control parameter, and  $\epsilon$  is the loss function that describes the regression vector without all the input data (Kisi and Cimen, 2011). These three parameters were selected based on a trial and error procedure. The combination of parameters that produced the lowest RMSE values for the calibration data sets were selected.

### **3.4.7 WA-SVR Models**

The WA-SVR models were trained in exactly the same way as the SVR models with the OnlineSVR software (2007) with the exception that the inputs were wavelet decomposed. The data for WA-SVR models was partitioned exactly like the data for SVR. The optimal parameters for the WA-SVR models were chosen using the same procedure used to find the parameters for SVR models.

### **3.4.8 Performance Measures**

To evaluate the performances of the aforementioned data driven models the following measures of goodness of fit were used:

$$\text{The coefficient of determination (R}^2\text{)} = \frac{\sum_{i=1}^N (\hat{y}_i - \bar{y}_i)}{\sum_{i=1}^N (y_i - \bar{y}_i)^2} \quad (28)$$

$$\text{where } \bar{y}_i = \frac{1}{N} \sum_{i=1}^N y_i \quad (29)$$

where  $\bar{y}_i$  is the mean value taken over  $N$ ,  $y_i$  is the observed value,  $\hat{y}_i$  is the forecasted value and  $N$  is the number of samples. The coefficient of determination measures the degree of correlation among the observed and predicted values. It is a measure of the strength of the model in developing a relationship among input and output variables. The higher the value of  $R^2$  (with 1 being the highest possible value), the better the performance of the model.

$$\text{The Root Mean Squared Error (RMSE)} = \sqrt{\frac{SSE}{N}} \quad (30)$$

where  $SSE$  is the sum of squared errors, and  $N$  is the number of data points used.  $SSE$  is given by:

$$SSE = \sum_{i=1}^N (\hat{y}_i - y_i)^2 \quad (31)$$

with the variables already having been defined. The RMSE evaluates the variance of errors independently of the sample size.

$$\text{The Mean Absolute Error (MAE)} = \sum_{i=1}^N \frac{|\hat{y}_i - y_i|}{N} \quad (32)$$

The MAE is used to measure how close forecasted values are to the observed values. It is the average of the absolute errors.

The results in this study are also compared to persistence forecasts.

$$PERS = 1 - \frac{SSE}{SSE_{naive}} \quad \text{where} \quad (33)$$

$$SSE_{naive} = \sum_i^N (y_i - y_{i-L})^2 \quad (34)$$

As mentioned above, *SSE* is the sum of squared errors.  $y_{i-L}$  is the estimate from a persistence model that takes the last observation (at time 1 minus the lead time (*L*)) (Tiwari and Chatterjee, 2010). A value of *PERS* smaller or equal to 0 indicates that the model under study performs worse or no better than the easy to implement naïve model. A *PERS* value of 1 is obtained when the model under study provides exact estimates of observed values.

### 3.5. Results and Discussion

In this present study the ability of the aforementioned models to effectively forecast SPI over different lead times was evaluated.

In the following sections, the forecast results for the best data driven models at each sub-basin are presented. The forecasts presented are from the validation data sets for time series of SPI 1 and SPI 3, which are mostly used to describe short-term drought (agricultural drought). SPI 1 is a good indicator of the deviation of precipitation from the long-term average. These two SPI time series are forecast over lead times of 1 and 3 months. Over a monthly time scale, forecasts of 1 month lead time are the shortest possible and forecasts of 3 months lead time represent drought conditions over a seasonal period.

All the data driven models had a *PERS* greater than 0. ARIMA models had a *PERS* of 0.38, ANN models had a *PERS* of 0.46, SVR models had a *PERS* of 0.41, WA-ANN models had a *PERS* of 0.59 and WA-SVR models had a *PERS* of 0.43.

**Table 3: Model Inputs and intermediate variables for the best data driven models (LT = monthly forecast lead time)**

Model	Input Structure	Output
ANN-LT1	SPI(t), SPI(t-1), SPI(t-2)	SPI(t+1)
ANN-LT3	SPI(t+2), SPI(t+1), SPI(t), SPI(t-1)	SPI(t+3)
SVR-LT1	SPI(t), SPI(t-1), SPI(t-2)	SPI(t+1)
SVR-LT3	SPI(t+2), SPI(t+1), SPI(t), SPI(t-1)	SPI(t+3)
WA-ANN-LT1	SPI(t), SPI(t-1), SPI(t-2)	SPI(t+1)
WA-ANN-LT3	SPI(t+2), SPI(t+1), SPI(t), SPI(t-1)	SPI(t+3)
WA-SVR-LT1	SPI(t), SPI(t-1), SPI(t-2)	SPI(t+1)
WA-SVR-LT3	SPI(t+2), SPI(t+1), SPI(t), SPI(t-1)	SPI(t+3)

### 3.5.1 SPI 1 forecasts

As shown in tables 4 and 5, the use of wavelet transforms improves the forecast ability of models as shown by the lower RMSE and MAE values for WA-ANN and WA-SVR models compared to the other data driven models. However, all SPI 1 forecasts exhibit low results in terms of  $R^2$ . Indeed the best SPI forecast for a 1 month lead time has an  $R^2$  of 0.3361. When the forecast lead time is increased to 3 months the forecast results predictably deteriorate across all the forecast measures. A possible explanation for the low correlation between predicted and observed SPI 1 values is the low level of autocorrelation within the data set. Figures 2 and 3 show the autocorrelation for both SPI 1 and SPI 3 at the same station. These figures indicate that there is greater autocorrelation within the SPI 3 time series as the lag time is increased. The SPI 1 time series is also more sensitive than an SPI 3 time series to any changes in monthly precipitation. As the SPI 1 is the shortest monthly SPI and is not made up of any other cumulative values, its sensitivity is higher than any other SPI value. This sensitivity to any fluctuations in monthly precipitation within the long-term precipitation record may also explain the poor model results in terms of  $R^2$ .

**Table 4: The best ARIMA, ANN and SVR models for 1 and 3 month forecasts of SPI 1.**

Column 3 is the ANN architecture detailing the number of nodes in the input, hidden and output layers respectively. In column 11 the parameters of the SVR models are given.

Basin	Station	ANN models	R <sup>2</sup>	RMSE	MAE	ARIMA (p,0,q)	R <sup>2</sup>	RMSE	MAE	SVR ( $\gamma, C, \epsilon$ )	R <sup>2</sup>	RMSE	MAE
1 month lead time													
Upper	Bantu Liben	3-4-1	0.2850	1.3302	1.3183	(1,0,1)	0.2291	1.3889	1.3664	0.02, 96, 0.002	0.1838	1.3456	1.3342
	Tullo Bullo	3-4-1	0.2430	1.3321	1.3017	(2,0,1)	0.2126	1.3811	1.3709	0.03, 95, 0.002	0.1837	1.3547	1.3240
	Ginchi	4-4-1	0.2321	1.3538	1.3012	(1,1,1)	0.2289	1.3943	1.3725	0.08, 90, 0.05	0.1548	1.3328	1.3202
	Sebeta	4-4-1	0.3170	1.3305	1.3096	(2,0,0)	0.2214	1.3756	1.3613	0.06, 100, 0.01	0.1635	1.3312	1.3301
	Ejersalele	5-4-1	0.2362	1.3513	1.3227	(1,1,1)	0.2235	1.3934	1.3853	0.05, 98, 0.007	0.1652	1.3287	1.3162
	Ziquala	3-4-1	0.2769	1.3619	1.3157	(1,0,1)	0.2117	1.3756	1.3614	0.04, 88, 0.08	0.1544	1.3403	1.3287
	Debre Zeit	4-4-1	0.2671	1.3470	1.3169	(1,0,1)	0.2072	1.3741	1.3561	0.05, 96, 0.06	0.1723	1.3448	1.3236
Middle	Koka	4-4-1	0.2551	1.3314	1.3138	(1,0,1)	0.2131	1.3920	1.3822	0.05, 100, 0.003	0.1535	1.3348	1.3139
	Modjo	3-4-1	0.2962	1.3312	1.3157	(1,1,1)	0.2230	1.3731	1.3644	0.08, 90, 0.08	0.1537	1.3356	1.3150
	Nazereth	4-4-1	0.3059	1.3465	1.3136	(1,0,0)	0.2014	1.3842	1.3706	0.07, 94, 0.03	0.1542	1.3317	1.3128
	Wolenchiti	3-4-1	0.2713	1.3157	1.3078	(2,1,1)	0.2206	1.3904	1.3698	0.07, 92, 0.004	0.1667	1.3477	1.3268
	Gelemsso	4-4-1	0.2950	1.3201	1.3041	(1,0,1)	0.2098	1.3863	1.3665	0.05, 93, 0.003	0.1259	1.3491	1.3281
	Dire Dawa	3-4-1	0.2894	1.3568	1.3144	(1,0,1)	0.2103	1.3802	1.3688	0.05, 88, 0.01	0.1482	1.3547	1.3445
	Lower	Dubti	3-4-1	0.2990	1.3482	1.3128	(1,0,0)	0.2112	1.3734	1.3605	0.08, 97, 0.05	0.1752	1.3531
Eliwuha		4-4-1	0.3180	1.3503	1.3105	(1,1,1)	0.2099	1.3841	1.3694	0.06, 98, 0.06	0.1834	1.3429	1.3319
Mersa		3-5-1	0.3583	1.3328	1.3115	(1,1,1)	0.2152	1.3711	1.3698	0.09, 100, 0.008	0.1744	1.3560	1.3344
Mille		3-4-1	0.2894	1.3356	1.3143	(2,0,1)	0.2172	1.3863	1.3835	0.06, 91, 0.007	0.1928	1.3632	1.3431
Bati		4-4-1	0.3060	1.3240	1.3021	(1,0,1)	0.2098	1.3705	1.3913	0.05, 93, 0.004	0.1845	1.3472	1.3315
3 month lead time													
Upper	Bantu Liben	3-4-1	0.1642	1.4804	1.4461	(1,0,0)	0.1648	1.5831	1.3808	0.05, 96, 0.002	0.1746	1.4673	1.4257
	Tullo Bullo	4-5-1	0.1721	1.4628	1.4571	(1,0,0)	0.1698	1.5843	1.3724	0.02, 92, 0.005	0.1657	1.4555	1.4447
	Ginchi	4-4-1	0.1323	1.4581	1.4320	(1,0,1)	0.1643	1.5936	1.3853	0.06, 99, 0.006	0.1530	1.4551	1.4433
	Sebeta	3-4-1	0.1724	1.4253	1.4169	(1,1,0)	0.1740	1.5832	1.3626	0.09, 90, 0.008	0.1604	1.4556	1.4447
	Ejersalele	3-4-1	0.1477	1.4612	1.4401	(1,0,1)	0.1591	1.5763	1.3756	0.08, 92, 0.006	0.1178	1.4646	1.4239
	Ziquala	4-4-1	0.1050	1.4658	1.4425	(2,1,1)	0.1623	1.5914	1.3754	0.07, 93, 0.004	0.1182	1.4637	1.4154
	Debre Zeit	3-4-1	0.1046	1.4421	1.4293	(1,0,1)	0.1478	1.5723	1.3722	0.05, 94, 0.006	0.1143	1.4653	1.4148
Middle	Koka	3-4-1	0.1106	1.4600	1.4131	(1,0,1)	0.1585	1.5634	1.3822	0.05, 87, 0.005	0.1149	1.4537	1.4149
	Modjo	3-4-1	0.1205	1.4199	1.4074	(1,0,1)	0.1675	1.5741	1.3725	0.05, 100, 0.003	0.1137	1.4623	1.4119
	Nazereth	3-4-1	0.1954	1.4134	1.4012	(1,1,1)	0.1669	1.5842	1.3698	0.08, 93, 0.01	0.1136	1.4639	1.4128
	Wolenchiti	4-4-1	0.1421	1.4124	1.4004	(2,1,1)	0.1714	1.5701	1.3866	0.08, 95, 0.002	0.1158	1.4529	1.4118
	Gelemsso	4-4-1	0.1530	1.4059	1.3957	(1,0,1)	0.1491	1.5777	1.3700	0.04, 94, 0.003	0.1147	1.4638	1.4130
	Dire Dawa	3-4-1	0.1349	1.4129	1.4099	(2,0,1)	0.1629	1.5862	1.3833	0.05, 85, 0.009	0.1148	1.4737	1.4619
Lower	Dubti	4-4-1	0.1673	1.4190	1.4060	(1,1,1)	0.1513	1.5732	1.3903	0.08, 97, 0.05	0.1134	1.4354	1.4349
	Eliwuha	4-4-1	0.1341	1.4159	1.4028	(1,0,1)	0.1644	1.5869	1.3711	0.09, 90, 0.007	0.1165	1.4716	1.4663
	Mersa	4-4-1	0.1427	1.4117	1.4106	(1,0,1)	0.1512	1.5991	1.3795	0.03, 95, 0.009	0.1172	1.4884	1.4642
	Mille	3-4-1	0.1750	1.4175	1.3943	(1,0,0)	0.1638	1.5745	1.3806	0.05, 100, 0.005	0.1135	1.4440	1.4332
	Bati	4-4-1	0.1776	1.4040	1.3924	(1,0,0)	0.1584	1.5702	1.3722	0.04, 98, 0.008	0.1122	1.4442	1.4313

**Table 5: The best WA-ANN and WA-SVR models for 1 and 3 month forecasts of SPI 1**

Column 3 is the ANN architecture detailing the number of nodes in the input, hidden and output layers respectively. In column 7 the parameters of the SVR models are given

Basin	Station	WA-ANN	R <sup>2</sup>	RMSE	MAE	WA-SVR	R <sup>2</sup>	RMSE	MAE
<b>1 month lead time</b>									
Upper	Bantu Liben	4-7-1	0.3064	1.1343	1.0871	0.02, 96, 0.002	0.2872	1.1983	1.1782
	Tullo Bullo	5-6-1	0.2600	1.0469	1.0392	0.03, 95, 0.002	0.2832	1.1895	1.1837
	Ginchi	4-7-1	0.2686	1.0483	1.0412	0.08, 90, 0.05	0.2777	1.1746	1.1348
	Sebeta	4-5-1	0.3006	1.0557	1.0482	0.06, 100, 0.01	0.2938	1.1839	1.0781
	Ejersalele	7-4-1	0.3361	1.3183	1.0972	0.05, 98, 0.007	0.2981	1.1238	1.0617
	Ziquala	6-4-1	0.3102	1.0652	1.0551	0.04, 88, 0.08	0.3163	1.1765	1.1033
	Debre Zeit	7-5-1	0.2754	1.1327	1.0834	0.05, 96, 0.06	0.2871	1.1389	1.0579
Middle	Koka	4-5-1	0.2625	1.1783	1.1643	0.05, 100, 0.003	0.2716	1.1293	1.1093
	Modjo	5-5-1	0.2638	1.0387	1.0331	0.08, 90, 0.08	0.2879	1.1389	1.1006
	Nazereth	4-6-1	0.2895	1.0536	1.0422	0.07, 94, 0.03	0.2183	1.1384	1.1289
	Wolenchiti	4-4-1	0.3145	1.0346	1.0312	0.07, 92, 0.004	0.2983	1.2840	1.2791
	Gelemsso	6-4-1	0.2653	1.0484	1.0312	0.05, 93, 0.003	0.2765	1.1132	1.0882
	Dire Dawa	4-5-1	0.2741	1.0534	1.0432	0.02, 96, 0.007	0.2598	1.0183	1.0175
Lower	Dubti	4-6-1	0.2838	1.1627	1.0934	0.08, 97, 0.05	0.2688	1.1844	1.1736
	Eliwuha	5-4-1	0.2940	1.3659	1.0995	0.06, 98, 0.06	0.2606	1.1930	1.1728
	Mersa	7-4-1	0.3158	1.1453	1.0753	0.09, 100, 0.008	0.3193	1.2914	1.1897
	Mille	5-4-1	0.2849	1.1483	1.0921	0.06, 91, 0.007	0.2793	1.1378	1.0926
	Bati	5-4-1	0.3056	1.0135	1.0126	0.05, 93, 0.004	0.2953	1.1469	1.1146
<b>3 month lead time</b>									
Upper	Bantu Liben	5-7-1	0.2420	1.1476	1.1351	0.05, 96, 0.002	0.2291	1.2236	1.2012
	Tullo Bullo	6-6-1	0.2398	1.1378	1.1231	0.02, 92, 0.005	0.1732	1.3243	1.3041
	Ginchi	5-7-1	0.2036	1.1323	1.0948	0.06, 99, 0.006	0.1938	1.1224	1.0864
	Sebeta	5-5-1	0.1723	1.1378	1.1073	0.09, 90, 0.008	0.1748	1.1453	1.0815
	Ejersalele	7-4-1	0.2007	1.1257	1.1066	0.08, 92, 0.006	0.1981	1.1234	1.0759
	Ziquala	7-4-1	0.1703	1.1921	1.1479	0.07, 93, 0.004	0.1838	1.1565	1.1037
	Debre Zeit	7-5-1	0.1463	1.1389	1.1224	0.05, 94, 0.006	0.1839	1.2104	1.2063
Middle	Koka	5-5-1	0.1741	1.1597	1.1487	0.05, 87, 0.005	0.2203	1.2143	1.1933
	Modjo	6-5-1	0.1414	1.1568	1.1507	0.05, 100, 0.003	0.1210	1.1330	1.1249
	Nazereth	5-6-1	0.1368	1.1281	1.1076	0.08, 93, 0.01	0.1303	1.2401	1.1837
	Wolenchiti	5-4-1	0.1244	1.1556	1.1365	0.08, 95, 0.002	0.1234	1.1304	1.1192
	Gelemsso	7-4-1	0.1829	1.0448	1.0871	0.04, 94, 0.003	0.1123	1.2430	1.2162
	Dire Dawa	5-5-1	0.1655	1.3851	1.3382	0.05, 85, 0.009	0.1241	1.2049	1.1897
Lower	Dubti	5-6-1	0.2027	1.1711	1.1598	0.08, 97, 0.05	0.1378	1.1381	1.1329
	Eliwuha	6-4-1	0.2126	1.1372	1.1149	0.09, 90, 0.007	0.1483	1.1378	1.1283
	Mersa	7-4-1	0.1997	1.1204	1.1043	0.03, 95, 0.009	0.1599	1.1293	1.1158
	Mille	6-4-1	0.1712	1.1600	1.1587	0.05, 100, 0.005	0.1418	1.1357	1.1175
	Bati	6-4-1	0.1576	1.0271	1.0641	0.04, 98, 0.008	0.1621	1.1422	1.1126

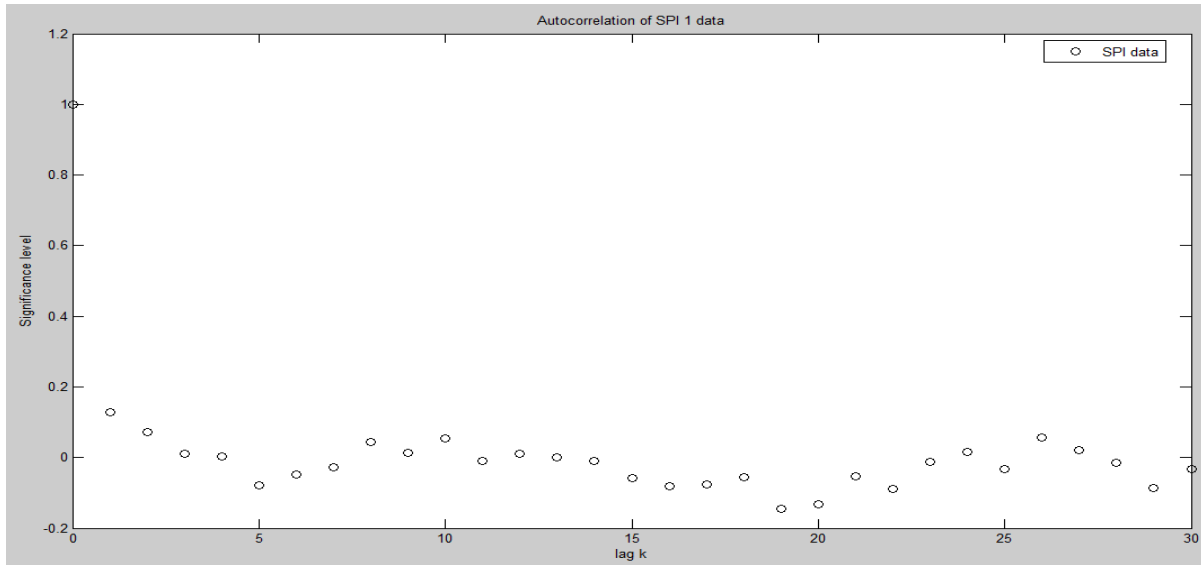


**Figure 2: Autocorrelation plot for the selection of candidate SPI 1 models.**

Figure 2 and 3 show the autocorrelations of SPI 1 and SPI 3 data respectively. These figures illustrate how the autocorrelation within the SPI 3 data is greater than SPI data as the lag is increased. This trend is a possible explanation for why results of SPI 1 forecasts have low  $R^2$  values.

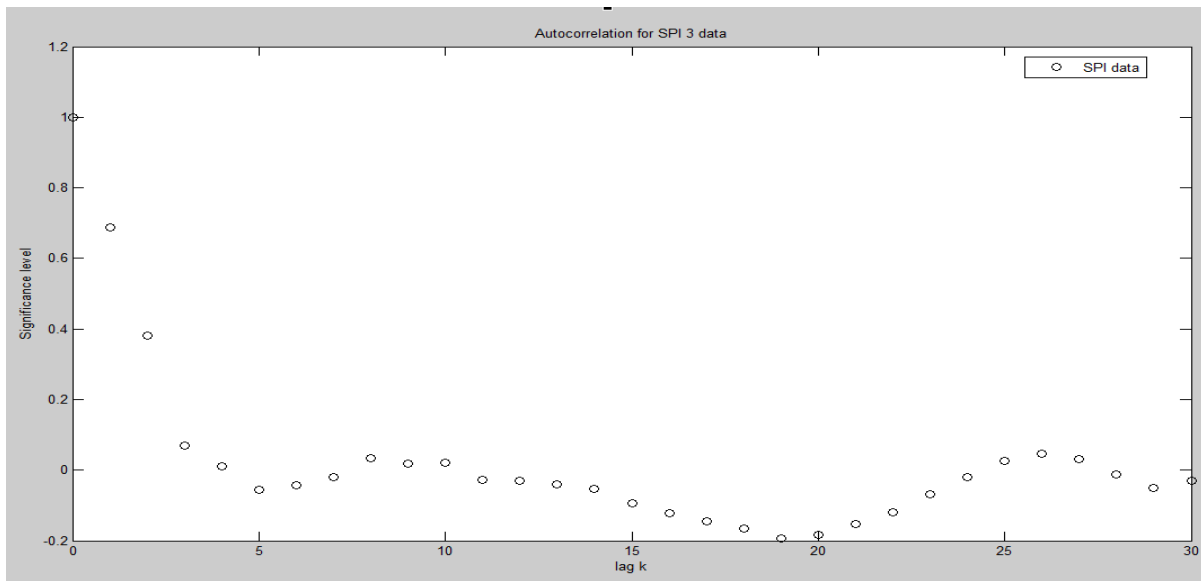


**Figure 3: Autocorrelation plot for the selection of candidate SPI 3 models.**

### 3.5.2 SPI 3 forecasts

The SPI 3 forecast results for all data driven models are presented in figures 6 and 7. Similar to the forecast results for SPI 1, as the forecast lead time is increased, the forecast accuracy deteriorates. In the Upper Awash basin, the best data driven model for SPI 3 forecasts of 1 month lead time was a WA-ANN model. The WA-ANN model at the Ziquala station had the best results in terms of RMSE and MAE, with forecast results of 1.1072 and 1.0918, respectively. The Ginchi station had the best WA-ANN model in terms of  $R^2$ , with forecast results of 0.8808. When the forecast lead time is increased to 3 months, the best models remain WA-ANN models. The Bantu Liben station had the model with the lowest RMSE and MAE values of 1.1098 and 1.0941, respectively. The Sebeta station had the best results in terms of  $R^2$ , with a value of 0.7301.

In the Middle Awash basin, for forecasts of 1 month lead time, WA-ANN and WA-SVR models had the best forecast results. The WA-ANN model at the Koka station had the best results in terms of  $R^2$  with a value of 0.9245. However, unlike the Upper Awash basin, the best forecast results in terms of RMSE and MAE were from a WA-SVR model. The WA-SVR model at the Modjo station had the lowest RMSE and MAE values of 1.1309 and 1.1018, respectively. For forecasts of 3 months lead time, WA-ANN models had the best results across all performance measures with the Koka station having the highest value of  $R^2$  at 0.7513 and the Gelemsso station having the lowest RMSE and MAE values of 1.1448 and 1.1334, respectively.

In the Lower Awash basin, for forecasts of 1 month lead time, the best results were from WA-ANN and WA-SVR models, similar to the Middle Awash basin. The highest value for  $R^2$  was 0.8008 and it was from the WA-ANN model at the Bati station. The lowest values for RMSE and MAE were 1.1023 and 1.0738, and were from the WA-SVR model at the Dubti station. For forecasts of 3 months lead time the best results were observed at the Bati station. The WA-ANN model at this station had the highest  $R^2$  value of 0.6006 and the WA-SVR model at this station had the lowest RMSE and MAE values of 1.1089 and 1.0884, respectively.

**Table 6: The best ARIMA, ANN and SVR models for 1 and 3 month forecasts of SPI 3**

Column 3 is the ANN architecture detailing the number of nodes in the input, hidden and output layers respectively. In column 11 the parameters of the SVR models are given.

Basin	Station	ANN models	R <sup>2</sup>	RMSE	MAE	ARIMA models	R <sup>2</sup>	RMSE	MAE	SVR ( $\gamma, C, \epsilon$ )	R <sup>2</sup>	RMS E	MAE
1 month lead time													
Upper	Bantu Liben	3-4-1	0.777	0.729	0.713	(5,1,0)	0.743	0.246	0.225	0.8, 98, 0.008	0.804	0.229	0.219
	Tullo Bullo	3-4-1	0.774	0.718	0.709	(3,0,2)	0.755	0.253	0.220	0.8, 94, 0.006	0.814	0.239	0.200
	Ginchi	4-4-1	0.725	0.744	0.729	(3,0,0)	0.698	0.232	0.224	0.5, 95, 0.007	0.753	0.203	0.192
	Sebeta	4-4-1	0.848	0.740	0.721	(3,1,1)	0.768	0.222	0.217	0.4, 90, 0.008	0.746	0.235	0.223
	Ejersalele	5-4-1	0.718	0.751	0.739	(1,0,0)	0.713	0.253	0.246	0.5, 95, 0.005	0.782	0.209	0.203
	Ziquala	3-4-1	0.735	0.715	0.704	(1,0,0)	0.718	0.246	0.236	0.6, 93, 0.004	0.792	0.239	0.214
	Debre Zeit	4-4-1	0.763	0.745	0.734	(3,0,0)	0.732	0.256	0.226	0.5, 95, 0.009	0.800	0.208	0.198
Middle	Koka	4-4-1	0.730	0.748	0.733	(3,1,0)	0.715	0.251	0.223	0.3, 97, 0.006	0.735	0.239	0.202
	Modjo	3-4-1	0.783	0.720	0.697	(5,0,1)	0.721	0.235	0.216	0.5, 94, 0.004	0.733	0.232	0.229
	Nazereth	4-4-1	0.732	0.717	0.702	(4,1,0)	0.727	0.235	0.218	0.8, 98, 0.01	0.792	0.183	0.164
	Wolenchiti	3-4-1	0.739	0.704	0.689	(3,0,2)	0.710	0.251	0.244	0.7, 98, 0.004	0.744	0.209	0.192
	Gelemsso	4-4-1	0.808	0.740	0.697	(3,0,0)	0.716	0.252	0.235	0.4, 88, 0.007	0.832	0.239	0.210
	Dire Dawa	3-4-1	0.777	0.707	0.697	(1,1,1)	0.711	0.252	0.233	0.6, 93, 0.004	0.800	0.223	0.211
Lower	Dubti	3-4-1	0.737	0.752	0.731	(2,0,0)	0.732	0.254	0.241	0.9, 92, 0.008	0.767	0.219	0.204
	Eliwuha	4-4-1	0.709	0.732	0.723	(1,1,1)	0.701	0.256	0.253	0.6, 94, 0.008	0.731	0.214	0.203
	Mersa	3-5-1	0.706	0.737	0.720	(2,0,1)	0.694	0.253	0.238	0.4, 96, 0.006	0.749	0.206	0.195
	Mille	3-4-1	0.730	0.744	0.724	(3,1,0)	0.726	0.251	0.249	0.6, 88, 0.007	0.754	0.215	0.202
	Bati	4-4-1	0.702	0.738	0.704	(5,0,0)	0.699	0.240	0.225	0.65, 91, 0.008	0.732	0.202	0.199
3 month lead time													
Upper	Bantu Liben	4-4-1	0.500	0.978	0.954	(4,0,0)	0.460	0.345	0.314	0.7, 99, 0.006	0.500	0.284	0.371
	Tullo Bullo	4-4-1	0.515	0.988	0.947	(3,1,0)	0.466	0.336	0.305	0.65, 100, 0.01	0.472	0.234	0.215
	Ginchi	5-4-1	0.516	0.949	0.942	(3,0,1)	0.454	0.263	0.254	0.8, 84, 0.004	0.475	0.236	0.218
	Sebeta	5-4-1	0.587	0.925	0.908	(3,1,2)	0.446	0.313	0.287	0.7, 87, 0.005	0.448	0.295	0.290
	Ejersalele	4-4-1	0.512	0.961	0.957	(1,0,0)	0.452	0.293	0.272	0.6, 93, 0.008	0.462	0.281	0.266
	Ziquala	4-4-1	0.462	0.996	0.974	(1,1,0)	0.446	0.293	0.265	0.85, 90, 0.007	0.466	0.239	0.227
	Debre Zeit	5-4-1	0.514	0.942	0.939	(1,0,1)	0.456	0.302	0.285	0.8, 96, 0.008	0.450	0.294	0.280
Middle	Koka	5-4-1	0.446	0.962	0.937	(1,0,1)	0.436	0.314	0.286	0.5, 99, 0.006	0.494	0.257	0.239
	Modjo	4-4-1	0.406	0.963	0.947	(2,1,0)	0.406	0.316	0.315	0.65, 97, 0.007	0.500	0.249	0.233
	Nazereth	5-4-1	0.450	0.938	0.920	(1,0,0)	0.436	0.326	0.322	0.6, 92, 0.011	0.451	0.251	0.240
	Wolenchiti	4-4-1	0.492	0.961	0.952	(1,1,1)	0.453	0.323	0.314	0.55, 85, 0.004	0.450	0.244	0.230
	Gelemsso	5-4-1	0.424	0.994	0.971	(3,0,0)	0.414	0.325	0.305	0.6, 90, 0.007	0.494	0.232	0.219
	Dire Dawa	4-4-1	0.435	0.986	0.959	(1,0,0)	0.416	0.327	0.325	0.6, 86, 0.01	0.524	0.249	0.233
Lower	Dubti	4-4-1	0.402	0.950	0.942	(1,0,0)	0.401	0.351	0.321	0.6, 90, 0.008	0.603	0.239	0.224
	Eliwuha	5-4-1	0.480	0.962	0.945	(1,0,0)	0.456	0.352	0.349	0.7, 92, 0.01	0.611	0.246	0.236
	Mersa	4-5-1	0.440	0.958	0.940	(2,0,2)	0.427	0.314	0.305	0.6, 93, 0.009	0.565	0.245	0.226
	Mille	4-4-1	0.461	0.941	0.903	(3,0,1)	0.454	0.354	0.348	0.8, 79, 0.001	0.559	0.242	0.227
	Bati	5-4-1	0.471	0.961	0.984	(1,0,1)	0.456	0.325	0.315	0.07, 87, 0.004	0.587	0.249	0.238

**Table 7: The best WA-ANN and WA-SVR models for 1 and 3 month forecasts of SPI 3.**

Column 3 is the ANN architecture detailing the number of nodes in the input, hidden and output layers respectively.

In column 7 the parameters of the SVR models are given

Basin	Station	WA-ANN	R <sup>2</sup>	RMSE	MAE	WA-SVR	R <sup>2</sup>	RMSE	MAE
<b>1 month lead time</b>									
<b>Upper</b>	Bantu Liben	4-7-1	0.7952	0.1300	0.0922	0.8, 98, 0.008	0.7228	0.1461	0.1038
	Tullo Bullo	5-6-1	0.8582	0.1539	0.0957	0.8, 94, 0.006	0.8349	0.1062	0.0837
	Ginchi	4-7-1	0.8808	0.1663	0.0598	0.5, 95, 0.007	0.8462	0.1293	0.1188
	Sebeta	4-5-1	0.8722	0.1742	0.1118	0.4, 90, 0.008	0.8029	0.1183	0.0961
	Ejersalele	7-4-1	0.7797	0.1700	0.1012	0.5, 95, 0.005	0.8193	0.1829	0.1711
	Ziquala	6-4-1	0.7997	0.1072	0.0918	0.6, 93, 0.004	0.7628	0.1830	0.1627
	Debre Zeit	7-5-1	0.8610	0.1819	0.0774	0.5, 95, 0.009	0.8271	0.1761	0.1647
<b>Middle</b>	Koka	4-5-1	0.9245	0.1849	0.1561	0.3, 97, 0.006	0.8282	0.1493	0.1328
	Modjo	5-5-1	0.8564	0.1975	0.1580	0.5, 94, 0.004	0.8398	0.1309	0.1018
	Nazereth	4-6-1	0.8993	0.1510	0.1455	0.8, 98, 0.01	0.8384	0.1930	0.1721
	Wolenchiti	4-4-1	0.7632	0.1781	0.1202	0.7, 98, 0.004	0.8429	0.1839	0.1683
	Gelemsso	6-4-1	0.8130	0.1409	0.1248	0.4, 88, 0.007	0.8287	0.1389	0.1104
	Dire Dawa	4-5-1	0.7816	0.1893	0.1735	0.6, 93, 0.004	0.8245	0.1738	0.1596
<b>Lower</b>	Dubti	4-6-1	0.7857	0.1105	0.1003	0.9, 92, 0.008	0.7283	0.1023	0.0738
	Eliwuha	5-4-1	0.7723	0.1217	0.0996	0.6, 94, 0.008	0.7911	0.1048	0.0173
	Mersa	7-4-1	0.7495	0.1127	0.1067	0.4, 96, 0.006	0.7238	0.1079	0.0934
	Mille	5-4-1	0.7507	0.1985	0.0875	0.6, 88, 0.007	0.7311	0.1281	0.0852
	Bati	5-4-1	0.8008	0.1039	0.0954	0.65, 91, 0.008	0.7256	0.1032	0.0818
<b>3 month lead time</b>									
<b>Upper</b>	Bantu Liben	5-7-1	0.5566	0.1098	0.0941	0.7, 99, 0.006	0.5817	0.2012	0.1871
	Tullo Bullo	6-6-1	0.6007	0.1566	0.1039	0.65, 100, 0.01	0.5829	0.1821	0.1734
	Ginchi	5-7-1	0.6204	0.1708	0.1143	0.8, 84, 0.004	0.5171	0.1782	0.1638
	Sebeta	5-5-1	0.7301	0.1820	0.1345	0.7, 87, 0.005	0.5281	0.1827	0.1739
	Ejersalele	7-4-1	0.7178	0.1843	0.1406	0.6, 93, 0.008	0.5812	0.1922	0.1782
	Ziquala	7-4-1	0.5598	0.1568	0.1343	0.85, 90, 0.007	0.5821	0.1881	0.1781
	Debre Zeit	7-5-1	0.6458	0.1906	0.1416	0.8, 96, 0.008	0.5721	0.1872	0.1721
<b>Middle</b>	Koka	5-5-1	0.7513	0.1904	0.1602	0.5, 99, 0.006	0.6248	0.2019	0.1921
	Modjo	6-5-1	0.6808	0.1996	0.1604	0.65, 97, 0.007	0.6093	0.1921	0.1829
	Nazereth	5-6-1	0.5942	0.1665	0.1424	0.6, 92, 0.011	0.6189	0.1991	0.1829
	Wolenchiti	5-4-1	0.6059	0.1809	0.1738	0.55, 85, 0.004	0.6018	0.1921	0.1829
	Gelemsso	7-4-1	0.5285	0.1498	0.1334	0.6, 90, 0.007	0.5728	0.1721	0.1617
	Dire Dawa	5-5-1	0.6256	0.1966	0.1828	0.6, 86, 0.01	0.6092	0.1921	0.1817
<b>Lower</b>	Dubti	5-6-1	0.5893	0.1487	0.1325	0.6, 90, 0.008	0.5034	0.1156	0.1039
	Eliwuha	6-4-1	0.5792	0.1908	0.1783	0.7, 92, 0.01	0.5056	0.1159	0.1129
	Mersa	7-4-1	0.5621	0.1884	0.1725	0.6, 93, 0.009	0.5051	0.1253	0.1090
	Mille	6-4-1	0.5630	0.1993	0.1403	0.8, 79, 0.001	0.5915	0.1494	0.1287
	Bati	6-4-1	0.6006	0.1670	0.1523	0.07, 87, 0.004	0.5838	0.1089	0.0884

### 3.5.3 Discussion

As shown in the forecast results for both SPI 1 and SPI 3, the use of wavelet analysis increased forecast accuracy for both 1 month and 3 month forecast lead times. Once the original SPI time series was decomposed using wavelet analysis it was found that the approximation series of the signal was disproportionately more important for future forecasts compared to the wavelet detail series of the signal. Irrespective of the number of decomposition levels, an absence of the approximation series would result in poor forecast results. Adding the approximation series to the wavelet details did not noticeably improve the forecast results compared to using the approximation series on its own in most models. Traditionally, the number of wavelet decompositions is either determined via trial and error or using the formula  $L = \log [N]$ , with  $N$  being the number of samples. Using this formula the optimal number of decompositions would be  $L = 3$ . In this study, the above method was repeated for wavelet decomposition levels 1 through 9 until the appropriate level was determined using the aforementioned performance measures.

In general, WA-ANN models were the best forecast models in each of the sub-basins. In the Upper Awash basin, WA-ANN models had the best forecast results in terms of  $R^2$  at all the stations. WA-SVR models had the second best forecast results in terms of  $R^2$  in four stations and ANN models had the second best results twice. With respect to RMSE the WA-ANN models had the best forecast results in five out of seven stations while WA-SVR models had the best forecast results twice. With respect to MAE, the Upper basin WA-ANN was the best model at 3 stations and the second best at 3 stations. WA-SVR was the best at 2 stations and the second best at one station. ANN was the best at one station and second best at one station. An ANN model having the best forecasts is unusual given the presence of WA-ANN and WA-SVR models. However, the ANN model in question had the best results regarding 1 out of 3 forecast criteria. ARIMA models had the best results at one station. The fact that ARIMA models produced the least accurate results was expected. Unlike the other models used in this study ARIMA models were linear in nature and are not as effective as ANNs or SVR models in forecasting non-linear trends in precipitation.

In the Middle Awash basin WA-ANN models were the best models in terms of  $R^2$  in 4 out of the 6 stations. In the other 2 stations WA-SVR models had the best results. In terms of RMSE, WA-SVR models had the best results in 4 out of 6 stations, while the WA-ANN models has the best results in the remaining 3 stations. In terms of MAE WA-ANN and WA-SVR models had the best results in 2 and 4 out of 6 stations respectively.

In the Lower Awash Basin WA-ANN models had the best results in terms of  $R^2$  in 4 out of 5 of the stations, while the WA-SVR model had the best forecast result in the remaining station. Conversely, the WA-SVR models had the best results in terms of RMSE and MAE in all 5 of the stations, while the WA-ANN models had the second best forecast results in all 5 of the stations.

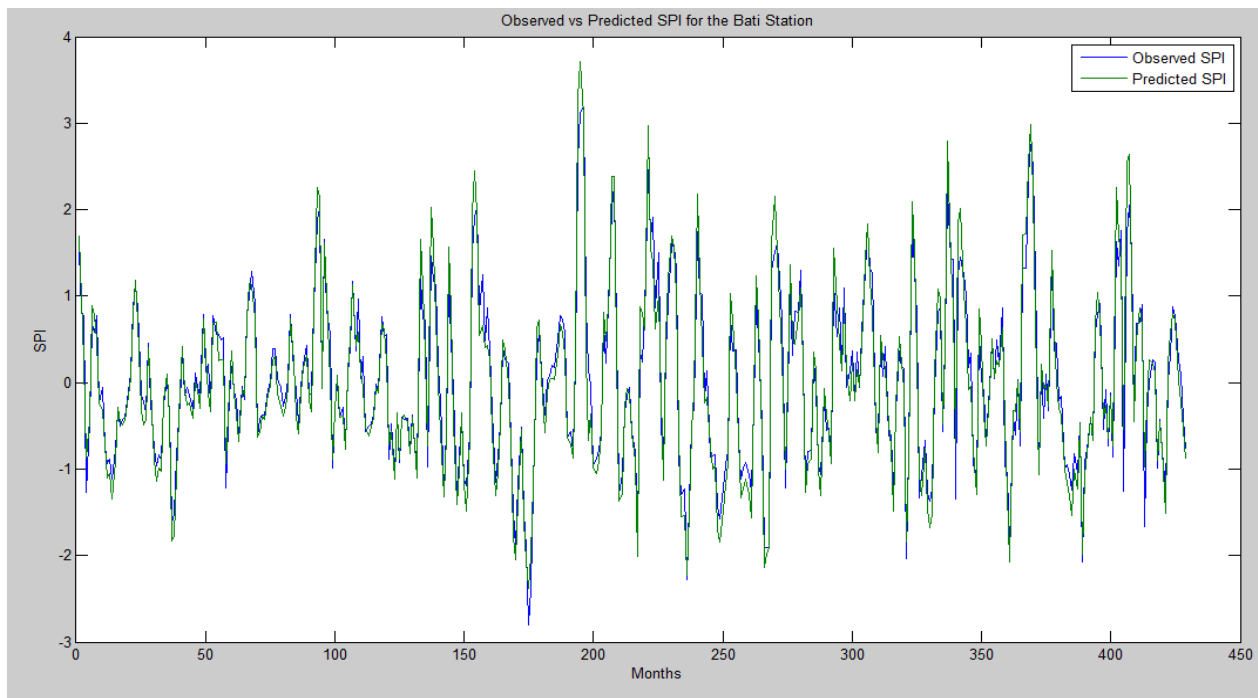


**Figure 4: SPI 3 forecast results for the best WA-ANN model at the Bati station for 1 month lead time.**

While both the WA-ANN and WA-SVR models were effective in forecasting SPI 3, most WA-ANN models had more accurate forecasts. In addition, as shown by Figures 3 and 4, the forecast from the WA-ANN model seems to be more effective in forecasting the extreme SPI values, whether indicative of severe drought or heavy precipitation. While the WA-SVR model closely mirrors the observed SPI trends, it seems to underestimate the extreme events, especially the extreme drought event at 170 months.

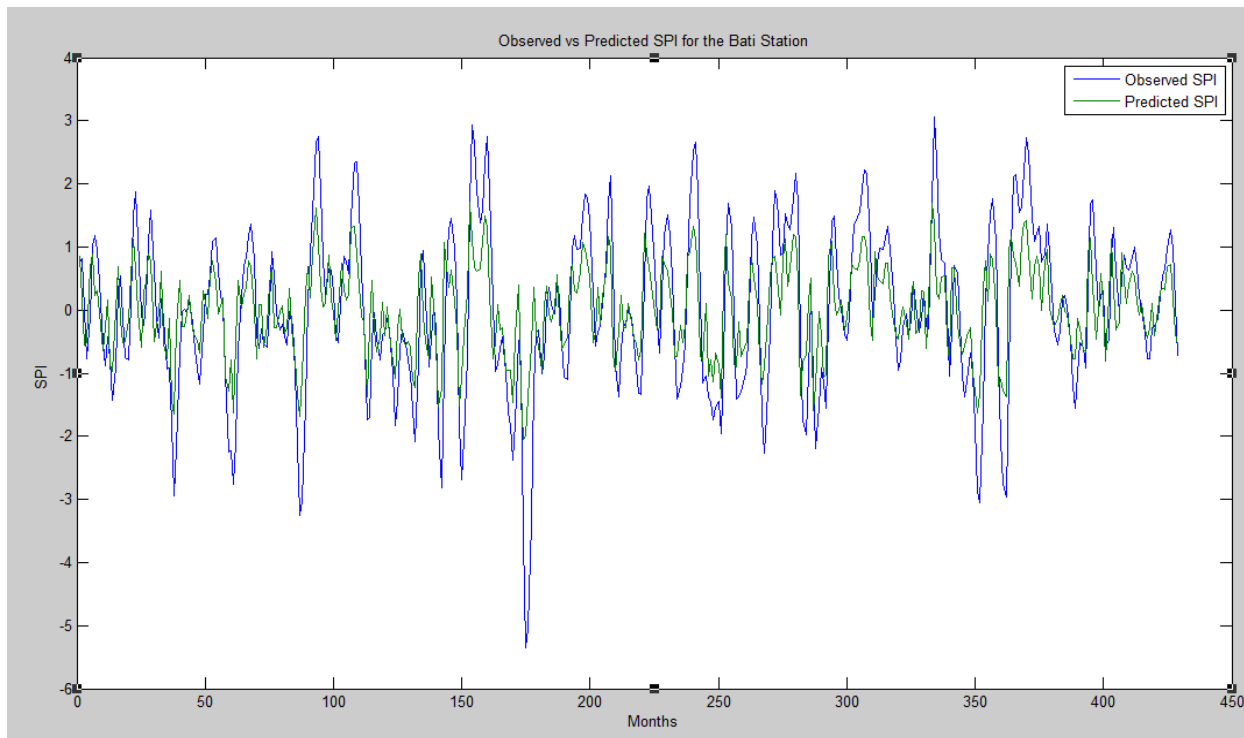


**Figure 5: SPI 3 forecast results for the best WA-SVR model at the Bati Station for 1 month lead time.**

The reason why WA-ANN models seem to be slightly more effective than WA-SVR models, and seem to be more effective in forecasting extreme events, is likely due to the inherent effectiveness of ANNs compared to SVR models, such as their simplicity in terms of development and their reduced computation time, as the wavelet analysis used for both machine learning techniques is the same. This observation is further supported by the fact that most ANN forecasts have better results than SVR models as shown in Table 4. Theoretically, SVR models should perform better than ANN models because they adhere to the structural risk minimization principle instead of the empirical risk minimization principle. They should, in theory, not be as susceptible to local minima or maxima. However, the performance of SVR models is highly dependent of the selection of the appropriate kernel and its three parameters. Given that there are no prior studies on the selection of these parameters for forecasts of the SPI, the selection was done via a trial and error procedure. This process is made even more difficult by the size of the data set (monthly data from 1970-2005), which contributes to the long computation time of SVR models. The uncertainty regarding the three SVR parameters increases the number of trials

required to obtain the optimal model. Due to the long computational time of SVR models the same amount of trials cannot be done as for ANN models. For ANN models, even in complex systems, the relationship between input and output variables does not need to be fully understood. Effective models can be determined by varying the number of neurons within the hidden layer. Producing several models with varying architectures is not computationally intensive and allows for a larger selection pool for the optimal model. In addition, the ability of wavelet analysis to effectively forecast local discontinuities likely reduces the susceptibility in ANN models when they are coupled.

This study also shows that the à trous algorithm is an effective tool for forecasting SPI time series. The à trous algorithm de-noises a given time series and improves the performances of both ANN and SVR models. The à trous algorithm is shift invariant, making it more applicable for forecasting studies, which includes drought forecasting. The fact that wavelet based models had the best results is likely due to the fact that wavelet decomposition was able to capture non-stationary features of the data.

### **3.6 Conclusion**

This study explored forecasting short-term drought conditions using five different data driven models in the Awash River basin, including newly proposed methods based on SVR and WA-SVR. With respect to wavelet analysis, this study found, for the first time, that the use of only the approximation series was effective in de-noising a given SPI time series. SPI 1 and SPI 3 were forecast over lead times of 1 and 3 months using ARIMA, ANN, SVR, WA-SVR and WA-ANN models. Forecast results for SPI 1 were low in terms of the coefficient of determination, likely a result of the low levels of autocorrelation of the data sets compared to SPI 3. Overall, the WA-ANN method, with a new method for determining the optimal number of neurons within the hidden layer, had the best forecast results with WA-SVR models also having very good results. Wavelet coupled models consistently showed lower values of RMSE and MAE compared to the other data driven models, possibly because wavelet decomposition de-noises a given time series subsequently allowing either ANN or SVR models to forecast the main signal rather than the main signal with noise.

Studies should also focus on different regions and try to compare the effectiveness of data driven methods in forecasting different drought indices. This study has not found a clear link between a particular sub-basin and performance indicating the need for further studies in different climates to determine whether there is a significant link between forecast accuracy and climate. The coupling of these data driven models with uncertainty analysis techniques such as bootstrapping should be investigated. In addition, coupling SVR models with genetic algorithms to make parameter estimation more efficient could be explored.

### **Acknowledgements**

An NSERC Discovery and FQNRT New Researcher Grant held by Dr. Jan Adamowski were used to fund this research. The data was obtained from the Meteorological Society of Ethiopia (NMSA). Their help is greatly appreciated.

### **References**

Abramowitz, M., Stegun, A. (eds.), (1965). Handbook of Mathematical Formulas, Graphs, and Mathematical Tables. Dover Publications, Inc., New York, USA.

Adamowski, J. (2008). Development of a short-term river flood forecasting method for snowmelt driven floods based on wavelet and cross-wavelet analysis. *Journal of Hydrology*. 353: 247-266.

Adamowski, J., Sun, K. (2010). Development of a coupled wavelet transform and neural network method for flow forecasting of non-perennial rivers in semi-arid watersheds. *Journal of Hydrology* 390: 85-91.

Adamowski, J., Chan, H.F. (2011). A wavelet neural network conjunction model for groundwater level forecasting. *Journal of Hydrology* 407: 28-40.

ASCE Task Committee on Application of Artificial Neural Networks in Hydrology, (2000a). Artificial neural networks in hydrology. I. Preliminary concepts. *Journal of Hydrologic Engineering*. 5 (2): 124–137.

ASCE Task Committee on Application of Artificial Neural Networks in Hydrology, 2000b. Artificial neural networks in hydrology. II. Hydrologic applications. *Journal of Hydrologic Engineering*. 5 (2): 115–123.

Asefa, T., Kemblowski, M., McKee, M., Khalil, A. (2006). Multi-time scale stream flow 505 predicitions: The support vector machines approach. *Journal of Hydrology*, 318 (1-4): 7-16.

Bacanli, U. G., Firat, M., Dikbas, F. (2008). Adaptive Neuro-Fuzzy Inference System for drought forecasting. *Stochastic Environmental Research and Risk Assessment* 23(8): 1143-1154.

- Barros, A. and Bowden G. (2008). Toward long-lead operational forecasts of drought: An experimental study in the Murray-Darling River Basin. *Journal of Hydrology* 357(3-4): 349-367.
- Bonaccorso B, Bordi I, Cancelliere A, Rossi G, Sutera A. (2003) Spatial variability of drought: an analysis of SPI in Sicily. *Water Resour Manag* 17:273–296.
- Box, G.E.P., Jenkins, G.M. (1976). *Time Series Analysis, Forecasting and Control*. Holden-Day, San Francisco.
- Box, G.E.P., Jenkins, G.M., Reinsel, G.C. (1994). *Time Series Analysis, Forecasting and Control*. Prentice Hall, Englewood Cliffs, NJ, USA.
- Byun, H.R., Wilhite, D.A., (1999). Objective quantification of drought severity and duration. *Journal of Climatology* 12: 2747–2756.
- Cacciamani, C., Morgillo, A., Marchesi, S., Pavan, V. (2007). Monitoring and Forecasting Drought on a Regional Scale: Emilia-Romagna Region. *Water Science and Technology Library* 62(1): 29-48
- Cancelliere, A., Di Mauro, G., Bonaccorso, B., Rossi, G. (2006). Drought forecasting using the Standardized Precipitation Index. *Water Resources Management* 21(5): 801-819.
- Cancelliere, A., Di Mauro, G., Bonaccorso, B., Rossi, G. (2007). Stochastic Forecasting of Drought Indices, G. Rossi et al. (eds.) *Methods and Tools for Drought Analysis and Management*. Springer
- Cannas, B., A. Fanni, Sias, G., Tronci, S., Zedda, M.K. (2006). River flow forecasting using neural networks and wavelet analysis. *Proceedings of the European Geosciences Union*
- Cimen, M., (2008). Estimation of daily suspended sediments using support vector machines. *Hydrol. Sci. J.* 53 (3), 656–666.
- Coulibaly, P., Anctil, F., Bobee, B. (2000). Daily reservoir inflow forecasting using artificial neural networks with stopped training approach. *Journal of Hydrology* 230: 244–257.
- Cutore, P., Di Mauro, G., Cancelliere, A. (2009). Forecasting Palmer Index Using Neural Networks and Climatic Indexes
- Desalegn, C., Babel, M.S., Das Gupta, A., Seleshi, B.A., Merrey, D. (2006). Farmers' perception about water management under drought conditions in the Awash River Basin, Ethiopia. *Int J Water Resour Dev* 22(4):589–602
- Edossa, D.C., Babel, M.S., Gupta, A.D. (2010). Drought Analysis on the Awash River Basin, Ethiopia. *Water Resource Management* 24: 1441-1460

Edwards, D.C., McKee, T.B., 1997. Characteristics of 20th Century Drought in the United States at Multiple Scales. Atmospheric Science Paper: 634.

Gao, J.B., Gunn, S.R., Harris, J., Brown, M. (2001). A probabilistic framework for SVM regression and error bar estimation. Mach. Learn. 46: 71–89.

Gibbs, W.J., Maher, J.V. (1967). Rainfall Deciles as Drought Indicators. Bureau of Meteorology Bull. 48. Commonwealth of Australia, Melbourne, Australia.

Guttman, N.B. (1999). Accepting the standardized precipitation index: a calculation algorithm. Journal of American Water Resource Association. 35 (2): 311–322.

Han, P., Wang, P., Zhang, S., Zhu, D. (2010). Drought forecasting with vegetation temperature condition index. Wuhan Daxue Xuebao (Xinxi Kexue Ban)/Geomatics and Information Science of Wuhan University 35 (10): 1202-1206+1259.

Hayes, M., (1996). Drought Indexes. National Drought Mitigation Center, University of Nebraska–Lincoln, p. 7 (available from University of Nebraska–Lincoln, 239LW Chase Hall, Lincoln, NE 68583).

Holder, R.L. (1985). Multiple linear regression in hydrology. pp.32. Institute of hydrology. Oxfordshire.

Karamouz, M., Rasouli, K., Nazil, S. (2009). Development of a Hybrid Index for Drought Prediction: Case Study. Journal of Hydrologic Engineering. 14: 617-627

Khan, M.S., Coulibaly, P. (2006). Application of support vector machine in lake water level prediction. Journal of Hydrologic Engineering 11(3): 199-205, American Society of Civil Engineering.

Kim, T., Valdes, J.B. (2003). Nonlinear Model for Drought Forecasting Based on a Conjunction of Wavelet Transforms and Neural Networks. Journal of Hydrologic Engineering 8: 319-328

Kisi, O., Cimen, M. (2009). Evapotranspiration modelling using support vector machines. Hydrological Science Journal 54 (5): 918-928. Taylor and Francis Ltd.

Kisi, O., Cimen, M. (2011). A wavelet-support vector machine conjunction model for monthly streamflow forecasting. Journal of Hydrology 399: 132-140.

Labat, D., Ababou, R., Mangin, A. (1999). Wavelet analysis in Karstic hydrology 2nd Part: rainfall–runoff cross-wavelet analysis. Comptes Rendus de l’Academie des Sciences Series IIA Earth and Planetary Science 329: 881–887

Lane, S.N., 2007. Assessment of rainfall–runoff models based upon wavelet analysis. Hydrological Processes 21: 586–607.

Linsley, R.K., Kohler, M.A., Paulhus, J.L.H. (1988). Hydrology for engineers. International Edition. McGraw-Hill, Singapore

Maity, R., Bhagwat, P.P., Bhatnagar, A. (2010). Potential of support vector regression for prediction of monthly streamflow using endogenous property. *Hydrological Processes* 24: 917-923

Mallat, S. G. (1998). A wavelet tour of signal processing, Academic, San Diego, 577.

Marj, A.F., Meijerink, A.M. (2011). Agricultural drought forecasting using satellite images, climate indices and artificial neural network. *International Journal of Remote Sensing* 32(24): 9707-9719

McKee, T.B., Doesken, N.J., Kleist, J. (1993). The Relationship of Drought Frequency and Duration to Time Scales, Paper Presented at 8th Conference on Applied Climatology. American Meteorological Society, Anaheim, CA.

Mersha, E. and Boken, V.K. (2005) Agricultural Drought in Ethiopia, In V.K Boken, A.P Cracknell and R.L Heathcote (ed.), *Monitoring and Predicting Agricultural Drought: A Global Study*. Oxford University Press

Mishra, A. K. and V. R. Desai (2005). Drought forecasting using stochastic models. *Stochastic Environmental Research and Risk Assessment* 19(5): 326-339.

Mishra, A. K. and V. R. Desai (2006). Drought forecasting using feed-forward recursive neural network. *Ecological Modelling* 198(1-2): 127-138.

Mishra, A. K. and V. P. Singh (2010). A review of drought concepts. *Journal of Hydrology* 391(1-2): 202-216.

Morid, S., Smakhtin, V., Bagherzadeh, K. (2007). Drought forecasting using artificial neural networks and time series of drought indices. *International Journal of Climatology* 27(15): 2103-2111.

Morid, S., Smakhtin, V., Moghaddasi, M. (2006). Comparison of seven meteorological indices for drought monitoring in Iran. *International Journal of Climatology* 26(7): 971-985.

Murtagh, F., Starcj, J.L., Renaud, O. (2003). On neuro-wavelet modeling. *Decision Support Systems* 37: 475-484.

Nason, G.P., Von Sachs, R. (1999). Wavelets in time-series analysis. *Philosophical Transactions of the Royal Society A: Mathematical, Physical and Engineering Sciences* 357 (1760): 2511-2526

Ntale, H. K. and T. Y. Gan (2003). Drought indices and their application to East Africa. *International Journal of Climatology* 23(11): 1335-1357.

- Ozger, M., Mishra, A.K., Singh, V.P. (2012). Long lead time drought forecasting using a wavelet and fuzzy logic combination model: A case study in Texas. *Journal of Hydrometeorology* 13(1): 284-297.
- Palmer, W. (1965). Meteorological drought. Tech. Rep., Vol.45, U.S. Weather Bureau, Washington, D.C., p. 58
- Parrella, F. (2007). Online Support Vector Regression. Master Thesis, University of Genoa
- Partal, T. (2009). Modelling evapotranspiration using discrete wavelet transform and neural networks. *Hydrological Processes* 23(25): 3545-3555.
- Partal, T. and O. Kisi (2007). Wavelet and neuro-fuzzy conjunction model for precipitation forecasting. *Journal of Hydrology* 342(1-2): 199-212.
- Paulo, A., Ferreira, E., Coelho, C., Pereira, L. (2005). Drought class transition analysis through Markov and Loglinear models, an approach to early warning. *Agricultural Water Management* 77(1-3): 59-81.
- Paulo, A., and Pereira, L., (2008). Stochastic Predictions of Drought Class Transitions. *Water Resources Mangement* 22(9): 1277-1296.
- Renaud, O., Starck, J., Murtagh F., (2002). Wavelet-based Forecasting of Short and Long Memory Time Series. Department of Economics. University of Geneve.
- Rossi, G., Castiglione, L., Bonaccorso, B. (2007). Guidelines for Planning and Implementing Drought Mitigation Measures, in G. Rossi et al. (eds), *Methods and Tools for Drought Analysis and Management*, 325-247
- Ross, T., Lott, N., (2003). A Climatology of 1980–2003 Extreme Weather and Climate Events. National Climatic Data Center Technical Report No. 2003-01. NOAA/ NESDIS. National Climatic Data Center, Asheville, NC.
- Saco, P., Kumar, P. (2000). Coherent modes in multiscale variability of streamflow over the United States. *Water Resources Research* 36 (4): 1049-1067.
- Shamseldin, A. Y. (2010). Artificial neural network model for river flow forecasting in a developing country. *Journal of Hydroinformatics* 12(1): 22.
- Smola, A.J. (1996). Regression Estimation with Support Vector Learning Machines, M.Sc. Thesis, Technische Universitat Munchen, Germany.
- Thom, H.C.S., (1958). A note on gamma distribution. *Monthly Weather Rev.* 86, 117–122.

Tiwari, M.K., Chatterjee, C. (2010). Development of an accurate and reliable hourly flood forecasting model using wavelet-bootstrap-ANN (WBANN) hybrid approach. *Journal of Hydrology* 394: 458-470.

Tsakiris, G., Vangelis, H. (2004). Towards a Drought Watch System based on spatial SPI. *Water Resources Management* 18 (1): 1-12.

Vapnik, V. (1995). *The Nature of Statistical Learning Theory*, Springer Verlag, New York, USA.

Wang, W.C., Chau, K.W., Cheng, C.T., Qiu, L. (2009). A comparison of performance of several artificial intelligence methods for forecasting monthly discharge time series. *Journal of Hydrology* 374 (3-4): 294-306.

Wanas, N., Auda, G., Kamel. M.S., Karray., F. (1998). On the optimal number of hidden nodes in a neural network. *Proceedings of the IEEE Canadian Conference on Electrical and Computer Engineering*. 918–921.

Wilks, D. S. (1995). *Statistical methods in the atmospheric sciences an introduction*, Academic, San Diego, 467.

Yuan, Z.-M. and Tan X.-S. (2010). Nonlinear Screening Indicators of Drought Resistance at Seedling Stage of Rice Based on Support Vector Machine. *Acta Agronomica Sinica* 36(7): 1176-1182.

Zeng, N., (2003). Drought in the Sahel. *Science* 302: 999–1000.

Zhang, B.L., Dong, Z.Y. (2001). An adaptive neural-wavelet model for short term load forecasting. *Electric Power System Research*. 59: 121–129.



## **Connecting Text to Chapter 4**

The chapter is a manuscript co-authored by the supervisor of this research Dr. Jan F. Adamowski, as well as Dr. Bahaa Khalil. This manuscript is being prepared for submission to the Journal of Hydrology. All literature cited in this chapter is listed in the reference section at the end of this chapter, as well as at the end of this thesis.

Chapter 4 covers the development of long-term SPI indices, namely SPI 12 and SPI 24 and the development of the five data driven forecasting models. SPI 12 and SPI 24 are computed as they are representative of long-term drought conditions such as hydrological drought. The methodology for the development of neural network architectures as well as the parameters for support vector regression is similar to the methods in Chapter 3. The process of wavelet decomposition is also discussed and is similar to the process used in Chapter 4. Once SPI 12 and SPI 24 are computed they are forecast by the five data driven models for lead times of 6 and 12 months, respectively. These forecasts are compared to determine which data driven model is the most effective drought forecasting tool for long-term drought conditions.

## Chapter 4

### Long-term SPI drought forecasting in the Awash River Basin in Ethiopia using wavelet-neural network and wavelet-support vector regression models

Belayneh, A., Adamowski, J., and Khalil, B.

Department of Bioresource Engineering, Faculty of Agricultural and Environmental Sciences,  
McGill University, Quebec, Canada, H9X 3V9 Email:

[anteneh.meshesha@mail.mcgill.ca](mailto:anteneh.meshesha@mail.mcgill.ca)

[jan.adamowski@mcgill.ca](mailto:jan.adamowski@mcgill.ca)

[bahaa.khalil@mail.mcgill.ca](mailto:bahaa.khalil@mail.mcgill.ca)

#### Abstract:

Long-term drought forecasts can be an effective tool for mitigating some of the more adverse consequences of drought. Data driven models are suitable forecast tools due to their minimal information requirements and rapid development times. This study compares the effectiveness of five data driven models for forecasting long-term (6 and 12 months lead time) drought conditions in the Awash River Basin of Ethiopia. The Standard Precipitation Index (in this case SPI 12 and SPI 24) was forecasted using a traditional stochastic model (ARIMA) and compared to machine learning techniques such as artificial neural networks (ANNs), where a new procedure was used to determine the optimal number of neurons in the hidden layer, and support vector regression (SVR). In addition to these three model types, wavelet transforms were used to pre-process the inputs for ANN and SVR models to form WA-ANN and WA-SVR models. This study proposed and tested, for the first time, new long-term SPI drought forecasting methods based on the SVR and WA-SVR methods. This study also tested a new approach in wavelet analysis, where only the approximation series were used to generate the inputs for WA-ANN and WA-SVR models. The performances of all models were compared using RMSE, MAE,  $R^2$  and a measure of persistence. The forecast results indicate that the coupled wavelet neural network (WA-ANN) models and the coupled wavelet support vector regression (WA-SVR) models were the best models for forecasting SPI 12 and SPI 24 values over lead times of 6 and 12 months in the Awash River Basin.

**Keywords:** ANN; Support vector regression; SPI; Drought forecasting; Wavelet transforms; Time series analysis

#### 4.1 Introduction

Long-term, accurate hydrologic forecasting can be an important tool for effective water management. Accurate long-term drought forecasts can enable water authorities to effectively plan and prepare for the consequences of a drought. Drought impacts span many sectors of a country's economy and its effects may even impact areas that are not experiencing a precipitation deficit. Given that extended periods of drought can lead to a disruption of the water supply, low agricultural yields and reduced flows for ecosystems, the ability to effectively

forecast and predict droughts is important. An example of a sub-Saharan country that is highly vulnerable to the impacts of drought is Ethiopia, which will be the focus of this research study. Between 1950 and 1988 there were 38 droughts in Ethiopia. A 1972-73 famine caused by drought claimed 200,000 lives in the Wollo province. Although the famine caused by the drought of 1984–85 remains well known to the world community, less serious, but nonetheless significant droughts occurred in the years 1987, 1988, 1991–92, 1993–94, 1999, and 2002 (Edossa et al., 2010).

There are many drought forecasting methods; however, as drought is a common phenomenon throughout the world, research is required to determine which forecasting method is most suitable for a given watershed. In order to accurately forecast drought and mitigate some of its adverse effects, a clear understanding of the main characteristics of drought are required. Drought is a natural phenomenon that occurs when precipitation is significantly lower than normal. Modeling deficits in precipitation can be done using either physical or data driven models. Although physical models are good at providing physical interpretation and insight into catchment processes, they have been criticized for a number of reasons that include: being difficult to implement for real time forecasting applications; requiring many different types of data that are often difficult to obtain; requiring knowledge of relationships between various input and output variables; being difficult to construct; and, resulting in models that are overly complex, leading to problems of over parameterization (Beven, 2006). This is in contrast to data driven models, which have found appeal due to their minimum information requirements, rapid development times, simplicity, and accuracy in hydrologic forecasting (Adamowski, 2008).

Of the various data driven models, stochastic models have been traditionally used to forecast droughts. Autoregressive integrated moving average models (ARIMA) (Mishra, 2005; Mishra and Desai, 2006; Mishra et al., 2007; Han et al., 2010) have been the most widely used stochastic models for hydrologic drought forecasting. One of the major limitations of stochastic models is that they are linear models and are not very effective in forecasting non-linear data, which is a very common characteristic of hydrologic data.

To overcome this limitation, researchers in the last two decades have increasingly begun to utilize artificial neural networks (ANNs) to forecast hydrological data. ANNs have been used in

several studies as a drought forecasting tool (Mishra and Desai, 2006; Morid et al., 2007; Bacanli et al., 2008; Barros and Bawden, 2008; Cutore et al., 2009; Karamouz et al., 2009; Marj and Meijerink, 2011). However, ANNs are limited in their ability to deal with non-stationarities in the data, a limitation also shared by stochastic models. In response to this limitation, wavelet analysis, which is an effective tool in dealing with non-stationary data, has recently been explored in hydrological forecasting.

Wavelet analysis has been applied to examine rainfall-runoff relationships in Karstic watersheds (Labat et al., 1999), to evaluate rainfall-runoff models (Lane, 2007), to forecast river flow (Adamowski, 2008; Adamowski, 2011; Ozger et al., 2012), to forecast groundwater levels (Adamowski and Chan, 2011), to forecast urban water demand (Chan et al., 2011) and for the purposes of drought forecasting (Kim and Valdes, 2003). Apart from the Kim and Valdes (2003) study, no other studies have explored the use of wavelet analysis for drought forecasting.

SVMs are a relatively new form of machine learning that was developed by Vapnik (1995). SVMs can be divided into two main techniques, the Support Vector Classification (SVC) and Support Vector Regression (SVR), which address problems of classification and regression, respectively (Gao et al., 2002). Since the main goal of this study is to forecast the SPI, the SVR was the method that was used. There are several studies where SVR was used in hydrological forecasting. Khan and Coulibaly (2006) found that a SVR model performed better than ANNs in 3-12 month predictions of lake water levels. Yu et al. (2006) was successful in using SVRs for predicting flood stages with 1-6 hour lead times and Han et al. (2007) found that SVRs performed better than other models for flood forecasting. Kisi and Cimen (2009) used SVRs to estimate daily evaporation. However, to date SVRs have not been used to forecast drought; this study assessed for the first time whether it is an effective forecasting tool for drought.

The main objective of this study was to compare the effectiveness of traditional drought forecasting methods such as ARIMA models with ANNs, ANNs with data pre-processed using wavelet transforms (WA-ANN), support vector regression (SVR), and a newly proposed drought forecasting method based on the coupling of wavelet transforms and support vector regression (WA-SVR), for long-term drought forecasting. The standardized precipitation index (SPI) was the drought index forecasted in this study, as it is a good indicator of the variability of East

African droughts (Ntale and Gan, 2003). SPI 12 and SPI 24 are forecast for lead times of 6 and 12 months; SPI 12 and SPI 24 are good indicators of long-term drought conditions. A SPI 12 forecast of 6 months lead time represents a 6 month warning time for SPI 12. A 6-month forecast lead time is a typical long-term forecast (Kim and Valdes, 2003 and Mishra and Singh, 2006). SPI 12 is a comparison of the precipitation for 12 consecutive months with the same 12 consecutive months during all the previous years of the long-term precipitation record, while SPI 24 is a comparison of the precipitation for 24 consecutive months with the same 24 consecutive months during all the previous years. These SPI values at these time scales are representative of hydrological drought conditions and are likely tied to streamflows, reservoir levels, and even groundwater levels at the longer time scales. These forecasts can complement current long-term drought forecasts in Ethiopia, where the normalized vegetation index (NDVI) is used to provide seasonal forecasts. The forecast lead times were chosen to represent a long warning time, and because 5 and 12 months represent the bimodal and annual rainfall patterns in the Awash Rainfall Basin.

## **4.2 Theoretical Development**

### **4.2.1 SPI**

The standardized Precipitation Index (SPI) was developed by McKee et al. (1993). The SPI index is based on precipitation alone making its evaluation relatively easy compared to other drought indices, namely the Palmer Index and the crop moisture index (Cacciamani et al., 2007). A major advantage of the SPI index is that it makes it possible to describe drought on multiple time scales (Tsakiris and Vangelis, 2004; Mishra and Desai, 2006; Cacciamani et al., 2007). The SPI is also standardized which makes it particularly well suited for the comparison of droughts in different time periods and regions with different climates (Cacciamani et al., 2007). The SPI was selected for these reasons and it was also determined to be the best drought index for representing the variability in East African droughts (Ntale and Gan, 2002).

The computation of the SPI requires fitting a probability distribution to aggregated monthly precipitation series (3, 6, 12, 24, 48 months). The probability density function is then transformed into a normal standardized index whose values classify the category of drought characterizing each place and time scale (Cacciamani et al., 2007). The SPI can only be

computed when sufficiently long (at least 30 years) and possibly continuous time-series of monthly precipitation data are available (Cacciamani et al., 2007).

#### 4.2.2 ARIMA Models

Autoregressive integrated moving average (ARIMA) models were included in this study to provide a traditional approach to drought forecasting as a basis of comparison for model performance with the other more recent data driven models that are explored in this research. Box and Jenkins (1976) developed ARIMA models for modeling non-stationary time series. A non-stationary time series can be defined as a time series that does not have a constant mean, variance or autocorrelation over time. The general non-seasonal ARIMA model is autoregressive (AR) to order  $p$  and moving average (MA) to order  $q$  and operates on  $d^{th}$  difference of the time series  $z_t$ ; thus a model of the ARIMA family is classified by three parameters ( $p, d, q$ ) which have zero or positive integral values.

The general non-seasonal ARIMA model may be written as (Box and Jenkins, 1976):

$$z_t = \frac{\theta(B)a_t}{\phi(B)\nabla^d} \quad (1)$$

$$\phi(B) = (1 - \phi_1 B - \phi_2 B^2 - \dots - \phi_p B^p) \quad (2)$$

and

$$\theta(B) = (1 - \theta_1 B - \theta_2 B^2 - \dots - \theta_q B^q) \quad (3)$$

where  $z_t$  is the observed time series.  $\phi(B)$  and  $\theta(B)$  are polynomials of order  $p$  and  $q$ , respectively. The orders  $p$  and  $q$  are the order of non-seasonal auto-regression and the order of non-seasonal moving average, respectively. Random errors  $a_t$  are assumed to be independently and identically distributed with a mean of zero and a constant variance.  $\nabla^d$  describes the differencing operation to data series to make the data series stationary and  $d$  is the number of regular differencing.

ARIMA model development follows three stages: identification, estimation and diagnostic check (Box et al., 1994). In the identification stage, data transformation is often needed in order to make the time series stationary. Stationarity is a necessary condition in building an ARIMA model that is useful for forecasting (Zhang, 2001). During the estimation stage, the model parameters are chosen. The parameters are estimated in order to minimize the overall measures

of error. The last stage of model building is the diagnostic checking of model adequacy. This stage checks if the model assumptions about the errors are satisfied. Several diagnostic statistics and plots of the residuals can be used to examine the goodness of fit of the tentative model to the observed data.

### 4.2.3 ANN Models

For the purposes of modeling hydrological data, especially considering that most hydrological data is usually nonlinear, artificial neural networks (ANNs) have become a popular data driven forecasting model in the last two decades. The advantage of using ANNs is their parsimonious data requirements, rapid execution time and ability to produce models where the relationship between inputs and outputs are not fully understood.

For this study, ANN models with feed-forward multi-layer perceptron (MLP) architecture were used. These ANN models were trained with the Levenberg Marquardt (LM) back propagation algorithm. MLPs consist of three layers: an input layer, a hidden layer and an output layer. The hidden layer contains the neuron-like processing elements that connect the input and output layers, and is given by (Kim and Valdes, 2003):

$$\hat{y}_k(t) = f_0 \left[ \sum_{j=1}^m w_{kj} \cdot f_n \left( \sum_{i=1}^N w_{ji} x_i(t) + (w_{j0}) + w_{k0} \right) \right] \quad (4)$$

where  $N$  is the number of samples,  $m$  is the number of hidden neurons,  $x_i(t)$  = the  $i^{th}$  input variable at time step  $t$ ;  $w_{ji}$  = weight that connects the  $i^{th}$  neuron in the input layer and the  $j^{th}$  neuron in the hidden layer;  $w_{j0}$  = bias for the  $j^{th}$  hidden neuron;  $f_n$  = activation function of the hidden neuron;  $w_{kj}$  = weight that connects the  $j^{th}$  neuron in the hidden layer and  $k^{th}$  neuron in the output layer;  $w_{k0}$  = bias for the  $k^{th}$  output neuron;  $f_0$  = activation function for the output neuron; and  $\hat{y}_k(t)$  is the forecasted  $k^{th}$  output at time step  $t$  (Kim and Valdes, 2003).

Neurons are organized in layers and each neuron is connected with the neurons in contiguous layers (Adamowski and Sun, 2010). Each neuron receives a weighted input that is an output from every neuron in the previous layer. The effective incoming signal then propagates forward

through a non-linear activation function, towards the neurons in the next layer (Adamowski and Sun, 2010).

The LM algorithm is based on the steepest gradient descent method and the Gauss-Newton iteration. For a given input, a desired output is obtained by adjusting the interconnection weights using the error convergence technique. Generally, the error in the output layer propagates in reverse through the hidden layer to the input layer to obtain the final output. The gradient descent method is utilized to calculate the weight of the network and adjusts the weight of interconnections to minimize the output error.

#### 4.2.4 Support Vector Regression

Support vector machines (SVM), which were developed by Vapnik (1995) as a tool for classification and regression, embody the structural risk minimization principle, unlike conventional neural networks which adhere to the empirical risk minimization principle (Vapnik, 1995). In contrast to ANNs, which seek to minimize training error, SVMs attempt to minimize the generalization error (Cao and Tay, 2001).

With SVR, the purpose is to estimate a functional dependency  $f(\vec{x})$  between a set of sampled points  $X = \{\vec{x}_1, \vec{x}_2, \dots, \vec{x}_n\}$  taken from  $R^n$  and target values  $Y = \{y_1, y_2, \dots, y_n\}$  with  $y_i \in R$  (the input and target vectors ( $x_i$ 's and  $y_i$ 's) refer to the monthly records of the SPI index). Assuming that these samples have been generated independently from an unknown probability distribution function  $P(\vec{x}, y)$  and a class of functions (Vapnik, 1995):

$$F = \left\{ f \mid f(\vec{x}) = (\vec{W}, \vec{x}) + B : \vec{W} \in R^n, R^n \rightarrow R \right\} \quad (5)$$

where  $\vec{W}$  and  $B$  are coefficients that have to be estimated from the input data. The main objective is to find a function  $f(\vec{x}) \in F$  that minimizes a risk functional (Cimen, 2008):

$$R \left[ f(\vec{x}) \right] = \int l(y - f(\vec{x}), \vec{x}) dP(\vec{x}, y) \quad (6)$$

where  $l$  is a loss function used to measure the deviation between the target,  $y$ , and estimate  $f(\vec{x})$ , values. The risk functional cannot be minimized directly since the probability distribution function  $P(\vec{x}, y)$  is unknown. However the empirical risk function can be computed (Cimen, 2008):

$$R_{emp} \left[ f(\vec{x}) \right] = \frac{1}{N} \sum_{i=1}^N l(y_i - f(\vec{x}_i)) \quad (7)$$

where  $N$  is the number of samples. This traditional empirical risk requires structural control or regularization. A regularized risk function with the smallest steepness among the functions that minimize the empirical risk function can be used as (Cimen, 2008):

$$R_{reg} \left[ f(\vec{x}) \right] = R_{emp} \left[ f(\vec{x}) \right] + \gamma \left\| \vec{W} \right\|^2 \quad (8)$$

where  $\gamma$  is a constant ( $\gamma \geq 0$ ). This additional term reduces the model space and thereby controls the complexity of the solution leading to the following form of this expression (Smola, 1996; Cimen, 2008):

$$R_{reg} \left[ f(\vec{x}) \right] = C_c \sum_{x_i \in X} l_{\epsilon}(y_i - f(\vec{x}_i)) + \frac{1}{2} \left\| \vec{W} \right\|^2 \quad (9)$$

where  $C_c$  is a positive constant that has to be chosen beforehand. The constant  $C_c$  that influences a trade-off between an approximation error and the regression (weight) vector  $\left\| \vec{W} \right\|^2$  is a design parameter. The loss function, which is called an  $\epsilon$ -insensitive loss function, has the advantage that it will not need all the input data for describing the regression vector  $\left\| \vec{W} \right\|^2$  and can be written as (Cimen, 2008):

$$l_{\epsilon}(y_1 - f(\vec{x}_i)) = \begin{cases} 0 & \text{for } |y_1 - f(\vec{x}_i)| < \epsilon \\ |y_1 - f(\vec{x}_i)| - \epsilon & \text{otherwise} \end{cases} \quad (10)$$

This function behaves as a biased estimator when it is combined with the regularization term  $(\gamma \left\| \vec{W} \right\|^2)$ . The loss is equal to 0 if the difference between the predicted and observed value is less than the loss function. The nonlinear regression function is given by the following expression ((Vapnik, 1995; Cimen, 2008):

$$f(x) = \sum_{i=1}^N (\alpha_i^* - \alpha_i) K(x, x_i) + B_s \quad (11)$$

where  $\alpha_i, \alpha_i^* \geq 0$  are the Lagrange multipliers,  $B_s$  is a bias term, and  $K(x, x_i)$  is the Kernel function (Kisi and Cimen, 2011). Instead of operations being performed in the feature space which potentially has high dimensionality the kernel function enables operations to be performed in the input space. A variety of functions such as polynomial functions, Gaussian radial basis functions, multi-layer perception functions, functions with splines, etc. are treated by SVR (Kisi and Cimen, 2011). In this study, the radial basis function (RBF) kernel was used.

#### 4.2.5 Wavelet Transforms

Wavelet transforms are mathematical functions that give a time-scale representation of a given time series and its relationships in order to analyse non-stationaries. Wavelet transforms can reveal trends in the data such as breakdown points, discontinuities local minima and maxima that other signal analysis techniques might not reveal. Wavelet analysis can also help de-noise a particular data set. Another advantage of wavelet analysis is the flexible choice of the mother wavelet according to the characteristics of the investigated time series (Adamowski and Sun, 2010).

Wavelet analysis begins by selecting a mother wavelet ( $\psi$ ). The continuous wavelet transform (CWT) is defined as the sum over all time of the signal multiplied by a scaled and shifted version of the wavelet function  $\psi$  (Nason and Von Sachs, 1999):

$$W(\tau, s) = \frac{1}{\sqrt{|s|}} \int_{-\infty}^{\infty} x(t) \psi^* \left( \frac{t - \tau}{s} \right) dt \quad (12)$$

where  $s$  is the scale parameter;  $\tau$  is the translation and  $*$  corresponds to the complex conjugate (Kim and Valdes, 2003). The CWT produces a continuum of all scales as the output with each scale corresponding to the width of the wavelet; hence, a larger scale means that more of a time series is used in the calculation of the coefficient than in smaller scales. The CWT is useful for processing different images and signals; however, it is not often used for forecasting because it takes time to compute. Instead, in forecasting applications, the discrete wavelet transform is more frequently used. The discrete wavelet transform (DWT) requires less computation time and is simpler to implement. DWT scales and positions are usually based on powers of two (dyadic

scales and positions). This is achieved by modifying the wavelet representation to (Cannas et al., 2006):

$$\psi_{j,m}(m) = \frac{1}{\sqrt{|s_0^j|}} \sum_k \psi\left(\frac{k - m\tau_0 s_0^j}{s_0^j}\right) x(k) \quad (13)$$

where  $j$  and  $m$  are integers that control the scale and translation respectively, while  $s_0 > 1$  is a fixed dilation step and  $\tau_0$  is a translation factor that depends on the dilation step. Discretizing, the wavelet results, in the time-space scale being sampled at discrete levels. The DWT has high-pass and low-pass filters. The original time series passes through high-pass and low-pass filters, and detailed coefficients and approximation series are obtained.

One of the inherent limitations of using the DWT for forecasting applications is that it is not shift invariant (i.e. if we change values at the beginning of our time series, all of the wavelet coefficients will change). To overcome this problem, a redundant algorithm, known as the à trous algorithm, can be used and is given by (Mallat, 1998):

$$C_{i+1}(k) = \sum_{l=-\infty}^{+\infty} h(l)c_i(k + 2^i l) \quad (14)$$

where  $h$  is the low pass filter and  $C_{i+1}(k)$  is the original time series. To extract the details,  $w_i(k)$ , that were eliminated in Eq. (14), the smoothed version of the signal is subtracted from the coarser signal that preceded it, given by (Murtagh et al., 2003):

$$w_i(k) = c_{i-1}(k) - c_i(k) \quad (15)$$

where  $c_i(k)$  is the approximation of the signal and  $c_{i-1}(k)$  is the coarser signal. Each application of Eq. (14) and (15) results in a smoother approximation and extracts a higher level of detail. Finally, the non-symmetric Haar wavelet can be used as the low pass filter for the à trous algorithm to prevent any future information from being used during the decomposition (Renaud et al., 2002).

### 4.3 Awash River Basin

In this study, the SPI was forecasted in the Awash River Basin in Ethiopia (Figure 1). Drought is a common occurrence in the Awash River Basin (Edossa et al., 2010). A survey conducted in the basin revealed that major droughts occurred every two years within the area (Desalegn et al., 2006). In some years almost the entire country is subjected to drought (Desalegn et al., 2006). Ethiopia's weather and climate are extremely variable both temporally and spatially. The heavy dependence of the population on rain-fed agriculture has made the people and the country's economy extremely vulnerable to the impacts of droughts. Current monthly and seasonal drought forecasts are done using the normalized vegetation index (NDVI). While the NDVI is an effective drought index it is sensitive to changes in vegetation and has limitations in areas where vegetation is minimal. Forecasts of SPI 12 and SPI 24 are not dependent on vegetative cover and can be used as another tool for drought forecasts within the basin and the country as a whole.

The mean annual rainfall of the basin varies from about 1,600 mm in the highlands to 160 mm in the northern point of the basin. The total amount of rainfall also varies greatly from year to year, resulting in severe droughts in some years and flooding in others. The total annual surface runoff in the Awash Basin amounts to some  $4,900 \times 10^6 \text{ m}^3$  (Edossa et al., 2010). The basin was divided into three smaller sub-basins based on altitude, climate, topography and agricultural development. The division of the Awash River Basin into three sub-basins allows for the analysis of the forecasting results based on differing physical conditions and to ensure the methods used in this study were effective in forecasting long-term drought in different conditions. Effective forecasts of the SPI can be used for mitigating the impacts of hydrological drought that manifests as a result of rainfall shortages in the area

The climate of the Awash River Basin varies between a mild temperate climate in the Upper Awash sub-basin to a hot semi-arid climate in both the Middle and Lower sub-basins. The Awash River Basin supports farming, from the growth of lowland crops such as maize and sesame to pastoral farming practices. Rainfall records from 1970-2005 were used to generate SPI 12 and SPI 24 time series from each station. The rainfall gauges for each sub-basin are shown in Table 5. Rainfall gauges were selected on the basis of how complete their records were.

### 4.3.1 Upper Awash Basin

The Upper Awash Basin has a temperate climate with annual mean temperatures ranging between 15-22°C and an annual precipitation of between 500-2000 mm (Edossa et al., 2010). Rainfall distribution in the Upper Awash Basin is unimodal. Seven rainfall gauges located in this sub-basin were chosen for this study (Table 5). These stations were chosen because their precipitation records from 1970-2005 were either complete or relatively complete. Any station which had over 10% of their records missing was not selected.

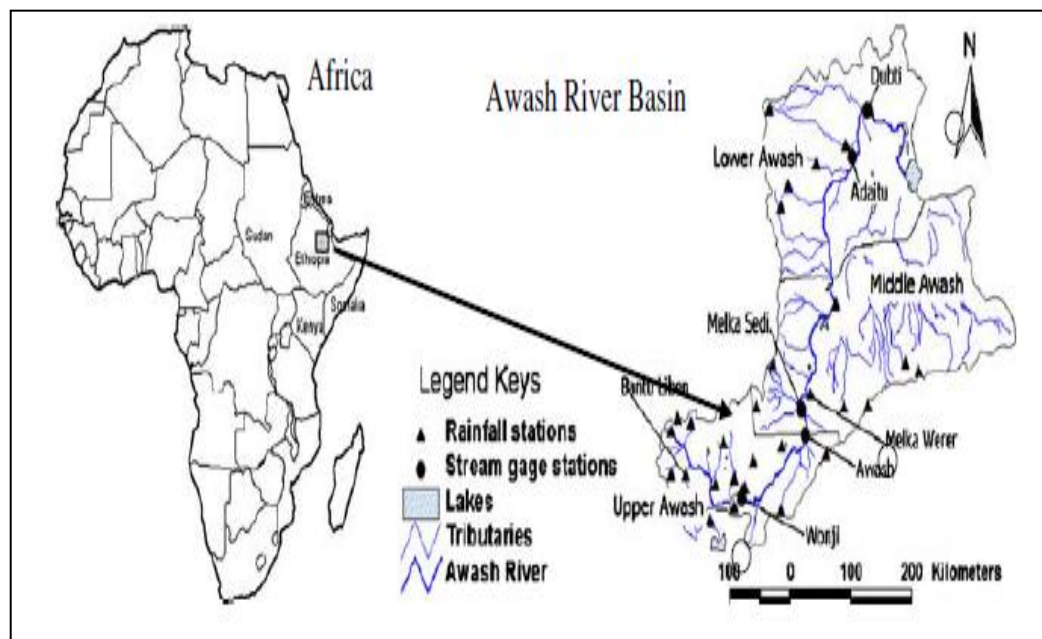


Figure 6: Awash River Basin (Source: Edossa et al., 2010).

### 4.3.2 Middle Awash Basin

The Middle Awash Basin is in the semi-arid climatic zone with a long hot summer and a short mild winter. Annual rainfall varies between 200-1500 mm (Edossa et al., 2010). The rainfall distribution is bimodal in this sub-basin. Minor rains normally occur in March and April and major rains from July to August. Six rainfall gauges located in this sub-basin were selected using the same criteria as in the Upper Awash Basin and are shown in Table 8.

### 4.3.3 Lower Awash Basin

The Lower Awash River Basin has a hot, semi-arid climate. The annual mean temperature of the region ranges between 22 and 32°C with average annual precipitation between 500 and 700 mm (Edossa et al., 2010). Five rainfall gauges were selected from this sub-basin using the same criteria used in the two other sub-basins and are shown in Table 5.

#### 4.3.4 Estimating Missing Rainfall

The normal ratio method, recommended by Linsley et al. (1988), was used to estimate the missing rainfall records stations that had incomplete precipitation records. With this method, rain depths for missing data are estimated from observations at three stations as close to, and as evenly spaced around the station with missing records, as possible. The distance matrix is established for all rain gauge stations in the basin based on their geographic locations in order to assess the proximity of stations with each other. All data sets were normalized using:

$$X_n = \frac{X_0 - X_{\min}}{X_{\max} - X_{\min}} \quad (16)$$

where  $X_0$  and  $X_n$  represent the original and normalized data respectively, while  $X_{\min}$  and  $X_{\max}$  represent the minimum and maximum value among the original data.

#### 4.4 Methodology

The methodology section details how the SPI is calculated as well as how the SPI is forecasted over long-term time scales using ARIMA, ANN, WA-ANN, SVR and WA-SVR models. In this section the best forecast results for each data driven model of SPI 12 and SPI 24 are presented. The data driven models were recursive models, where a model is forecast one lead time ahead and the subsequent forecasts include the output from the previous forecast as an input. Hence, a forecast of 6 months lead time will have the outputs from forecasts of lead times of 1-5 months (Table 9). For example, if a forecast of 12 months lead time has an input of SPI (t+8), it is the forecast of a SPI value at 8 months lead time. This output can subsequently be used as an input in a model with a greater lead time.

**Table 8: Descriptive Statistics for Awash Basin.**

Basin	Station	Mean Annual Precipitation (mm)	Max Annual Precipitation (mm)	Standard Deviation (mm)
Upper Awash Basin	Bantu Liben	91	647	111
	Tullo Bullo	94	575	114
	Ginchi	97	376	90
	Sebeta	111	1566	172
	Ejersalele	67	355	75
	Ziquala	100	583	110
	Debre Zeit	73	382	81
Middle Awash Basin	Koka	97	376	90
	Modjo	76	542	92
	Nazereth	73	470	85
	Wolenchiti	76	836	95
	Gelemsso	77	448	75
	Dire Dawa	51	267	54
Lower Awash Basin	Dubti	15	192	23
	Eliwuha	44	374	57
	Mersa	87	449	89
	Mille	26	268	40
	Bati	73	357	80

#### 4.4.1 SPI Calculation

SPI calculation begins by selecting a suitable probability density function to describe the precipitation data (Cacciamani et al., 2007). The cumulative probability of an observed precipitation amount is computed after an appropriate density function is chosen. The inverse normal (Gaussian) function is then applied to the probability (Cancelliere et al., 2007). For each rainfall gauge in this study the gamma distribution function was selected to fit the rainfall data. The SPI is a z-score and represents an event departure from the mean, expressed in standard deviation units. The SPI is a normalized index in time and space and this feature allows for the comparison of SPI values among different locations. SPI values can be categorized according to classes (Cacciamani et al., 2007). Normal conditions are established from the aggregation of two classes:  $-1 < \text{SPI} < 0$  (mild drought) and  $0 \leq \text{SPI} \leq 1$  (slightly wet). SPI values are positive or negative for greater or less than mean precipitation, respectively. Variance from the mean is a

probability indication of the severity of the flood or drought that can be used for risk assessment (Morid et al., 2006). The more negative the SPI value for a given location, the more severe the drought. The time series of the SPI can be used for drought monitoring by setting application-specific thresholds of the SPI for defining drought beginning and ending times. Accumulated values of the SPI can be used to analyze drought severity. In this study, an SPI\_SL\_6 program developed by the National Drought Mitigation Centre, University of Nebraska-Lincoln, was used to compute time series of drought indices (SPI) for each station in the basin and for each month of the year at different time scales.

#### **4.4.2 Model Inputs**

Two sets of inputs were developed from the SPI data. The monthly SPI was delayed ((t-1), (t-2), (t-3), etc) by an appropriate monthly time scale. The same delayed SPI data was decomposed using wavelet transforms. The optimal number of delays was determined by trial and error, with the number of delays that exhibit the highest model performance, as measured by RMSE in the training data set, being selected.

#### **4.4.3 ARIMA Models**

ARIMA models were included in this study to provide a traditional approach to hydrological time series forecasting that can be used as a basis of comparison for model performance with the aforementioned newer data driven models. Based on the Box and Jenkins approach, ARIMA models for the SPI time series were developed based on three steps: model identification, parameter estimation and diagnostic checking. The details on the development of ARIMA models for SPI time series can be found in the works of Mishra and Desai (2005) and Mishra et al., (2007).

In an ARIMA model, the value of a given times series is a linear aggregation of  $p$  previous values and a weighted sum of  $q$  previous deviations (Mishra and Desai, 2006). These ARIMA models are autoregressive to order  $p$  and moving average to order  $q$  and operate on  $d^{th}$  difference of the given times series. Hence, an ARIMA models is distinguished with three parameters ( $p, d, q$ ) that can each have a positive integer value or a value of zero.

#### 4.4.4 ANN Models

ANN models were created with the MATLAB (R.2010a) ANN toolbox and trained using the LM back propagation algorithm due to its efficiency and short computation time (Adamowski and Chan, 2011). The activation function for the hidden layer was a hyperbolic tangent sigmoid function; a linear function was used as the activation function for the output layer.

In the ANN toolbox the “newff” function was used. This function creates a feed-forward back-propagation network and assigns random initial weights. The default initialization for the first layer was done using the Nguyen-Widrow layer initialization function. This function generates initial weight and bias values for a layer so that the active regions of the layer’s neurons are distributed approximately evenly over the input space. This method results in several advantages over purely random weights and biases, including the fact that few neurons are wasted (since the active regions of all the neurons are in the input space), and training is faster (since each area of the input space has active neuron regions).

The ANN models had between 5-10 neurons in the input layer. The input data were normalized between 0 and 1. There are various methods to select the optimal number of nodes in the hidden layer of ANN models. One such method is trial and error. Another method, developed by Wanas et al. (1998) empirically determined that the optimal number of hidden nodes is equal to  $\log(N)$ , where  $N$  is the number of samples. Mishra and Desai (2006) determined that the optimal number of hidden neurons is  $2n+1$ , where  $n$  is the number of input layers. This study used all three methods to determine the optimal number of nodes in the hidden layer. For example, if using the method proposed by Wanas et al. (1998) gives a result of 4 hidden neurons and using the method proposed by Mishra and Desai (2006) gives 7 hidden neurons, the optimal number of hidden neurons is between 4 and 7, and thereafter the optimal number is determined using trial and error.

For all the ANN models, 80% of the data was used to train the models, while the remaining 20% of the data was used to test and validate the models with 10% used for testing and validation, respectively.

#### **4.4.5 SVR Models**

The OnlineSVR software created by Parrella (2007) was used to develop the SVR models for this study. All SPI data was partitioned into two sets: a calibration set (90% of the data) and a validation set (10% of the data). Unlike ANNs, the data can only be partitioned into two sets with the calibration set being equivalent to the training and testing sets found in ANNs. Similar to ANN models, all the input data for the SVR models were normalized between 0 and 1.

A nonlinear radial basis function (RBF) was used for the SVR models. As a result, each SVR model consisted of three parameters that were selected: gamma ( $\gamma$ ), cost (C), and epsilon ( $\epsilon$ ). A trial and error procedure was used to select the optimal combination of these three parameters. The combination of parameters that produced the lowest RMSE values for the training data sets was selected.

#### **4.4.6 Wavelet Decomposition**

The aim of the coupled models (WA-ANN and WA-SVR) is to predict the SPI 12 and 24 for lead times of 6 and 12 months ahead, given the current and previous SPIs. The à trous algorithm for the wavelet transform, which has been previously used for drought forecasts (Kim and Valdes, 2003), performs successive convolutions while a non-symmetric modified Haar wavelet transform developed by Karran, Morin and Adamowski (2012), is used as the low pass filter to prevent any future information from being used during the decomposition. The energy content of the Haar wavelet is concentrated over the narrowest support band (Karran et al., 2012). This property leads to the Haar wavelet having good localization properties, making it the most suitable wavelet for change detection studies (Karran et al., 2012).

In the proposed model, the SPI data for each of the rainfall stations was decomposed into sub-series of approximations and details (DWs). The process consists of a number of successive filtering steps. The decomposition process is then iterated, with successive approximation signals being decomposed in turn. As a result, the original SPI time series is broken down into many lower resolution components.

In this study, each original SPI time series was decomposed between 1 and 9 levels. After decomposition, the subsequent approximation series was either chosen on its own, in combination with relevant detail series or the relevant detail series were added together. This process was done for all decomposition levels until the decomposition level that yielded the best results was determined. The appropriate decomposition level varied between models. With most SPI time series, choosing just the approximation series resulted in the best forecast results. In some cases the summation of the approximation series with a decomposed detail series yielded the best forecast results. The appropriate approximation series was used as an input to the ANN and SVR models.

#### **4.4.7 WA-ANN Models**

The method of training for WA-ANN models is very similar to the method for training the ANN models. Unlike the ANN models, where the inputs are composed of the normalized SPI data, the inputs for the WA-ANN were made up of the approximations obtained via wavelet decomposition. The model architecture for WA-ANN models consists of 5-10 neurons in the input layer, 4-7 neurons in the hidden layer and one neuron in the output layer. The selection of the optimal number of neurons in both the input and hidden layers was done in the same way as for the ANN models. 80% of the data used to train the models and the remaining 20% used to test and validate the models with 10% of the data used to train and validate the models, respectively.

#### **4.4.8 WA-SVR Models**

Similar to the SVR models, the WA-SVR models were trained with the OnlineSVR software (2007). In addition, the data sets for the WA-SVR models were partitioned into a calibration and a validation set. 90% of the data was used in the calibration set, while the final 10% of the data was used in the validation set.

The three parameters for WA-SVR were selected using a trial and error procedure similar to the procedure used for SVR models. The inputs for the WA-SVR models were decomposed in the same way as WA-ANN models, with the approximation being chosen as an input in most cases

and the approximation being summed with the relevant details in some instances (when this was found to be more effective).

#### 4.4.9 Performance Measures

The following measures of goodness of fit were used to evaluate the forecast performance of all the aforementioned models:

$$\text{The coefficient of determination (R}^2\text{)} = \frac{\sum_{i=1}^N (y_i - \bar{y}_i)^2}{\sum_{i=1}^N (y_i - \hat{y}_i)^2} \quad (17)$$

$$\text{where } \bar{y}_i = \frac{1}{N} \sum_{i=1}^N y_i \quad (18)$$

where  $\bar{y}_i$  is the mean value taken over  $N$ ,  $y_i$  is the observed value,  $\hat{y}_i$  is the forecasted value and  $N$  is the number of data points. The coefficient of determination measures the degree of association among the observed and predicted values. The higher the value of  $R^2$  (with 1 being the highest possible value), the better the performance of the model.

$$\text{The Root Mean Squared Error (RMSE)} = \sqrt{\frac{SSE}{N}} \quad (19)$$

where  $SSE$  is the sum of squared errors, and  $N$  is the number of samples used.  $SSE$  is given by:

$$SSE = \sum_{i=1}^N (y_i - \hat{y}_i)^2 \quad (20)$$

with the variables already having been defined. The RMSE evaluates the variance of errors independently of the sample size.

$$\text{The Mean Absolute Error (MAE)} = \frac{\sum_{i=1}^N |\hat{y}_i - y_i|}{N} \quad (21)$$

The MAE is used to measure how close forecasted values are to the observed values. It is the average of the absolute errors.

The results in this study were also compared to persistence forecasts.

$$PERS = 1 - \frac{SSE}{SSE_{naive}} \quad (22)$$

where

$$SSE_{naive} = \sum (y_1 - y_{1-L})^2 \quad (23)$$

As mentioned above, *SSE* is the sum of squared errors.  $y_{1-L}$  is the estimate from a persistence model that takes the last observation (at time 1 minus the lead time (L)) (Tiwari and Chatterjee, 2010). A value of *PERS* smaller or equal to 0 indicates that the model under study performs worse or no better than the easy to implement naïve model. A *PERS* value of 1 is obtained when the model under study provides exact estimates of observed values.

#### 4.5 Results and Discussion

In this study the best forecast models for SPI 12 and SPI 24 are presented for forecast lead times of 6 and 12 months. As mentioned in section 1, SPI 12 and SPI 24 are good indicators of long term drought conditions. A SPI 12 forecast of 6 months lead time represents a 6 month warning time for SPI 12. A 6 month forecast lead time is a typical long-term forecast (Kim and Valdes, 2003 and Mishra and Singh, 2006) and is representative of the bimodal rainfall pattern present in the Awash River Basin, while a 12 month forecast lead time is able to show any variation in precipitation from year to year.

Table 9 shows the inputs used for the best data driven models. The performance results of the best models for each station are presented in Table 7 and Table 8. As mentioned earlier, models that have a persistence index between 0 and 1 perform better than a naïve model. All the data driven models had a persistence index greater than 0. ARIMA models had a *PERS* of 0.36, ANN models had a *PERS* of 0.46, SVR models had a *PERS* of 0.41, WA-ANN models had a *PERS* of 0.58 and WA-SVR models had a *PERS* of 0.48 respectively. The results presented are based on the validation data sets.

**Table 9: Model Inputs and intermediate variables for the best data driven models (LT = forecast lead time in months)**

Model	Input Structure	Output
ANN-LT6	SPI(t), SPI(t+4), SPI(t+5)	SPI(t+6)
ANN-LT12	SPI(t+6), SPI(t+10), SPI(t+11)	SPI(t+12)
SVR-LT6	SPI(t+3), SPI(t+4), SPI(t+5)	SPI(t+6)
SVR-LT12	SPI(t+9), SPI(t+10), SPI(t+11)	SPI(t+12)
WA-ANN-LT6	SPI(t+2), SPI(t+3), SPI(t+5)	SPI(t+6)
WA-ANN-LT12	SPI(t+2), SPI(t+7), SPI(t+11)	SPI(t+12)
WA-SVR-LT6	SPI(t+2), SPI(t+4), SPI(t+5)	SPI(t+6)
WA-SVR-LT12	SPI(t), SPI(t+10), SPI(t+11)	SPI(t+12)

#### 4.5.1 SPI 12 Forecasts

For SPI 12 forecasts of 6 months lead time the performance results of the best data driven models are presented in Table 10 . In the Upper Awash Basin, the best WA-ANN model for SPI 12 forecasts of 6 months lead time exhibited the best results. In terms of  $R^2$ , the best WA-ANN model was from the Ejersalele station and had a performance result of 0.9090. The model had a corresponding RMSE value of 0.2066 and a MAE of 0.1821. The WA-ANN model that had the lowest RMSE value was the Sebeta station, which had an RMSE value of 0.2012 and a corresponding  $R^2$  value of 0.8815. In the Middle Awash Basin the WA-ANN models exhibited the best forecast results. The best WA-ANN model from the Wolenchiti station had the best results in terms of  $R^2$  (0.9332) and a corresponding RMSE and MAE of 0.2015 and 0.1892, respectively. The Gelemsso station had the lowest RMSE value of 0.2 and a corresponding  $R^2$  value of 0.9204. In the Lower Awash Basin, the best forecast results in terms of RMSE were from a WA-ANN model. This model (Mille station) had a RMSE value of 0.2021 and a corresponding  $R^2$  of 0.9065. The WA-ANN model from the Eliwuha Station had the best results in terms of  $R^2$  with a value of 0.9326 and corresponding RMSE and MAE results of 0.2088 and 0.1804, respectively.

The best forecast results of SPI 12 for a 12 month lead time were also WA-ANN models. In the Upper Awash Basin the best model had forecast results of 0.83 in terms of  $R^2$  and results of 0.2206 and 0.2128 of RMSE and MAE, respectively. Similar to the Upper Basin, the best

forecast results for the Middle Basin were from the WA-ANN model with forecast results of 0.8292, 0.2334 and 0.2243 in terms of  $R^2$ , RMSE and MAE, respectively. In the Lower Awash Basin the WA-ANN models again exhibited the best forecast results. The forecast results from the Mille station were 0.8588, 0.2255 and 0.2023 in terms of  $R^2$ , RMSE and MAE, respectively.

#### 4.5.2 SPI 24 Forecasts

The forecast results for SPI 24 are shown in Table 12 and 13. For forecasts of 6 months lead time the best results were exhibited by WA-ANN models. The Bantu Liben station had the best results in terms of  $R^2$  with a forecast result of 0.9665 and corresponding RMSE and MAE values of 0.1968 and 0.1803, respectively. The Ejersalele station had the best results in terms of RMSE and MAE with results of 0.1778 and 0.1632, respectively. In the Lower Awash basin, WA-ANN models showed the best results in terms of  $R^2$  with the Gelemsso station having a forecast result of 0.9407. However, the best model results in terms of RMSE and MAE were from a WA-SVR model. The best WA-SVR model from the Dire Dawa station had forecast results of 0.2063 and 0.1872, respectively. This pattern is repeated in the Lower Awash basin with the best WA-ANN model exhibiting the highest  $R^2$  value of 0.9450 (Bati station) and the lowest RMSE and MAE values of 0.2100 and 0.1993 exhibited by a WA-SVR model.

For SPI 24 forecasts of 12 months lead time the data driven models that exhibited the best results were again WA-ANN and WA-SVR models. In the Upper Awash Basin the best models were from the Ginchi station. A WA-ANN model exhibited the highest  $R^2$  value of 0.8637 and a WA-SVR model had the lowest RMSE value of 0.2743 and the lowest MAE value of 0.2414. Similar to the results in the Upper basin, a WA-ANN model had the highest  $R^2$  value and a WA-SVR model had the lowest RMSE and MAE values in the Middle Awash Basin. The Meisso station in the Middle Awash Basin had the highest correlation between observed and predicted values with a  $R^2$  of 0.8659. The Dire Dawa station had the best results in terms of RMSE and MAE with results of 0.2664 and 0.2054, respectively. In the Lower Awash Basin the best forecast performance came from a WA-ANN model. The best forecast model from the Mersa station had results of 0.8602, 0.2819 and 0.2613 in terms of  $R^2$ , RMSE and MAE, respectively.

**Table 10: The best ARIMA, ANN and SVR models for 6 and 12 month forecasts of SPI 12.**

Column 3 is the ANN architecture detailing the number of nodes in the input, hidden and output layers respectively. In column 11 the parameters of the SVR models are given.

Basin	Station	ANN models	R <sup>2</sup>	RMSE	MAE	ARIMA (p,d,q)	R <sup>2</sup>	RMSE	MAE	SVR ( $\gamma, C, \epsilon$ )	R <sup>2</sup>	RMSE	MAE
6 month lead time													
Upper	Bantu Liben	5-4-1	0.7013	0.3737	0.3051	(5,0,0)	0.5912	0.8757	0.7714	0.4, 99, 0.008	0.7343	0.2427	0.2063
	Tullo Bullo	5-4-1	0.7269	0.3869	0.3191	(4,0,0)	0.5291	0.8662	0.7552	0.5, 98, 0.007	0.7382	0.2418	0.2137
	Ginchi	5-4-1	0.7120	0.3834	0.3592	(5,1,1)	0.5391	0.8851	0.7459	0.4, 94, 0.008	0.7028	0.2535	0.1984
	Sebeta	5-4-1	0.6993	0.3784	0.3516	(4,0,0)	0.5827	0.8789	0.7407	0.4, 96, 0.008	0.7320	0.2805	0.2007
	Ejersalele	5-4-1	0.7103	0.3751	0.3458	(3,1,0)	0.5261	0.8846	0.7539	0.5, 90, 0.006	0.7127	0.2997	0.1984
	Ziquala	6-4-1	0.7201	0.3765	0.3271	(4,0,0)	0.5713	0.8623	0.7436	0.3, 89, 0.005	0.7382	0.2690	0.2052
	Debre Zeit	5-4-1	0.7063	0.3816	0.3190	(5,0,0)	0.5718	0.8778	0.7399	0.6, 86, 0.01	0.7112	0.2886	0.2064
Middle	Koka	5-4-1	0.7222	0.3663	0.3048	(5,1,0)	0.5721	0.8629	0.7358	0.4, 87, 0.002	0.7346	0.2854	0.2134
	Modjo	5-4-1	0.7064	0.3673	0.3281	(3,110)	0.5329	0.8600	0.7333	0.6, 88, 0.008	0.7326	0.2917	0.2044
	Nazereth	6-4-1	0.6990	0.3843	0.3289	(5,1,2)	0.5729	0.8555	0.7296	0.8, 93, 0.008	0.7123	0.2701	0.2099
	Wolenchiti	6-4-1	0.7139	0.3722	0.3481	(5,0,0)	0.5537	0.8665	0.7388	0.9, 90, 0.008	0.7044	0.2884	0.1987
	Gelemsso	5-4-1	0.7045	0.3619	0.3581	(4,0,0)	0.5572	0.8751	0.7459	0.8, 91, 0.007	0.7150	0.2891	0.2147
	Dire Dawa	5-4-1	0.7123	0.3781	0.3440	(5,0,1)	0.5928	0.8731	0.7443	0.4, 92, 0.005	0.7329	0.2838	0.1885
Lower	Dubti	6-4-1	0.7077	0.3409	0.3103	(5,0,0)	0.5472	0.8928	0.7607	0.8, 93, 0.008	0.7346	0.3054	0.1851
	Eliwuha	5-4-1	0.7565	0.3296	0.3019	(4,0,1)	0.5534	0.8857	0.7798	0.8, 95, 0.008	0.7653	0.3136	0.1953
	Mersa	5-4-1	0.7142	0.3464	0.3340	(5,1,0)	0.5236	0.8989	0.7908	0.7, 94, 0.008	0.7543	0.2850	0.1966
	Mille	6-4-1	0.7000	0.3642	0.3214	(4,1,1)	0.5347	0.8949	0.7875	0.5, 90, 0.006	0.7123	0.2995	0.2202
	Bati	6-4-1	0.7210	0.3434	0.3097	(5,0,0)	0.5237	0.8928	0.7940	0.5, 87, 0.009	0.7547	0.2831	0.2162
12 month lead time													
Upper	Bantu Liben	5-4-1	0.5129	0.4120	0.3742	(4,0,0)	0.4421	0.9556	0.7577	0.4, 90, 0.01	0.6087	0.3723	0.2582
	Tullo Bullo	6-4-1	0.5438	0.4082	0.3802	(5,0,0)	0.4471	0.8951	0.7428	0.7, 88, 0.008	0.6054	0.3747	0.2498
	Ginchi	6-4-1	0.5346	0.4309	0.3781	(4,0,1)	0.4472	0.9015	0.7343	0.5, 91, 0.007	0.6078	0.3794	0.2352
	Sebeta	5-4-1	0.5456	0.4456	0.3981	(5,0,0)	0.4638	0.9123	0.7295	0.6, 97, 0.003	0.6123	0.3912	0.2807
	Ejersalele	6-4-1	0.5422	0.4021	0.3448	(5,0,0)	0.4537	0.9286	0.7416	0.6, 100, 0.01	0.6078	0.3466	0.2051
	Ziquala	7-4-1	0.5437	0.4358	0.3891	(4,0,1)	0.4682	0.9526	0.7321	0.8, 99, 0.03	0.6234	0.3556	0.2599
	Debre Zeit	5-4-1	0.5124	0.4009	0.3556	(5,0,0)	0.4462	0.9680	0.7287	0.6, 98, 0.006	0.6294	0.3466	0.2147
Middle	Koka	5-4-1	0.5474	0.4225	0.3997	(5,1,0)	0.4728	0.9751	0.7654	0.5, 93, 0.01	0.6052	0.3560	0.2478
	Modjo	6-4-1	0.5273	0.3996	0.3568	(4,1,0)	0.4572	0.9725	0.7755	0.5, 96, 0.008	0.6350	0.3482	0.2034
	Nazereth	7-4-1	0.4911	0.3960	0.3477	(3,1,1)	0.4438	0.9645	0.7725	0.8, 88, 0.004	0.6339	0.3396	0.2038
	Wolenchiti	7-4-1	0.5358	0.4180	0.3689	(3,0,0)	0.4589	0.9545	0.7785	0.8, 96, 0.008	0.6267	0.3114	0.1963
	Gelemsso	5-4-1	0.5441	0.4322	0.3889	(3,0,1)	0.4578	0.9592	0.7752	0.6, 94, 0.009	0.6290	0.3300	0.2115
Dire Dawa	5-4-1	0.5291	0.3900	0.3770	(3,0,0)	0.4280	0.9678	0.7690	0.5, 96, 0.008	0.6443	0.3466	0.2016	
Lower	Dubti	6-4-1	0.5127	0.3976	0.3782	(2,0,2)	0.4627	0.9285	0.7904	0.6, 96, 0.004	0.6239	0.3359	0.2212
	Eliwuha	4-4-1	0.5371	0.4304	0.3623	(5,0,0)	0.4632	0.9204	0.7837	0.8, 94, 0.008	0.6219	0.3087	0.1958
	Mersa	5-4-1	0.5312	0.4105	0.3785	(4,1,1)	0.4436	0.9158	0.7798	0.7, 95, 0.008	0.6350	0.3783	0.2587
	Mille	6-4-1	0.5279	0.3996	0.3574	(3,0,0)	0.4588	0.9007	0.7672	0.75, 90, 0.007	0.6438	0.3320	0.2144
	Bati	7-4-1	0.5230	0.4032	0.3703	(4,0,0)	0.4547	0.9890	0.7837	0.5, 96, 0.008	0.6387	0.3783	0.2426

**Table 11: The best WA-ANN and WA-SVR models for 6 and 12 month forecasts of SPI 12**

Column 3 is the ANN architecture detailing the number of nodes in the input, hidden and output layers respectively. In column 7 the parameters of the SVR models are given.

Basin	Station	WA-ANN	R <sup>2</sup>	RMSE	MAE	WA-SVR	R <sup>2</sup>	RMSE	MAE
<b>6 month lead time</b>									
<b>Upper</b>	Bantu Liben	5-6-1	0.8696	0.2023	0.1933	0.4, 99, 0.008	0.8507	0.2409	0.1934
	Tullo Bullo	5-6-1	0.8712	0.2048	0.1930	0.5, 98, 0.007	0.8419	0.2230	0.1935
	Ginchi	5-5-1	0.8276	0.2095	0.1831	0.4, 94, 0.008	0.8144	0.2314	0.2136
	Sebeta	5-5-1	0.8815	0.2013	0.1833	0.4, 96, 0.008	0.8380	0.2343	0.2214
	Ejersalele	7-5-1	0.9090	0.2066	0.1821	0.5, 90, 0.006	0.8363	0.2221	0.2054
	Ziquala	6-5-1	0.8616	0.2057	0.1830	0.3, 89, 0.005	0.8330	0.2413	0.2138
	Debre Zeit	7-4-1	0.8601	0.2066	0.1850	0.6, 86, 0.01	0.8344	0.2321	0.2234
<b>Middle</b>	Koka	4-4-1	0.8731	0.2061	0.1776	0.4, 87, 0.002	0.8714	0.2221	0.1844
	Modjo	5-4-1	0.8953	0.2083	0.1828	0.6, 88, 0.008	0.8732	0.2245	0.2054
	Nazereth	7-6-1	0.8403	0.2097	0.1804	0.8, 93, 0.008	0.8704	0.2537	0.2375
	Wolenchiti	7-4-1	0.9332	0.2015	0.1892	0.9, 90, 0.008	0.8644	0.2518	0.2210
	Gelemsso	6-5-1	0.9204	0.2000	0.1845	0.8, 91, 0.007	0.8726	0.2167	0.2017
	Dire Dawa	7-6-1	0.9129	0.2001	0.1928	0.4, 92, 0.005	0.8968	0.2212	0.2036
<b>Lower</b>	Dubti	4-4-1	0.9231	0.2060	0.1847	0.8, 93, 0.008	0.8640	0.2185	0.2084
	Eliwuha	5-4-1	0.9326	0.2088	0.1804	0.8, 95, 0.008	0.8671	0.2440	0.2213
	Mersa	5-4-1	0.8343	0.2183	0.2036	0.7, 94, 0.008	0.8325	0.2388	0.2228
	Mille	5-5-1	0.9065	0.2021	0.1928	0.5, 90, 0.006	0.8686	0.2438	0.2383
	Bati	6-4-1	0.9005	0.2183	0.1997	0.5, 87, 0.009	0.8441	0.2467	0.2341
<b>12 month lead time</b>									
<b>Upper</b>	Bantu Liben	5-6-1	0.8034	0.2235	0.2115	0.4, 90, 0.01	0.7535	0.2484	0.2228
	Tullo Bullo	6-6-1	0.8105	0.2320	0.2110	0.7, 88, 0.008	0.7547	0.2574	0.2320
	Ginchi	6-5-1	0.8261	0.2416	0.2128	0.5, 91, 0.007	0.7533	0.2455	0.2030
	Sebeta	5-5-1	0.8049	0.2314	0.2126	0.6, 97, 0.003	0.7148	0.2734	0.2622
	Ejersalele	8-6-1	0.8162	0.2208	0.2128	0.6, 100, 0.01	0.7342	0.2645	0.2406
	Ziquala	7-5-1	0.8300	0.2206	0.2128	0.8, 99, 0.03	0.7604	0.2922	0.2711
	Debre Zeit	8-5-1	0.8221	0.2411	0.2132	0.6, 98, 0.006	0.7336	0.2861	0.2727
<b>Middle</b>	Koka	5-4-1	0.8024	0.2474	0.2264	0.5, 93, 0.01	0.7140	0.2750	0.2522
	Modjo	6-4-1	0.8292	0.2334	0.2242	0.5, 96, 0.008	0.7643	0.2645	0.2449
	Nazereth	8-6-1	0.7942	0.2428	0.2293	0.8, 88, 0.004	0.7733	0.2595	0.2144
	Wolenchiti	8-5-1	0.8046	0.2365	0.2247	0.8, 96, 0.008	0.7843	0.2817	0.2733
	Gelemsso	7-6-1	0.8272	0.2354	0.2216	0.6, 94, 0.009	0.7721	0.2996	0.2717
	Dire Dawa	8-6-1	0.8219	0.2362	0.2117	0.5, 96, 0.008	0.7813	0.2674	0.2241
<b>Lower</b>	Dubti	5-5-1	0.8549	0.2406	0.2052	0.6, 96, 0.004	0.7443	0.2745	0.2620
	Eliwuha	6-4-1	0.8473	0.2719	0.2534	0.8, 94, 0.008	0.7641	0.3012	0.2639
	Mersa	6-4-1	0.8006	0.2492	0.2308	0.7, 95, 0.008	0.7241	0.2859	0.2714
	Mille	7-5-1	0.8588	0.2255	0.2023	0.75, 90, 0.007	0.7541	0.2942	0.2524
	Bati	8-4-1	0.8437	0.2350	0.2248	0.5, 96, 0.008	0.7134	0.2611	0.2418

**Table 12: The best ARIMA, ANN and SVR models for 6 and 12 month forecasts of SPI 24.**

Column 3 is the ANN architecture detailing the number of nodes in the input, hidden and output layers respectively. In column 11 the parameters of the SVR models are given.

Basin	Station	ANN models	R <sup>2</sup>	RMSE	MAE	ARIMA (p,d,q)	R <sup>2</sup>	RMSE	MAE	SVR (γ,C,ε)	R <sup>2</sup>	RMSE	MAE
6 month lead time													
Upper	Bantu Liben	4-4-1	0.7832	0.2775	0.2404	(5,1,0)	0.6486	0.5867	0.5735	0.8, 93, 0.08	0.7754	0.3192	0.2967
	Tullo Bullo	4-4-1	0.7756	0.3728	0.3110	(5,0,0)	0.6526	0.5860	0.5721	0.6, 95, 0.08	0.7694	0.3118	0.2872
	Ginchi	5-4-1	0.7949	0.3302	0.3238	(4,1,0)	0.6302	0.5853	0.5707	0.8, 94, 0.06	0.7581	0.3027	0.2883
	Sebeta	5-4-1	0.7682	0.3421	0.3325	(5,0,1)	0.6682	0.5844	0.5688	0.9, 93, 0.08	0.7961	0.3338	0.2991
	Ejersalele	6-4-1	0.7881	0.3347	0.3131	(5,1,0)	0.6427	0.5832	0.5665	0.8, 93, 0.08	0.7515	0.3546	0.3029
	Ziquala	4-4-1	0.7947	0.3619	0.3421	(5,0,1)	0.6362	0.5822	0.5644	0.5, 99, 0.05	0.7862	0.2627	0.2534
	Debre Zeit	5-4-1	0.8007	0.3332	0.3217	(4,1,0)	0.6291	0.5815	0.5631	0.6, 100, 0.04	0.7932	0.2922	0.2639
Middle	Koka	4-4-1	0.7763	0.3510	0.3429	(4,1,0)	0.6640	0.6017	0.5804	0.65, 90, 0.08	0.7868	0.3402	0.3103
	Modjo	4-4-1	0.7915	0.2836	0.2629	(5,0,0)	0.6526	0.6046	0.5421	0.7, 92, 0.06	0.7637	0.3115	0.2951
	Nazereth	4-4-1	0.8013	0.3701	0.3405	(5,0,0)	0.6227	0.6075	0.5728	0.8, 94, 0.07	0.7870	0.2835	0.2691
	Wolenchiti	4-4-1	0.7844	0.3302	0.3026	(4,0,1)	0.5721	0.5927	0.5721	0.6, 94, 0.08	0.7619	0.3143	0.3065
	Gelemsso	5-4-1	0.7916	0.2262	0.2202	(5,0,0)	0.6676	0.5821	0.5626	0.45, 96, 0.01	0.7738	0.3498	0.3431
	Dire Dawa	5-4-1	0.8042	0.2662	0.2632	(3,1,1)	0.6742	0.5780	0.5581	0.4, 89, 0.03	0.7887	0.2933	0.2788
	Dubti	4-4-1	0.8041	0.3397	0.3187	(5,0,0)	0.6248	0.5819	0.5355	0.4, 94, 0.07	0.7983	0.3141	0.2874
Lower	Eliwuha	5-4-1	0.7965	0.3129	0.3017	(5,0,0)	0.6574	0.5827	0.5282	0.5, 97, 0.06	0.7831	0.3149	0.2932
	Mersa	4-4-1	0.7715	0.3252	0.3230	(5,0,1)	0.6285	0.5881	0.5580	0.6, 92, 0.1	0.7845	0.3156	0.2744
	Mille	4-4-1	0.7852	0.3302	0.3160	(4,1,1)	0.6305	0.5944	0.5257	0.5, 96, 0.07	0.7748	0.3162	0.2864
	Bati	5-4-1	0.7914	0.2786	0.2645	(5,1,0)	0.6340	0.5595	0.5295	0.8, 98, 0.05	0.7681	0.2958	0.2804
	12 month lead time												
Upper	Bantu Liben	5-4-1	0.7122	0.3545	0.3422	(4,1,1)	0.5442	0.7470	0.6946	0.55, 88, 0.08	0.7259	0.3256	0.3179
	Tullo Bullo	5-4-1	0.7084	0.3817	0.3430	(4,0,0)	0.4724	0.7442	0.6625	0.55, 94, 0.09	0.7314	0.3271	0.2933
	Ginchi	6-4-1	0.7294	0.3620	0.3467	(5,1,0)	0.5078	0.7414	0.6379	0.65, 96, 0.08	0.7219	0.3282	0.3074
	Sebeta	6-4-1	0.7164	0.3632	0.3474	(5,0,10)	0.5939	0.7377	0.6200	0.85, 99, 0.06	0.7083	0.3387	0.3188
	Ejersalele	7-4-1	0.7231	0.3640	0.3493	(5,1,0)	0.5025	0.7330	0.5876	0.8, 88, 0.09	0.7296	0.3667	0.3594
	Ziquala	5-4-1	0.7017	0.3692	0.3508	(5,0,1)	0.5145	0.7288	0.5804	0.6, 91, 0.06	0.7139	0.3786	0.3683
	Debre Zeit	6-4-1	0.7138	0.3649	0.3462	(5,1,0)	0.5341	0.7261	0.5421	0.55, 94, 0.07	0.7038	0.3016	0.2886
Middle	Koka	5-4-1	0.7243	0.3908	0.3658	(5,1,0)	0.4412	0.8622	0.7525	0.55, 94, 0.07	0.7144	0.3577	0.3149
	Modjo	5-4-1	0.7129	0.3816	0.3710	(4,0,1)	0.4780	0.8637	0.7777	0.6, 91, 0.05	0.7233	0.3783	0.3684
	Nazereth	5-4-1	0.7055	0.3831	0.3540	(5,0,0)	0.5123	0.8654	0.8069	0.4, 95, 0.08	0.7168	0.3362	0.3293
	Wolenchiti	5-4-1	0.7064	0.3705	0.3657	(5,0,0)	0.4471	0.8762	0.8186	0.45, 100, 0.09	0.7235	0.3630	0.3529
	Gelemsso	6-4-1	0.7215	0.3534	0.3290	(4,1,1)	0.5659	0.8889	0.8300	0.6, 98, 0.08	0.7242	0.3768	0.3710
	Dire Dawa	6-4-1	0.7146	0.3412	0.3148	(5,1,0)	0.5216	0.9035	0.7709	0.65, 92, 0.05	0.7023	0.3687	0.3433
	Dubti	5-4-1	0.7179	0.3716	0.3580	(5,0,0)	0.5158	0.8854	0.7244	0.5, 88, 0.09	0.7253	0.3398	0.3158
Lower	Eliwuha	6-4-1	0.7189	0.3715	0.3471	(4,0,1)	0.4265	0.8643	0.7275	0.25, 100, 0.1	0.7018	0.3420	0.3261
	Mersa	5-4-1	0.7230	0.3628	0.3485	(5,0,0)	0.4940	0.8560	0.7308	0.55, 94, 0.06	0.7189	0.3649	0.3383
	Mille	5-4-1	0.7046	0.3624	0.3586	(5,1,1)	0.4710	0.8473	0.7629	0.8, 93, 0.08	0.7219	0.3207	0.2915
	Bati	6-4-1	0.7136	0.3708	0.3600	(5,1,0)	0.4915	0.8312	0.7729	0.88, 95, 0.07	0.7061	0.3387	0.2916

**Table 13: The best WA-ANN and WA-SVR models for 6 and 12 month forecasts of SPI 24.**

Column 3 is the ANN architecture detailing the number of nodes in the input, hidden and output layers respectively. In column 7 the parameters of the SVR models are given.

Basin	Station	WA-ANN	R <sup>2</sup>	RMSE	MAE	WA-SVR	R <sup>2</sup>	RMSE	MAE
<b>6 month lead time</b>									
Upper	Bantu Liben	5-6-1	0.9665	0.1968	0.1803	0.8, 93, 0.08	0.8832	0.2461	0.2108
	Tullo Bullo	5-6-1	0.8737	0.2748	0.2459	0.6, 95, 0.08	0.8569	0.2368	0.2268
	Ginchi	5-5-1	0.9254	0.2850	0.2671	0.8, 94, 0.06	0.8740	0.2475	0.2148
	Sebeta	5-5-1	0.8864	0.1821	0.1723	0.9, 93, 0.08	0.8742	0.2581	0.2331
	Ejersalele	7-5-1	0.8791	0.1778	0.1632	0.8, 93, 0.08	0.8683	0.2287	0.2023
	Ziquala	6-5-1	0.8978	0.2546	0.2395	0.5, 99, 0.05	0.8869	0.2192	0.2133
	Debre Zeit	7-4-1	0.8894	0.2576	0.2319	0.6, 100, 0.04	0.8858	0.2298	0.2048
Middle	Koka	5-4-1	0.9276	0.2828	0.2792	0.65, 90, 0.08	0.8958	0.3102	0.2962
	Modjo	5-4-1	0.9166	0.2561	0.2481	0.7, 92, 0.06	0.8938	0.2407	0.2281
	Nazereth	7-6-1	0.8515	0.2817	0.2743	0.8, 94, 0.07	0.8828	0.2512	0.2371
	Wolenchiti	7-4-1	0.9014	0.2115	0.2049	0.6, 94, 0.08	0.8892	0.2218	0.2106
	Gelemsso	6-5-1	0.9407	0.2258	0.2054	0.45, 96, 0.01	0.8935	0.2773	0.2694
	Dire Dawa	7-6-1	0.9215	0.2335	0.2149	0.4, 89, 0.03	0.8865	0.2487	0.2124
Lower	Dubti	5-4-1	0.8953	0.2618	0.2531	0.4, 94, 0.07	0.8938	0.3094	0.2870
	Eliwuha	5-4-1	0.9122	0.2190	0.2015	0.5, 97, 0.06	0.9024	0.2100	0.1993
	Mersa	5-4-1	0.9359	0.2340	0.2217	0.6, 92, 0.1	0.8953	0.2206	0.1916
	Mille	5-5-1	0.9322	0.2483	0.2386	0.5, 96, 0.07	0.8982	0.2442	0.2086
	Bati	6-4-1	0.9450	0.2236	0.2159	0.8, 98, 0.05	0.8953	0.2386	0.2114
<b>12 month lead time</b>									
Upper	Bantu Liben	5-6-1	0.8372	0.3342	0.3025	0.55, 88, 0.08	0.8171	0.3531	0.3388
	Tullo Bullo	6-6-1	0.8518	0.3351	0.3090	0.55, 94, 0.09	0.8385	0.3237	0.3104
	Ginchi	6-5-1	0.8637	0.3373	0.3191	0.65, 96, 0.08	0.8284	0.2743	0.2414
	Sebeta	5-5-1	0.8331	0.3325	0.3282	0.85, 99, 0.06	0.8398	0.3548	0.3302
	Ejersalele	8-6-1	0.8277	0.3372	0.3362	0.8, 88, 0.09	0.8420	0.3353	0.3209
	Ziquala	7-5-1	0.8316	0.3245	0.3083	0.6, 91, 0.06	0.8554	0.3560	0.3422
	Debre Zeit	8-5-1	0.8341	0.3274	0.3161	0.55, 94, 0.07	0.8042	0.3367	0.3325
Middle	Koka	5-4-1	0.8207	0.3121	0.3028	0.55, 94, 0.07	0.8215	0.3480	0.3204
	Modjo	6-4-1	0.8419	0.3061	0.2931	0.6, 91, 0.05	0.8013	0.3591	0.3396
	Nazereth	8-6-1	0.8101	0.3011	0.2876	0.4, 95, 0.08	0.8396	0.3629	0.3419
	Wolenchiti	8-5-1	0.8134	0.2948	0.2844	0.45, 100, 0.09	0.8400	0.3159	0.2760
	Gelemsso	7-6-1	0.8178	0.2879	0.2753	0.6, 98, 0.08	0.8223	0.2777	0.2697
	Dire Dawa	8-6-1	0.8659	0.2853	0.2762	0.65, 92, 0.05	0.8548	0.3410	0.3163
Lower	Dubti	5-5-1	0.8303	0.2827	0.2749	0.5, 88, 0.09	0.8472	0.3051	0.2827
	Eliwuha	6-4-1	0.8462	0.2874	0.2697	0.25, 100, 0.1	0.8494	0.3184	0.3073
	Mersa	6-4-1	0.8602	0.2819	0.2613	0.55, 94, 0.06	0.8512	0.3263	0.3113
	Mille	7-5-1	0.8406	0.2835	0.2637	0.8, 93, 0.08	0.8522	0.3107	0.2962
	Bati	8-4-1	0.8086	0.2839	0.2620	0.88, 95, 0.07	0.8538	0.3019	0.2794

### 4.5.3 Discussion

This study has shown that data driven models can be an effective means of forecasting drought at forecast lead times of 6 and 12 months in the Awash River Basin. The results indicate that machine learning techniques (ANNs and SVR) are more effective than a traditional stochastic model such as an ARIMA model in forecasting SPI 12 and SPI 24 at the aforementioned lead times. This is likely due to the fact that ANN and SVR models are effective in modeling non-linear components of time series data. Furthermore, the use of wavelet analysis as a pre-processing tool improved the forecast results for both ANN and SVR models. As might be expected, the results also indicate that as the forecast lead time is increased the correlation between observed and predicted values, as measured by  $R^2$ , decreases considerably. While the RMSE and the MAE decrease with increasing forecast lead time, their decrease is not as pronounced. This pattern is a likely result of the autocorrelation of the data sets since both data sets have a strong autocorrelation when the lag is increased. However, an increase in forecast lead time from 6 to 12 months did not result in poor results, especially when wavelet analysis was used, which highlights the effectiveness of this pre-processing method for ANN and SVR models in predicting the SPI.

The results from all the data driven models generally show that SPI 24 forecasts were more accurate than SPI 12 forecasts. Both SPI 12 and SPI 24 are long-term SPI and each new month has less impact on the period of sum precipitation (McKee et al., 1993) compared to short-term precipitation. As a result, monthly variation in precipitation has a smaller impact for both these SPI than for short-term SPI. However, as SPI 24 is a longer term SPI its sensitivity to changes in precipitation is less than that of SPI 12. This lack of sensitivity may explain why the forecast results for SPI 24 are generally better than those of SPI 12.

From the tables provided it can be seen that the ability of wavelet analysis to improve forecast results is more pronounced for SPI 12 than SPI 24. Given the higher sensitivity to changes in monthly precipitation for SPI 12 it seems that wavelet analysis reduces the sensitivity of shorter term SPI values to variations in monthly precipitation. In addition, the above tables show variability in forecast accuracy between the three sub-basins. However, a clear trend with regards to forecast accuracy and a given sub-basin is not apparent in the results. It seems the

characteristics of the individual rainfall station are more responsible for the forecast results than the general climatology of a given sub-basin.

Figure 7 shows that the forecast results of the WA-ANN model closely mirrors that of the observed SPI 24. The WA-ANN model seems to overestimate some of the peak events shown in the observed SPI 24 time series. The dry period around 165 months and the wet periods around 80 and 350 months are examples of this. In terms of the application of these forecasts, overestimating the severity of a drought may enable water resource managers and agricultural systems to be prepared for some of the adverse consequences of a given drought.

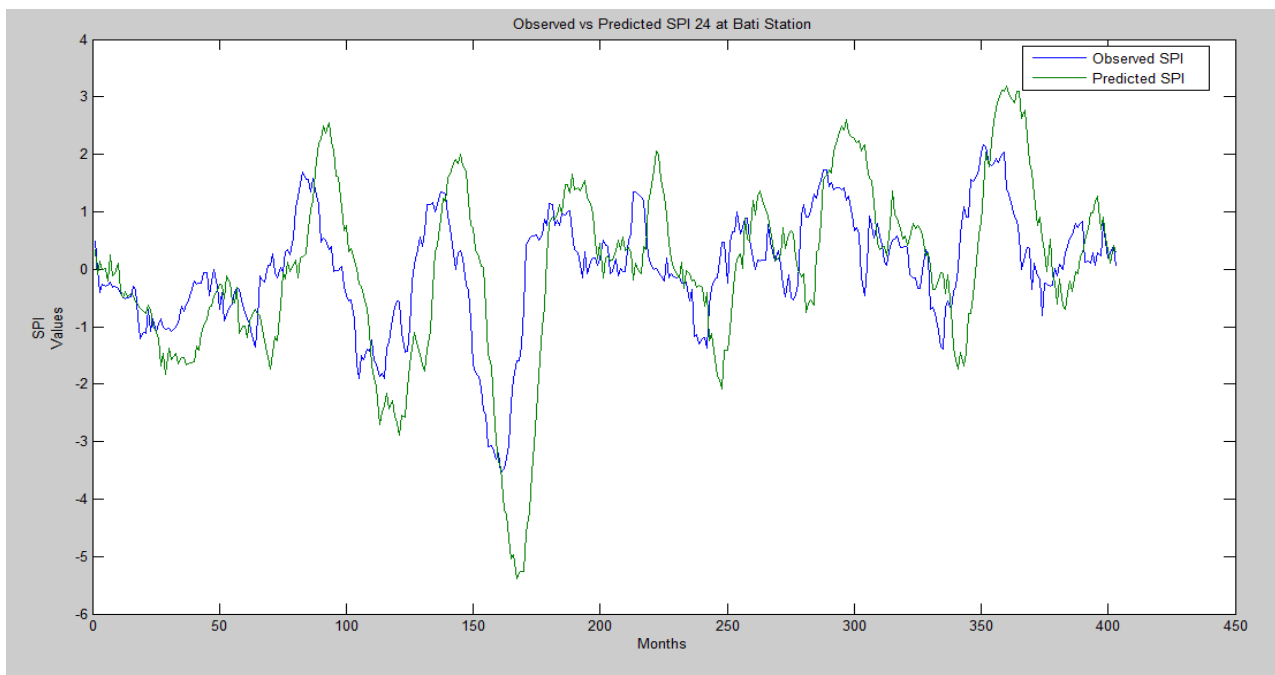


**Figure 7: SPI 24 forecast results for the best WA-ANN model at the Bati station for 6 months lead time.**

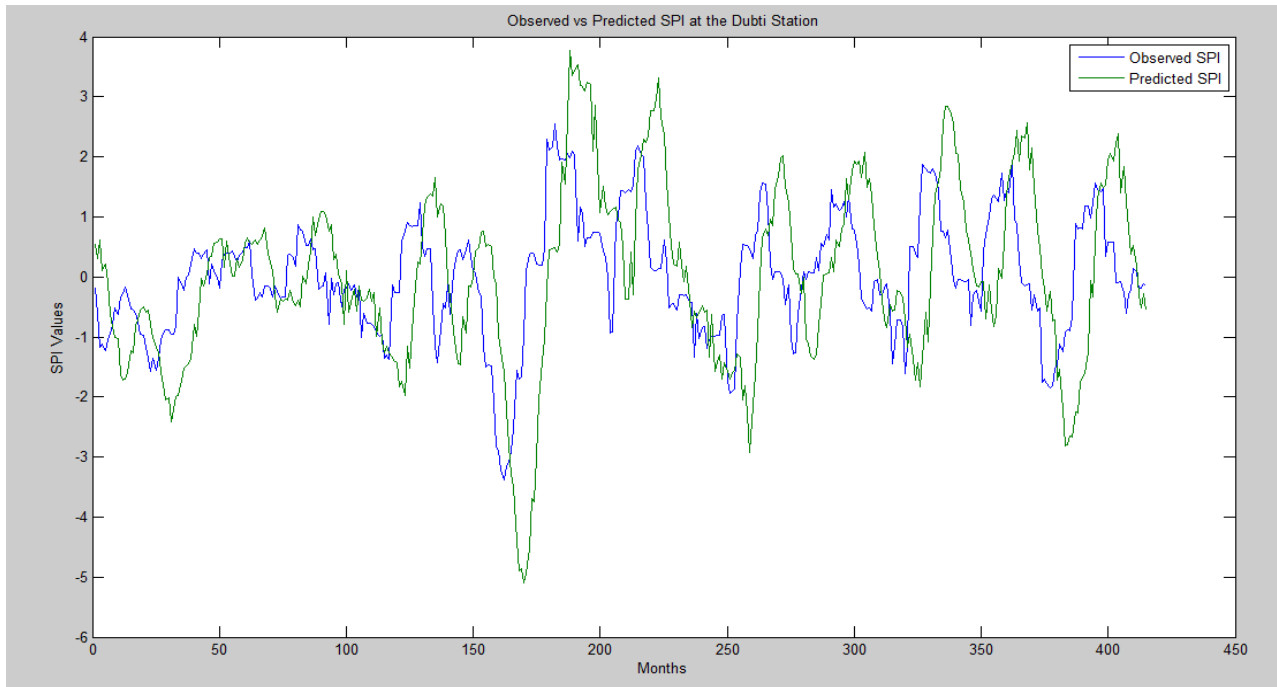


**Figure 8: SPI 12 forecast results for the best WA-ANN model at the Dubti Station for 6 months lead time.**

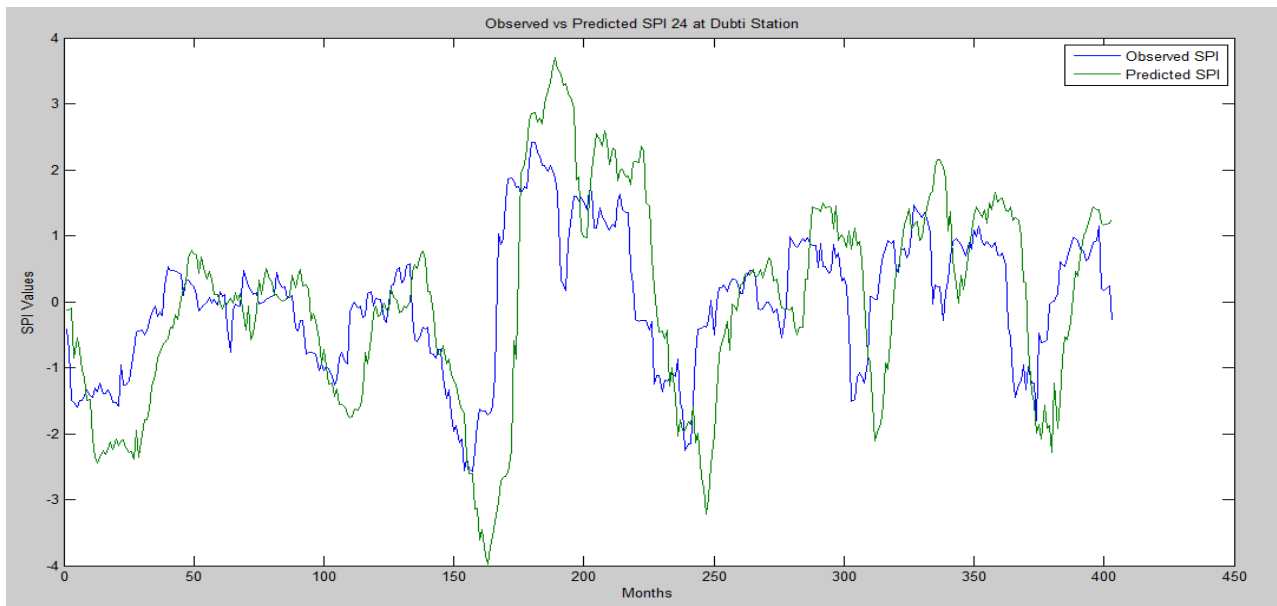


**Figure 9: SPI 24 forecast results for the best WA-ANN model at the Dubti Station for 6 months lead time.**

Figures 8 and 9 show a comparison of SPI 12 and SPI 24 forecasts (6 months lead time) for the Dubti station. For both SPI values, the predicted values for SPI 12 and SPI 24 closely mirror the observed values. The models do seem to overestimate the severity of peak events. The figures

show that the level of overestimation is higher for SPI 24 forecasts than for SPI 12 forecasts. It seems WA-ANN models overestimate the severity of a drought for SPI 24 more than for SPI 12.

The best forecast results in all three sub-basins are consistently either WA-ANN or WA-SVR models. The improved results due to wavelet analysis show that the à trous algorithm is an effective pre-processing tool for ANN and SVR models that forecast SPI 12 and SPI 24. The à trous algorithm is shift invariant making it more applicable for forecasting studies, which includes drought forecasting. The results confirm that wavelet analysis enhances the ability of ANN and SVR models to address the non-stationary components in the data.

Given the similar nature of wavelet analysis conducted on both these model types, the fact that WA-ANN models have slightly better results than SVR models can be attributed to ANN models outperforming SVR models. In using ANN models, even in complex systems, the relationship between input and output variables does not need to be fully understood. Effective models can be determined by changing the number of neurons within the hidden layer. Producing several models with different architectures is not computationally intensive and allows for a larger selection pool for the optimal model. SVR models however, require a lot more computation time, especially for a large data set. The uncertainty regarding the three SVR parameters increases the number of trials required to obtain the optimal model. Due to the long computational time of SVR models the same amount of trials cannot be done compared to ANN models and the selection pool for the best model is smaller than the selection pool for ANN models. ANN models adhere to the empirical risk minimization function, which sometimes makes them susceptible to local minima or maxima. However, given the ability of wavelet transforms to de-noise time series data and not be affected by these local discontinuities, this susceptibility can be overcome and the performance of ANN models improved as shown by the good results for WA-ANN models.

#### **4.6 Conclusion**

The ability of five data driven models to forecast the SPI 12 and SPI 24 over 6 and 12 month time scales was investigated in this study. This study proposed and evaluated, for the first time, the use of the SVR and WA-SVR methods for long-term drought forecasting. This study also, for the first time, utilized the approximation series (without the detail series) after wavelet

decomposition to generate the inputs for WA-ANN and WA-SVR models. In addition, a new approach for determining the optimal number of hidden neurons was tested in this study, which involved a combination of two traditional empirical approaches with a trial and error procedure.

Overall, coupled wavelet-neural network (WA-ANN and WA-SVR) models were found to provide the best results for forecasts of SPI 12 and SPI 24 in the Awash River Basin, especially for SPI 24. WA-ANN models showed a higher coefficient of determination between observed and predicted SPI compared to simple ANNs, ARIMA, and SVR models. Wavelet coupled models also consistently showed lower values of RMSE and MAE compared to the other data driven models. The coupled models provide more accurate results because pre-processing the original SPI time series with wavelet decompositions improves the forecast results over time series that do not use wavelet decompositions. Wavelet analysis seems to de-noise the SPI time series and subsequently allow the ANN and SVR model to model the main signal without the noise. Wavelet analysis also seems to reduce the sensitivity to changes in monthly precipitation within the SPI time series especially for SPI 12 compared to SPI 24. This reduction in sensitivity would be more pronounced in short-term SPI as they are inherently more sensitive to changes in monthly precipitation than long-term SPI.

This study focused on long-term drought forecasts of SPI 12 and SPI 24 in the Awash River Basin. Further studies need to be done to determine which of these data driven models is suitable for forecasting long-term SPI values in other locations with different climates and different physical characteristics. Considering the fact that the Middle and Lower Awash sub-basins have a very similar climate, studies of areas with different climates should be conducted to determine whether there is a significant link between forecast accuracy and climate. This study found that the characteristics of the station had more of an effect on forecast accuracy than the general climatology of the area. Future studies should also attempt to couple data driven drought forecasting models with uncertainty analysis, such as bootstrapping.

### **Acknowledgements**

This research was partially funded by an NSERC Discovery Grant held by Jan Adamowski. The data was obtained from National Meteorological Agency of Ethiopia. Their help is greatly appreciated.

## References:

- Abramowitz, M., Stegun, A. (eds.), (1965). Handbook of Mathematical Formulas, Graphs, and Mathematical Tables. Dover Publications, Inc., New York, USA.
- Adamowski, J. (2008). Development of a short-term river flood forecasting method for snowmelt driven floods based on wavelet and cross-wavelet analysis. *Journal of Hydrology*. 353: 247-266.
- Adamowski, J., Sun, K. (2010). Development of a coupled wavelet transform and neural network method for flow forecasting of non-perennial rivers in semi-arid watersheds. *Journal of Hydrology* 390: 85-91.
- Adamowski, J., Chan, H.F. (2011). A wavelet neural network conjunction model for groundwater level forecasting. *Journal of Hydrology* 407: 28-40.
- Asefa, T., Kemblowski, M., McKee, M., Khalil, A. (2006). Multi-time scale stream flow 505 predicitions: The support vector machines approach. *Journal of Hydrology*, 318 (1-4): 7-16.
- Bacanli, U. G., M. Firat, et al. (2008). Adaptive Neuro-Fuzzy Inference System for drought forecasting. *Stochastic Environmental Research and Risk Assessment* 23(8): 1143-1154.
- Barros, A. and G. Bowden (2008). Toward long-lead operational forecasts of drought: An experimental study in the Murray-Darling River Basin. *Journal of Hydrology* 357(3-4): 349-367.
- Beven, K. (2006). A manifesto for the equifinality thesis. *Journal of Hydrology*. 320: 18-36.
- Bonaccorso B, Bordi I, Cancelliere A, Rossi G, Sutera A (2003) Spatial variability of drought: an analysis of SPI in Sicily. *Water Resour Manag* 17:273–296
- Cancelliere, A., Di Mauro, G., Bonaccorso, B., Rossi, G. (2006). Drought forecasting using the Standardized Precipitation Index. *Water Resources Management* 21(5): 801-819.
- Cancelliere, A., Di Mauro, G., Bonaccorso, B., Rossi, G. (2007). Stochastic Forecasting of Drought Indices, G. Rossi et al. (eds.) *Methods and Tools for Drought Analysis and Management*. Springer
- Cannas, B., A. Fanni, Sias, G., Tronci, S., Zedda, M.K. (2006). River flow forecasting using neural networks and wavelet analysis. *Proceedings of the European Geosciences Union*
- Cao, L., Tay, F. (2001). Financial Forecasting Using Support Vector Machines. *Neural Computing and Applications*. 10: 184-192
- Cimen, M., 2008. Estimation of daily suspended sediments using support vector machines. *Hydrol. Sci. J.* 53 (3), 656–666.

- Conway, A.J., Macpherson, K., Brown, J. (1998). Delayed Time Series Predictions with Neural Networks. *Neurocomputing*. 18(1-3): 81-89.
- Coulibaly, P., Anctil, F., Bobee, B., 2000. Daily reservoir inflow forecasting using artificial neural networks with stopped training approach. *Journal of Hydrology* 230: 244–257.
- Cutore, P., Di Mauro, G., Cancelliere, A. (2009). Forecasting Palmer Index Using Neural Networks and Climatic Indexes
- Desalegn, C., Babel, M.S., Das Gupta, A., Seleshi, B.A., Merrey, D. (2006). Farmers' perception about water management under drought conditions in the Awash River Basin, Ethiopia. *Int J Water Resour Dev* 22(4):589–602
- Edossa, D.C., Babel, M.S., Gupta, A.D. (2010). Drought Analysis on the Awash River Basin, Ethiopia. *Water Resource Management* 24: 1441-1460
- Edwards, D.C., McKee, T.B., 1997. Characteristics of 20th Century Drought in the United States at Multiple Scales. *Atmospheric Science Paper* 634,
- Gao, J.B., Gunn, S.R., Harris, J., Brown, M., 2001. A probabilistic framework for SVM regression and error bar estimation. *Mach. Learn.* 46: 71–89.
- Gibbs, W.J., Maher, J.V., 1967. Rainfall Deciles as Drought Indicators. *Bureau of Meteorology Bull.* 48. Commonwealth of Australia, Melbourne, Australia.
- Guttman, N.B., 1999. Accepting the standardized precipitation index: a calculation algorithm. *Journal of American Water Resource Association*. 35 (2): 311–322.
- Han, P., Wang, P., Zhang, S., Zhu, D. (2010). Drought forecasting with vegetation temperature condition index. *Wuhan Daxue Xuebao (Xinxi Kexue Ban)/Geomatics and Information Science of Wuhan University* 35 (10): 1202-1206+1259.
- Holder, R.L. (1985). Multiple linear regression in hydrology. pp.32. Institute of hydrology. Oxfordshire.
- Karamouz, M., Rasouli, K., Nazil, S. (2009). Development of a Hybrid Index for Drought Prediction: Case Study. *Journal of Hydrologic Engineering*. 14: 617-627.
- Karran, D., Morin, E., Adamowski, J., (2012). Daily Streamflow Forecasting in Four Different Watersheds using Wavelet Transforms Coupled with Multiple Linear Regression, Neural Networks, and Support Vector Regression.
- Khan, M.S., Coulibaly, P. (2006). Application of support vector machine in lake water level prediction. *Journal of Hydrologic Engineering* 11(3): 199-205, American Society of Civil Engineering.

- Kim, T., Valdes, J.B. (2003). Nonlinear Model for Drought Forecasting Based on a Conjunction of Wavelet Transforms and Neural Networks. *Journal of Hydrologic Engineering* 8: 319-328
- Kisi, O., Cimen, M., (2009). Evapotranspiration modelling using support vector machines. *Hydrological Science Journal* 54 (5): 918-928. Taylor and Francis Ltd.
- Kisi, O. (2011). A wavelet-support vector machine conjunction model for monthly streamflow forecasting. *Journal of Hydrology* 399: 132-140.
- Labat, D., Ababou, R., Mangin, A. (1999). Wavelet analysis in Karstic hydrology 2nd Part: rainfall–runoff cross-wavelet analysis. *Comptes Rendus de l’Academie des Sciences Series IIA Earth and Planetary Science* 329: 881–887
- Lane, S.N., 2007. Assessment of rainfall–runoff models based upon wavelet analysis. *Hydrological Processes* 21: 586–607.
- Linsley, R.K., Kohler, M.A., Paulhus, J.L.H. (1988). *Hydrology for engineers*. International Edition. McGraw-Hill, Singapore
- Maity, R., Bhagwat, P.P., Bhatnagar, A. (2010). Potential of support vector regression for prediction of monthly streamflow using endogenous property. *Hydrological Processes* 24: 917-923
- Mallat, S. G. (1998). *A wavelet tour of signal processing*, Academic, San Diego, 577.
- McKee, T.B., Doesken, N.J., Kleist, J. (1993). The Relationship of Drought Frequency and Duration to Time Scales, Paper Presented at 8th Conference on Applied Climatology. American Meteorological Society, Anaheim, CA.
- Mishra, A. K. and V. R. Desai (2005). Drought forecasting using stochastic models. *Stochastic Environmental Research and Risk Assessment* 19(5): 326-339.
- Mishra, A. K. and V. R. Desai (2006). Drought forecasting using feed-forward recursive neural network. *Ecological Modelling* 198(1-2): 127-138.
- Mishra, A. K. and V. P. Singh (2010). A review of drought concepts. *Journal of Hydrology* 391(1-2): 202-216.
- Morid, S., V. Smakhtin, et al. (2007). Drought forecasting using artificial neural networks and time series of drought indices. *International Journal of Climatology* 27(15): 2103-2111.
- Morid, S., V. Smakhtin, et al. (2006). Comparison of seven meteorological indices for drought monitoring in Iran. *International Journal of Climatology* 26(7): 971-985.
- Murtagh, F., Starcj, J.L., Renaud, O. (2003). On neuro-wavelet modeling. *Decision Support Systems* 37: 475-484.

- Ntale, H. K. and T. Y. Gan (2003). Drought indices and their application to East Africa. *International Journal of Climatology* 23(11): 1335-1357.
- Palmer, W. (1965). Meteorological drought. Tech. Rep., Vol.45, U.S. Weather Bureau, Washington, D.C., p. 58
- Parrella, F. (2007). Online Support Vector Regression. Master Thesis, University of Genoa
- Partal, T. (2009). Modelling evapotranspiration using discrete wavelet transform and neural networks. *Hydrological Processes* 23(25): 3545-3555.
- Partal, T. and O. Kisi (2007). Wavelet and neuro-fuzzy conjunction model for precipitation forecasting. *Journal of Hydrology* 342(1-2): 199-212.
- Rossi, G., Castiglione, L., Bonaccorso, B. (2007). Guidelines for Planning and Implementing Drought Mitigation Measures, in G. Rossi et al. (eds), *Methods and Tools for Drought Analysis and Management*, 325-247, Springer
- Ross, T., Lott, N., (2003). A Climatology of 1980–2003 Extreme Weather and Climate Events. National Climatic Data Center Technical Report No. 2003-01. NOAA/ NESDIS. National Climatic Data Center, Asheville, NC. <<http://www.ncdc.noaa.gov/ol/reports/billionz.html>>.
- Shamseldin, A. Y. (2010). Artificial neural network model for river flow forecasting in a developing country. *Journal of Hydroinformatics* 12(1): 22.
- Smola, A.J. (1996). Regression Estimation with Support Vector Learning Machines, M.Sc. Thesis, Technische Universitat Munchen, Germany.
- Thom, H.C.S., (1958). A note on gamma distribution. *Monthly Weather Rev.* 86, 117–122.
- Tiwari, M.K., Chatterjee, C. (2010). Development of an accurate and reliable hourly flood forecasting model using wavelet-bootstrap-ANN (WBANN) hybrid approach. *Journal of Hydrology* 394: 458-470
- Vapnik, V. (1995). *The Nature of Statistical Learning Theory*, Springer Verlag, New York, USA.
- Wang, W.C., Chau, K.W., Cheng, C.T., Qiu, L. (2009). A comparison of performance of several artificial intelligence methods for forecasting monthly discharge time series. *Journal of Hydrology* 374 (3-4): 294-306.
- Wanas, N., Auda, G., Kamel. M.S., Karray., F. (1998). On the optimal number of hidden nodes in a neural network. *Proceedings of the IEEE Canadian Conference on Electrical and Computer Engineering*. 918–921.

Wilks, D. S. (1995). *Statistical methods in the atmospheric sciences an introduction*, Academic, San Diego, 467.

Yuan, Z.-M. and Tan X.-S. (2010). Nonlinear Screening Indicators of Drought Resistance at Seedling Stage of Rice Based on Support Vector Machine. *Acta Agronomica Sinica* 36(7): 1176-1182.

Zeng, N., (2003). Drought in the Sahel. *Science* 302: 999–1000.

Zhang, B.L., Dong, Z.Y. (2001). An adaptive neural-wavelet model for short term load forecasting. *Electric Power System Research*. 59: 121–129.

## Chapter 5: Summary and Conclusions

### 5.1 Summary

Accurate drought forecasts are increasingly important in light of growing demands on water resources as well as the growing uncertainty regarding water resources due to climate change. Given the high dependence of the population of Ethiopia on rain fed agriculture, the importance of accurate drought forecasts is heightened. This study attempted to compare various data driven models to forecast drought on both short-term and long-term time scales in the Awash River Basin of Ethiopia. The Standard Precipitation Index (SPI) is the drought index that is forecast over multiple lead times. Five data driven models were used to forecast the SPI; a traditional stochastic model (ARIMA), two machine learning techniques (ANN and SVR) and machine learning techniques pre-processed using wavelet analysis (WA-ANN and WA-SVR). To date, although WA-ANN models have been used to forecast the Palmer Index (Kim and Valdes, 2003) in Mexico, they have not been used to forecast the SPI, while SVR and WA-SVR models have not been explored to forecast drought until the present study.

The SPI was chosen for this study due to its many advantages over other drought indices, such as its standardization and relative ease of computation, as well as its ability to quantify different types of drought. In addition, the SPI had been computed for the Awash River Basin in previous studies (Edossa et al., 2010), and it was determined to be an effective drought index for East African droughts (Ntale and Gan, 2003).

The Awash River Basin was divided into three sub-basins, the Upper Awash Basin, the Middle Awash Basin and the Lower Awash Basin. Short-term and long-term drought forecasts were explored for all three sub-basins. Short-term drought forecasts constituted 1 and 3 month lead time forecasts of SPI 1 and SPI 3, while long-term forecasts constituted 6 and 12 month lead time forecasts of SPI 12 and SPI 24. SPI 1 is representative of short-term drought conditions. Its application can be related to short-term soil moisture deficits and crop stress. SPI 3 compares the precipitation for that period with the same 3 month period over the historical record. SPI 3 can be very effective in showing seasonal precipitation trends. SPI 1 and SPI 3 are useful indicators for agricultural drought. Hence, accurate forecasts of SPI 1 and SPI 3 can result in an early warning

system for agricultural systems and allow farmers to switch to more drought resistant crops. These forecasts can also augment current 10 day and monthly drought forecasts done by the NMSA of Ethiopia.

SPI 12 and SPI 24 are representative of long-term precipitation patterns. SPI 12 is a comparison of the precipitation for 12 consecutive months with the same 12 consecutive months during all the previous years of available data. Because these time scales are the cumulative result of shorter periods that may be above or below normal, the longer SPIs tend toward zero unless a specific trend is taking place. SPI 12 and SPI 24 are representative of hydrological drought conditions, which tend to affect streamflows, surface water levels and groundwater levels. With the demands on water due to agricultural and industrial development, coupled with growing population and climate change, water scarcity is a common feature in various parts of the world. These periods of water scarcity put an even greater stress on a region's water supply. With the onset of climate change, droughts occur with more frequency and severity. Given the fact that the consequences of a drought accumulate over a period of time and, in extreme conditions, linger long enough to lead to a famine, effective forecasts of these indices will help water resource managers prepare for any shortages in the water supply as well as mitigate the detrimental effects of droughts.

The forecast models used in this study were recursive models, which mean that a model is forecast one time-step ahead and the network is applied recursively, using the previous predictions as inputs for the subsequent forecasts. Hence, a forecast of 3 months lead time will have the outputs from forecasts of lead times of 1 and 2 months. A forecast of 6 months lead time will have the outputs from forecasts of lead times of 1-5 months. All the ANN models in this study had a feed-forward Multi-layer perceptron (MLP) architecture, and they were all trained with the Levenberg Marquardt (LM) back propagation algorithm. All SVR models used the radial basis function (RBF) kernel.

The number of wavelet decompositions can traditionally be determined using either a trial and error procedure or according to the formula  $L = \text{int}[\log(N)]$ , with  $N$  being the number of samples (Tiwari and Chatterjee, 2010). Once a time series is decomposed into its approximation and detail series, either the detail series are added together or added together along with the

approximation series to generate a new time series that is then subsequently used as the input to ANN or SVR models. In this study, each time series was decomposed between 1 and 9 times. To determine the appropriate decomposition level, the approximations were added to the detail series, the detail series were added on their own, and a new method where the approximation series' were taken on their own as well; these were then all compared. For almost all SPI time series, taking the approximation series on its own provided the best results as measured by  $R^2$ , RMSE and MAE, with the summation of the detail series with approximation providing the best results in only a few limited cases. With regards to wavelet analysis the à trous algorithm was used with a non-symmetric Haar wavelet as the low pass filter to prevent any future information from being used during wavelet decomposition.

## **5.2 Short-term Drought Forecasts**

In order to forecast drought on short-term time scales, SPI 1 and SPI 3 were computed and forecast over lead times of 1 and 3 months. SPI 1 reflects relatively short-term drought conditions and is closely related to short-term soil moisture and crop stress. In addition, SPI 1 is very similar to the percent of normal drought index and is an accurate representation of monthly precipitation because the index is normalized. One limitation of the SPI 1 is that in areas where rainfall is normally low during a month, large negative or positive SPI values may result even though the deviation from the mean is relatively small. Also, in areas with typically low normal monthly precipitation values, SPI 1 values may give the impression of a severe drought in a month where the climatology is typically dry.

SPI 3 compares the precipitation over a specific 3 month period with the precipitation totals from the same 3 month period for all the years included in the historical record (35 years in the case of this study). SPI 3 reflects short and medium-term moisture conditions and provides a seasonal estimation of precipitation. In agriculturally productive regions, SPI 3 is more effective at highlighting available moisture conditions than the Palmer Index. Given the importance of agriculture to the economy of Ethiopia, accurate forecasts of the SPI 3 are very important. As with the SPI 1, the SPI 3 may be misleading in regions where it is normally dry during that 3 month period. Large negative or positive SPIs may be associated with precipitation totals not very different from the mean.

The aforementioned SPI values were forecast over lead times of 1 and 3 months. For short-term forecasts a 1 month lead time is the shortest possible monthly lead time. Forecasts of 3 months lead time represent drought conditions over a seasonal period.

### **5.2.1 SPI 1 Forecasts**

The SPI forecasts were primarily evaluated using the  $R^2$ , RMSE and MAE. The results from the SPI 1 forecasts indicate that the best forecast models are the WA-ANN models followed by WA-SVR models. However, both 1 month and 3 month forecasts had low results in terms of  $R^2$  across all forecast models. A possible explanation for the low correlation between predicted and observed SPI 1 values is the low level of autocorrelation within the data set. In addition, SPI 1 is more sensitive to variation in precipitation from month to month. This sensitivity can result in less accurate forecasts compared to SPI 3 which is a cumulative of 3 consecutive months and as a result is less sensitive to variations in precipitation from month to month.

### **5.2.2 SPI 3 Forecasts**

The results of the SPI 3 forecasts were markedly better than the results from the SPI 1 forecasts, especially with respect to  $R^2$ . As mentioned earlier, SPI 3 is not as sensitive to changes in precipitation from month to month compared to SPI 1, which is a likely reason why the forecasts are better. Again, wavelet analysis improved the forecast results as exhibited by the results of WA-ANN and WA-SVR models. However, the improvements due to wavelet analysis are slightly more significant for SPI 1 than for SPI 3, especially for forecast lead times of 3 months. As stated previously, the forecasts of SPI 3 are not as sensitive to changes in precipitation and thus good results are obtained without wavelet analysis. The ability of wavelet analysis to improve these forecasts exists as shown but is not as high as the improvement seen in SPI 1 forecasts because forecasts of SPI 1 without the use of wavelet analysis suffer due to the sensitivity of SPI 1 to slight changes in precipitation over the long-term record.

## **5.3 Long-term SPI Forecasts**

In order to forecast drought on long-term time scales, SPI 12 and SPI 24 were computed and forecast over lead times of 6 and 12 months. The SPI at these time scales reflects long-term

precipitation patterns. SPI 12 is a comparison of the precipitation for 12 consecutive months with the same 12 consecutive months during all the previous years of the long-term precipitation record (which is 35 years in this study). These time scales are the cumulative result of shorter periods that may be above or below normal; the longer SPI values tend toward zero unless a specific trend is taking place. These SPI values at these time scales are probably tied to streamflows, reservoir levels, and even groundwater levels at the longer time scales. Forecast lead times of 6 and 12 months represent the bimodal and annual rainfall patterns in the Awash River Basin, respectively.

### **5.3.1 SPI 12 and SPI 24 Forecasts**

All the data driven models had good forecast results for SPI 12 compared to both SPI 1 and SPI 3. As with short-term SPI forecasts, WA-ANN and WA-SVR models had the best forecast results. The ability of wavelet analysis to model local discontinuities and to de-noise time series data is a reason why ANN and SVR model forecasts improved with the use of wavelet transforms. When the forecast lead time is increased the performance of all the data driven models deteriorated. SPI 12 is not very sensitive to any variation in monthly precipitation within the long-term record, as it is calculated from 12 consecutive months. The fact that fluctuations in monthly precipitation do not impact SPI 12 leads to more accurate forecast results compared to short-term SPI values.

Similar to the forecast for SPI 12, all the data driven models produced good SPI 24 forecasts. Wavelet analysis improved the results of both ANN and SVR models and those models that had their data pre-processed with wavelet transforms had the best forecast results.

### **5.4 General Forecasting Observations**

The forecast results for all the data driven models for both short and long-term SPI were better than using an easily implemented naïve model, as shown by the *PERS* values of the models. Forecast results for long-term SPI were better than forecast results for short-term SPI. As mentioned earlier, long-term SPI are less sensitive to variations in monthly precipitation within the historical record and thus have better forecast results. In this study, it was shown that data

driven models underestimate the severity of drought events for short-term forecasts and overestimate the severity of drought events for long-term forecasts.

There also does not seem to be any discernable relationship between the accuracy of forecasts and a given sub-basin. Even though the sub-basins each have distinct climatology, data driven models do not markedly perform better in any sub-basin. The performance of a given model is dependent on the characteristics of the individual station and not the overall climatology of the sub-basin.

## **5.5 Contribution to Research**

In the field of hydrologic forecasting the use of wavelet transforms is a relatively new phenomenon. The use of wavelet transforms in this study contributes significantly to the existing literature on hydrological forecasting. With regards to drought forecasting, to date, the only other study to utilize wavelet transforms was a study by Kim and Valdes (2003), which explored the use of a WA-ANN model to forecast the Palmer Index. This study expands, in a significant way, on the research of Kim and Valdes (2003) and explores the use of a WA-ANN model to forecast the SPI index, for the first time. Furthermore, this study explores, for the first time, the use of SVR and WA-SVR models as tools for drought forecasting. The results of this study confirm that wavelet transforms help improve the results of ANN and SVR models for drought forecasting. The results also show that WA-ANN and WA-SVR models are effective drought forecasting tools in the Awash River Basin in Ethiopia for both short and long-term drought conditions, and should be explored in other basins.

When using wavelet transforms for hydrologic forecasting, determining the appropriate level of decomposition and transformation is important. Traditionally, the number of decompositions is determined either by trial and error or using the formula  $L = \text{int}[\log(N)]$ , with  $N$  being the number of samples (Tiwari and Chatterjee, 2010). After an appropriate decomposition level is determined, the relevant detailed series are added together to generate an input time series for ANN or SVR models. This study proposed a new method, where all wavelet decomposition levels are considered (which in this study was 1-9). For all the levels the approximation series were taken individually, or added to the detailed series, or the detailed series were added together

without the approximation series. Overall, this study found that using the approximation series on their own, without the detail series, as an input to models resulted in the best forecasts

This study also proposed a new method for determining the optimal number of neurons in the hidden layer of ANN models. The number of neurons in the hidden layer are either traditionally determined using a trial and error procedure or are determined empirically to be either  $\log(N)$ , where  $N$  is the number of samples (Wanas et al., 1998) or  $2n+1$ , where  $n$  is the number of input layers (Mishra and Desai, 2006). This study combined all three approaches. The two empirical methods helped establish upper and lower bounds for the optimal number of neurons. After an interval was determined, a trial and error procedure was used to determine the optimal number of neurons in the hidden layer.

Drought forecasts in Ethiopia are carried out by the Meteorological Services Agency (NMSA). These forecasts include monthly forecasts as well as seasonal forecasts. The NMSA uses the normalized vegetation index (NDVI) as a drought index. The results of the present study indicate that data driven models, and especially wavelet-ANN and wavelet-SVR are effective in forecasting the SPI drought index in the Awash River Basin in Ethiopia. Given some of the limitations of a satellite based index such as the NDVI, using WA-ANN and WA-SVR data driven approaches can complement the already existing drought forecasting method used in Ethiopia and other regions of the world.

## **5.6 Future Research**

While this study did contribute new research to the field of drought forecasting there are still areas that need to be expanded upon. For instance, this study forecast the SPI drought index because the study by Ntale and Gan, (2002) determined that the SPI is the best drought index for showing the variability of East African droughts. Future studies could attempt to assess whether other drought indices are more effective in the context of the Awash River Basin. Other studies could compare multiple drought indices within the basin.

With respect to wavelet analysis, this study used the à trous wavelet transform with a modified Haar wavelet as a low pass filter. Future studies could experiment with different wavelet transforms to see whether they are effective in drought forecasting within the region. Wavelet

transforms were only applied to the machine learning techniques in this study. Future studies could attempt to use wavelet decomposed data as inputs to stochastic models such as ARIMA models. Future studies could also try to determine whether there is a relationship between a particular wavelet transform and a data driven model in terms of forecasting accuracy.

All drought forecasts were done with the understanding that rain-fed agriculture is the primary method of agriculture in Ethiopia. Future studies could investigate the impact of irrigation on drought conditions. In the context of irrigation systems a drought index that utilizes more than just precipitation as an input may be appropriate.

Future studies should also attempt to quantify time shift error as it is a part of forecasting problems with regression models. The use of wavelet ensemble models should also be explored. Combining data driven models with data from climatology models is another avenue for future research. Drought forecasts given future climate projections and scenarios would also be very useful risk assessment tools. This study does not couple any of the forecasts with any uncertainty analysis. The coupling of the models developed in this study with any uncertainty analysis methods such as bootstrapping would be very useful. In addition, the coupling of SVR models with genetic algorithms to make parameter estimation more efficient should be explored.

## **5.7 Conclusions**

All data driven models in this study were found to forecast SPI 3, SPI 12 and SPI 24 reasonably well across all lead times. The forecast results for SPI 1 were not very accurate, especially as measured by  $R^2$ . WA-ANN and WA-SVR models provided the best forecast results for all the aforementioned SPI time series. As expected, the use of wavelet analysis improved the forecast results of both ANN and SVR models. One advantage of using ANN models compared to SVR models was the relative ease of computation. Several ANN models could be trained in order to obtain a suitable forecast model within a short period of time. However, training SVR models took a much longer time. Given that the parameters for SVR models were selected using trial and error, the computation time for these models was considerably longer than for ANN models.

The improvement from using wavelet analysis was more pronounced in short-term SPI than in long-term SPI. The sensitivity of short-term SPI to monthly precipitation changes is reduced

when the SPI time series is wavelet decomposed. However, the ability of wavelet analysis to improve SPI 1 is limited, as this particular time series is very sensitive to monthly changes in precipitation and shows low levels of autocorrelation within the data set.

The forecast results did not vary significantly in each sub-basin. The climatology of the Upper Awash Basin is temperate, while the climatology of the Middle and Lower basins are semi-arid. The forecasts results do not indicate a trend with respect to any of the sub-basins.

Data driven models, and especially WA-ANN and WA-SVR models, can be effective in forecasting drought in the Awash River Basin. SPI 3, which is a short-term drought indicator that is closely linked with agricultural drought, is forecast well, and these forecasts can find great application in the Awash River Basin and Ethiopia as a whole given the importance of agriculture in the region. The forecasts for SPI 12 and SPI 24 are even better and can be utilized as long-term planning tools for water resource managers within the country.

## **References:**

- Abramowitz, M., Stegun, A. (eds.), (1965). Handbook of Mathematical Formulas, Graphs, and Mathematical Tables. Dover Publications, Inc., New York, USA.
- Adamowski, J. (2008). Development of a short-term river flood forecasting method for snowmelt driven floods based on wavelet and cross-wavelet analysis. *Journal of Hydrology*. 353: 247-266.
- Adamowski, J., Sun, K. (2010). Development of a coupled wavelet transform and neural network method for flow forecasting of non-perennial rivers in semi-arid watersheds. *Journal of Hydrology* 390: 85-91.
- Adamowski, J., Chan, H.F. (2011). A wavelet neural network conjunction model for groundwater level forecasting. *Journal of Hydrology* 407: 28-40.
- American Meteorological Society. (1997) Meteorological drought- Policy statement. *Bull. Amer. Meteor. Soc.* 78:847-849
- Anyamba, A., Tucker, C.J., Huete, A.R, Boken, V.K. (2005). Monitoring Drought Using Coarse-Resolution Polar-Orbiting Satellite Data, In V.K Boken, A.P Cracknell and R.L Heathcote (ed.), *Monitoring and Predicting Agricultural Drought: A Global Study*. Oxford University Press
- ASCE Task Committee on Application of Artificial Neural Networks in Hydrology, (2000a). Artificial neural networks in hydrology. I. Preliminary concepts. *Journal of Hydrologic Engineering*. 5 (2): 124–137.

ASCE Task Committee on Application of Artificial Neural Networks in Hydrology, 2000b. Artificial neural networks in hydrology. II. Hydrologic applications. *Journal of Hydrologic Engineering*. 5 (2): 115–123.

Asefa, T., Kemblowski, M., McKee, M., Khalil, A. (2006). Multi-time scale stream flow 505 predicitions: The support vector machines approach. *Journal of Hydrology*, 318 (1-4): 7-16.

Bacanli, U. G., M. Firat, et al. (2008). Adaptive Neuro-Fuzzy Inference System for drought forecasting. *Stochastic Environmental Research and Risk Assessment* 23(8): 1143-1154.

Barros, A. and G. Bowden (2008). Toward long-lead operational forecasts of drought: An experimental study in the Murray-Darling River Basin. *Journal of Hydrology* 357(3-4): 349-367.

Beven, K. (2006). A manifesto for the equifinality thesis. *Journal of Hydrology*. 320: 18-36.

Boken V.K. (2005). Agricultural Drought and Its Monitoring and Prediction: Some Concepts, In V.K Boken, A.P Cracknell and R.L Heathcote (ed.), *Monitoring and Predicting Agricultural Drought: A Global Study*. Oxford University Press

Bonaccorso B, Bordi I, Cancelliere A, Rossi G, Sutera A (2003) Spatial variability of drought: an analysis of SPI in Sicily. *Water Resour Manag* 17:273–296.

Bordi, I. and Sutera, A. (2007). Drought Monitoring and Forecasting at Large Scale, In G. Rossi et al. (eds.) *Methods and Tools for Drought Analysis and Management*. Springer

Box, G.E.P., Jenkins, G.M. (1976). *Time Series Analysis, Forecasting and Control*. Holden-Day, San Francisco.

Box, G.E.P., Jenkins, G.M., Reinsel, G.C. (1994). *Time Series Analysis, Forecasting and Control*. Prentice Hall, Englewood Cliffs, NJ, USA.

Cancelliere, A., Di Mauro, G., Bonaccorso, B., Rossi, G. (2006). Drought forecasting using the Standardized Precipitation Index. *Water Resources Management* 21(5): 801-819.

Cancelliere, A., Di Mauro, G., Bonaccorso, B., Rossi, G. (2007). Stochastic Forecasting of Drought Indices, G. Rossi et al. (eds.) *Methods and Tools for Drought Analysis and Management*. Springer

Cannas, B., A. Fanni, Sias, G., Tronci, S., Zedda, M.K. (2006). River flow forecasting using neural networks and wavelet analysis. *Proceedings of the European Geosciences Union*

Cao, L., Tay, F. (2001). Financial Forecasting Using Support Vector Machines. *Neural Computing and Applications*. 10: 184-192

Cimen, M., 2008. Estimation of daily suspended sediments using support vector

machines. *Hydrol. Sci. J.* 53 (3), 656–666.

Conway, A.J., Macpherson, K., Brown, J. (1998). Delayed Time Series Predictions with Neural Networks. *Neurocomputing.* 18(1-3): 81-89.

Coulibaly, P., Anctil, F., Bobee, B., 2000. Daily reservoir inflow forecasting using artificial neural networks with stopped training approach. *Journal of Hydrology* 230: 244–257.

CSA. (1999). *Statistical Abstract*. Central Statistical Authority. Addis Ababa, Ethiopia

Cutore, P., Di Mauro, G., Cancelliere, A. (2009). Forecasting Palmer Index Using Neural Networks and Climatic Indexes

Desalegn, C., Babel, M.S., Das Gupta, A., Seleshi, B.A., Merrey, D. (2006). Farmers' perception about water management under drought conditions in the Awash River Basin, Ethiopia. *Int J Water Resour Dev* 22(4):589–602

Edossa, D.C., Babel, M.S., Gupta, A.D. (2010). Drought Analysis on the Awash River Basin, Ethiopia. *Water Resource Management* 24: 1441-1460

Edwards, D.C., McKee, T.B., 1997. Characteristics of 20th Century Drought in the United States at Multiple Scales. *Atmospheric Science Paper* 634,

Engida, M. (1999). Annual Rainfall and Potential Evapotranspiration in Ethiopia. *Ethiop. J. Nat. Resources* 1:137-154.

Environment Canada, 2004. Threats to Water Availability in Canada. National Water Research Institute, Burlington, Ontario. NWRI Scientific Assessment Report Series No. 3 and ACSD Science Assessment Series No. 1. p. 128.

Gao, J.B., Gunn, S.R., Harris, J., Brown, M., 2001. A probabilistic framework for SVM regression and error bar estimation. *Mach. Learn.* 46: 71–89.

Gibbs, W.J., Maher, J.V., 1967. Rainfall Deciles as Drought Indicators. Bureau of Meteorology Bull. 48. Commonwealth of Australia, Melbourne, Australia.

Glantz, M.H. (1994). *Drought follows the plow*. University Press, Cambridge, Great Britain.

Guttman, N.B., 1999. Accepting the standardized precipitation index: a calculation algorithm. *Journal of American Water Resource Association.* 35 (2): 311–322.

Han, P., Wang, P., Zhang, S., Zhu, D. (2010). Drought forecasting with vegetation temperature condition index. *Wuhan Daxue Xuebao (Xinxi Kexue Ban)/Geomatics and Information Science of Wuhan University* 35 (10): 1202-1206+1259.

- Heim, R.R.Jr. (2002). A review of twentieth-century drought indices used in the United States. *Bull. Amer. Meteor. Soc.* 83: 1149-1165.
- Holder, R.L. (1985). *Multiple linear regression in hydrology*. pp.32. Institute of hydrology. Oxfordshire.
- Hwang, Y., Carbone, G.J. (2009). Ensemble Forecasts of Drought Indices Using a Conditional Residual Resampling Technique. *Journal of Applied Meteorology and Climatology*. 48: 1289-1301.
- Karamouz, M., Rasouli, K., Nazil, S. (2009). Development of a Hybrid Index for Drought Prediction: Case Study. *Journal of Hydrologic Engineering*. 14: 617-627.
- Khan, M.S., Coulibaly, P. (2006). Application of support vector machine in lake water level prediction. *Journal of Hydrologic Engineering* 11(3): 199-205, American Society of Civil Engineering.
- Kim, T., Valdes, J.B. (2003). Nonlinear Model for Drought Forecasting Based on a Conjunction of Wavelet Transforms and Neural Networks. *Journal of Hydrologic Engineering* 8: 319-328
- Kisi, O., Cimen, M. (2009). Evapotranspiration modelling using support vector machines. *Hydrological Science Journal* 54 (5): 918-928. Taylor and Francis Ltd.
- Kisi, O. (2011). A wavelet-support vector machine conjunction model for monthly streamflow forecasting. *Journal of Hydrology* 399: 132-140.
- Kogan, F.N. (1997). Global drought watch from space. *Bull. Am. Meteorol. Soc.* 78: 621–636.
- Labat, D., Ababou, R., Mangin, A. (1999). Wavelet analysis in Karstic hydrology 2nd Part: rainfall–runoff cross-wavelet analysis. *Comptes Rendus de l’Academie des Sciences Series IIA Earth and Planetary Science* 329: 881–887
- Lane, S.N., 2007. Assessment of rainfall–runoff models based upon wavelet analysis. *Hydrological Processes* 21: 586–607.
- Linsley, R.K., Kohler, M.A., Paulhus, J.L.H. (1988). *Hydrology for engineers*. International Edition. McGraw-Hill, Singapore
- Lloyd-Hughes, B., Saunders, M.A., 2002. A drought climatology for Europe. *Int. J. Climatol.* 22, 1571–1592.
- Mabbutt, J.A. (1984). A new global assessment of the status and trends of desertification. *Environ. Conserv.* 11:100-113. Vikas Publishing House, New Delhi, India

- Maity, R., Bhagwat, P.P., Bhatnagar, A. (2010). Potential of support vector regression for prediction of monthly streamflow using endogenous property. *Hydrological Processes* 24: 917-923
- Mallat, S. G. (1998). *A wavelet tour of signal processing*, Academic, San Diego, 577.
- McKee, T.B., Doesken, N.J., Kleist, J. (1993). The Relationship of Drought Frequency and Duration to Time Scales, Paper Presented at 8th Conference on Applied Climatology. American Meteorological Society, Anaheim, CA.
- Mishra, A. K. and V. R. Desai (2005). Drought forecasting using stochastic models. *Stochastic Environmental Research and Risk Assessment* 19(5): 326-339.
- Mishra, A. K. and V. R. Desai (2006). Drought forecasting using feed-forward recursive neural network. *Ecological Modelling* 198(1-2): 127-138.
- Mishra, A. K. and V. P. Singh (2010). A review of drought concepts. *Journal of Hydrology* 391(1-2): 202-216.
- Morid, S., V. Smakhtin, et al. (2007). Drought forecasting using artificial neural networks and time series of drought indices. *International Journal of Climatology* 27(15): 2103-2111.
- Morid, S., V. Smakhtin, et al. (2006). Comparison of seven meteorological indices for drought monitoring in Iran. *International Journal of Climatology* 26(7): 971-985.
- Murtagh, F., Starcj, J.L., Renaud, O. (2003). On neuro-wavelet modeling. *Decision Support Systems* 37: 475-484.
- Ntale, H. K. and T. Y. Gan (2003). Drought indices and their application to East Africa. *International Journal of Climatology* 23(11): 1335-1357.
- Palmer, W. (1965). *Meteorological drought*. Tech. Rep., Vol.45, U.S. Weather Bureau, Washington, D.C., p. 58
- Parrella, F. (2007). *Online Support Vector Regression*. Master Thesis, University of Genoa
- Partal, T. (2009). Modelling evapotranspiration using discrete wavelet transform and neural networks. *Hydrological Processes* 23(25): 3545-3555.
- Partal, T. and O. Kisi (2007). Wavelet and neuro-fuzzy conjunction model for precipitation forecasting. *Journal of Hydrology* 342(1-2): 199-212.
- Rossi, G., Castiglione, L., Bonaccorso, B. (2007). Guidelines for Planning and Implementing Drought Mitigation Measures, in G. Rossi et al. (eds), *Methods and Tools for Drought Analysis and Management*, 325-247, Springer

Ross, T., Lott, N. (2003). A Climatology of 1980–2003 Extreme Weather and Climate Events. National Climatic Data Center Technical Report No. 2003-01. NOAA/ NESDIS. National Climatic Data Center, Asheville, NC. <<http://www.ncdc.noaa.gov/ol/reports/billionz.html>>.

Sanford, S. (1978). Towards a definition of Drought, In: M.T Hinchey (ed.), Symposium on Drought in Botswana. Hanover, New Jersey: University Press of New England

Shamseldin, A. Y. (2010). Artificial neural network model for river flow forecasting in a developing country. *Journal of Hydroinformatics* 12(1): 22.

Smith, L.C., Turcotte, D.L., Isacks, B.L. (1998). Stream flow characterization and feature detection using a discrete wavelet transform. *Hydrological Processes* 12, 233–249.

Smola, A.J. (1996). Regression Estimation with Support Vector Learning Machines, M.Sc. Thesis, Technische Universitat Munchen, Germany.

Thom, H.C.S., (1958). A note on gamma distribution. *Monthly Weather Rev.* 86, 117–122.

Tiwari, M.K., Chatterjee, C. (2010). Development of an accurate and reliable hourly flood forecasting model using wavelet-bootstrap-ANN (WBANN) hybrid approach. *Journal of Hydrology* 394: 458-470

Vapnik, V. (1995). *The Nature of Statistical Learning Theory*, Springer Verlag, New York, USA.

Wang, W.C., Chau, K.W., Cheng, C.T., Qiu, L. (2009). A comparison of performance of several artificial intelligence methods for forecasting monthly discharge time series. *Journal of Hydrology* 374 (3-4): 294-306.

Wanas, N., Auda, G., Kamel. M.S., Karray., F. (1998). On the optimal number of hidden nodes in a neural network. *Proceedings of the IEEE Canadian Conference on Electrical and Computer Engineering.* 918–921.

Wilks, D. S. (1995). *Statistical methods in the atmospheric sciences an introduction*, Academic, San Diego, 467.

Yuan, Z.-M. and Tan X.-S. (2010). Nonlinear Screening Indicators of Drought Resistance at Seedling Stage of Rice Based on Support Vector Machine. *Acta Agronomica Sinica* 36(7): 1176-1182.

Zeng, N., (2003). Drought in the Sahel. *Science* 302: 999–1000.

Zhang, B.L., Dong, Z.Y. (2001). An adaptive neural-wavelet model for short term load forecasting. *Electric Power System Research.* 59: 121–129.